

DISS. ETH NO. 24088

DEVELOPMENT OF A GRK2-INHIBITORY PEPTIDE

A thesis submitted to attain the degree of

DOCTOR OF SCIENCES of ETH ZURICH

(Dr. sc. ETH Zurich)

presented by

MURIEL GRÄMER

MSc ETH

born on 25.03.1987

citizen of Gommiswald-Dorf SG

accepted on the recommendation of

Prof. Dr. Ursula Qitterer

Prof. Dr. Cornelia Halin Winter

2017

Table of contents

1	SUMMARY	1
2	ZUSAMMENFASSUNG	3
3	ABBREVIATIONS	5
4	INTRODUCTION	10
4.1	G protein-coupled receptor signalling	10
4.1.1	Characteristics of G protein-coupled receptors	10
4.1.2	Heterotrimeric G proteins are classical signal transducers	11
4.1.2.1	The α -subunit of heterotrimeric G proteins	11
4.1.2.2	The $\beta\gamma$ -complex of heterotrimeric G proteins	12
4.1.2.3	Coupling specificity of GPCRs	13
4.1.3	Arrestins are mediators of GPCR signalling and desensitization	13
4.1.3.1	Arrestins are signal transducers	13
4.1.3.2	Arrestins mediate GPCR sequestration	15
4.1.4	GPCR biased signalling	16
4.2	Physiological roles of G protein-coupled receptor kinases	16
4.2.1	GRKs are multi-domain kinases	16
4.2.1.1	The visual subfamily	17
4.2.1.2	The β ARK subfamily	17
4.2.1.3	The GRK4 subfamily	18
4.2.2	GRKs are multifunctional proteins	18
4.2.2.1	Receptor desensitization	18
4.2.2.2	Phosphorylation of non-receptor substrates	18
4.2.2.3	Kinase-independent functions of GRK2	19
4.3	Pathophysiological roles of GRK2	19
4.3.1	Heart failure	19
4.3.2	Hypertension	20
4.3.3	Diabetes mellitus	21
4.3.4	Obesity	21
4.3.5	Osteoporosis	21
4.3.6	Cancer	22
4.3.7	Potential of a GRK2-inhibitor	22

4.4	Approaches to GRK2-inhibition	22
4.4.1	GRK2-inhibition via the N-terminal domain	23
4.4.2	Targeting the central kinase domain	24
4.4.3	Targeting the C-terminal interaction with G β y	25
4.4.4	Peptide GRK2-inhibitors	27
4.4.5	Other GRK2-inhibitors	27
4.5	The therapeutic potential of peptide drugs	28
4.5.1	Characteristics of peptides	28
4.5.2	Modifications	29
4.5.3	Displacement assay	29
4.5.4	Gene therapy	29
4.6	Peptide phage display library screen for candidate drugs	30
4.6.1	Principle of a phage display library screen	30
4.6.2	Peptide libraries	31
4.6.3	Applications of phage display technology	31
4.7	Aim	32
5	MATERIALS AND METHODS	33
5.1	Molecular cloning	33
5.2	Protein procedures	40
5.3	Peptide phage display library screening	47
5.4	<i>In vitro</i> phosphorylation assay	50
5.5	Cell culture	52
5.6	Establishment of transgenic mouse lines	54
5.7	Statistical analysis	55
6	RESULTS	56
6.1	Cloning, protein expression and purification of GRK2 domains	56
6.1.1	Generation of GRK2 domain-containing plasmids	56
6.1.2	Protein expression and purification of GRK2 domains	58
6.2	Peptide phage display library screening with GRK2CTD as bait	63

6.2.1	Panning procedure	63
6.2.2	Phage ELISA	64
6.2.3	Peptide results	65
6.3	Development of a GRK2-interacting peptide based on the panning results	65
6.3.1	BLAST sequence analysis	65
6.3.2	Sequence elongation based on WDR76	67
6.3.3	An ELISA shows selective binding of GRK2CTD to WD3	67
6.4	The GRK2-interacting peptide shows GRK2-inhibitory features	68
6.4.1	WD3 interferes with the binding of GRK2CTD to Gβ3	68
6.4.1.1	GRK2CTD binds to Gβ3 and Gβ3-s	68
6.4.1.2	WD3 inhibits the binding of GRK2CTD to Gβ3	69
6.4.2	Assessment of kinase activity	70
6.4.2.1	WD3 inhibits the phosphorylation of the splicing factor SRSF1 by GRK2	70
6.4.2.2	An ELISA shows binding of SRSF1 to GRK2	71
6.4.3	Inhibition of GRK2-mediated receptor desensitization	72
6.4.3.1	Generation of plasmids expressing WD-Peptides	73
6.4.3.2	WD3 increases the bradykinin-stimulated Ca ²⁺ -signal in HEK293A cells	73
6.5	In vivo characterization of the GRK2-inhibitory peptide	74
6.5.1	Generation of a plasmid for cardiac-specific expression of WD3	74
6.5.2	Establishment of a transgenic mouse model	75
6.5.3	Genotyping of transgenic animals by PCR	75
6.5.4	The GRK2-inhibitory peptide shows a cardioprotective effect <i>in vivo</i>	76
7	DISCUSSION	77
7.1	Identification of a GRK2-interacting peptide	78
7.1.1	Protein expression and purification of GRK2-domains	78
7.1.2	A phage display library screen identifies several peptides	78
7.1.3	A protein database search was performed for the peptides	79
7.1.4	Sequence elongation of the peptide sequence ASTLIVF	81
7.1.5	A GRK2-interacting peptide is identified by ELISA	81
7.2	The GRK2-interacting peptide shows GRK2-inhibitory features <i>in vitro</i>	82
7.2.1	The GRK2-inhibitory peptide interferes with the Gβ-GRK2CTD interaction	82
7.2.2	The GRK2-inhibitory peptide inhibits GRK2 activity in an <i>in vitro</i> phosphorylation assay	83
7.2.3	The GRK2-inhibitory peptide inhibits desensitization of the GPCR B2R	84

7.3	The GRK2-interacting peptide WD3 shows GRK2-inhibitory features <i>in vivo</i>	85
7.4	Evaluation of the GRK2-inhibitory peptide	85
7.4.1	Potency and selectivity	85
7.4.2	Mechanism of action	86
7.4.3	Safety of GRK2-inhibition	86
7.5	Outlook	87
7.5.1	Further development of the prototype	87
7.5.2	Research Applications	87
8	CONCLUSION	89
9	ACKNOWLEDGMENTS	90
10	CURRICULUM VITAE	91
11	PUBLICATIONS	92
12	REFERENCES	93
13	APPENDIX	119
13.1	Sequencing of GRK2NTD6xCHis	119
13.2	Sequencing of 6xNHisGRK2KD	120
13.3	Sequencing of GRK2KD6xCHis	121
13.4	Sequencing of 6xNHisGRK2CTD	122
13.5	Sequencing of GRK2CTD6xCHis	123
13.6	Sequencing of pcDNA3WD1	124
13.7	Sequencing of pcDNA3WD2	125
13.8	Sequencing of pcDNA3WD3	125
13.9	Sequencing of pMHCWD3	126

1 Summary

G protein-coupled receptor (GPCR) kinases (GRKs) are most prominently known for phosphorylating agonist-occupied receptors resulting in signal attenuation.

GRK2, the most thoroughly investigated GRK isoform, is recognized as a potential drug target for disorders such as heart failure and hypertension. However, efforts to find a GRK2-inhibitor have been futile.

The ubiquitously expressed GRK2 displays a tri-domain structure with the central kinase domain harbouring the enzyme active site, flanked by an amino terminal domain mediating receptor recognition and a carboxyl terminal domain (GRK2CTD) involved in localization to the plasma membrane. More specifically, G β γ -interaction with GRK2CTD is required for kinase translocation to the plasma membrane towards receptor substrates. Blocking of this interaction with β ARKct, a G β γ -scavenging peptide derived from the carboxyl terminal domain of GRK2, successfully inhibits GRK2 activity and prevents heart failure development in animal models. Moreover, interfering with G β γ binding of GRK2 confers subtype-specificity, because membrane localization of other GRK isoforms employs different mechanisms. In a similar manner, compounds specifically interacting with GRK2CTD would be expected to block GRK2 function. Nevertheless, such an approach, to our knowledge, was not investigated to date.

Therefore, in this study, a peptide phage display library screen was used as an approach towards finding of GRK2 domain-specific interaction partners. Specifically, the focus was to identify peptides that interact with GRK2CTD. The peptides' inhibitory features were subsequently characterized in different *in vitro* assays and *in vivo*.

The three GRK2 domains were purified individually from bacterial cultures. In a next step, GRK2CTD was used as bait in a peptide phage display library screen, which yielded the following 7-mer peptide sequences: ASTLIVF, IRYVPQT, HGGVRLY, HYTDFRW, IVSLQTP, and HYIDFRW.

To investigate sequence homology with known proteins, a protein data base search was performed. Peptide sequence IVSLQTP is partially contained in the nuclear-factor of activated T-cells and peptide ASTLIVF shares sequence identity with the WD repeat-containing protein 76 (WDR76). WDR76 is structurally related to G β γ , another WD repeat-containing protein and, as mentioned before, a known GRK2 interaction and activation partner. Based on WDR76, the original peptide sequence (ASTLIVF) was elongated carboxyl (WD1) and amino (WD3) terminally. WD1 and WD3 were used for further experiments.

For WD3, the interaction with GRK2CTD could be confirmed by ELISA technique, whereas WD1 did not significantly interact with GRK2CTD.

To study the effect of WD1 and WD3 on the G β γ -GRK2CTD interaction essential for kinase activity, an inhibition ELISA with recombinant G β 3 purified from bacterial culture and GRK2CTD was established. In this assay, WD3 successfully blocked the G β 3-GRK2CTD protein-protein interaction. In contrast, WD1 did not interfere with the binding of GRK2CTD to G β 3.

In addition to its role in receptor phosphorylation and subsequent desensitization, GRK2 also phosphorylates a number of cytosolic non-receptor substrates.

To investigate, whether WD1 and WD3 influence GRK2 kinase activity, an *in vitro* phosphorylation assay using a soluble substrate of GRK2 was performed. WD3 reduced GRK2-mediated phosphorylation of this non-receptor substrate, whereas WD1 did not display any inhibitory effect.

The impact of WD1 and WD3 on desensitization of the GPCR bradykinin receptor type 2 was assessed *in vitro* in HEK cells. Additionally, another peptide (WD2), which was elongated based on the original peptide sequence both amino and carboxyl terminally, was tested. Only WD3 increased bradykinin-stimulated calcium signalling, indicating reduced GRK2-mediated receptor desensitization.

To further investigate the properties of WD3 *in vivo*, a transgenic mouse model with cardiac-specific expression was established. In a pressure overload model of cardiac dysfunction, WD3 retarded signs of heart failure *in vivo*.

Taken together, modification of a phage display-derived peptide yielded a peptide prototype with GRK2-inhibitory features *in vitro* and *in vivo*. By employing a novel strategy to GRK2-inhibition, it could serve as a lead structure for further development into a candidate drug compound.

2 Zusammenfassung

G-protein-gekoppelte Rezeptorkinasen (GRKs) phosphorylieren und regulieren dadurch aktivierte G-protein-gekoppelte Rezeptoren (GPCRs), was zu einer Signaldämpfung führt. GRK2, die am besten untersuchte GRK-Isoform, gilt als ein möglicher Angriffspunkt für die Behandlung von Krankheiten wie Herzinsuffizienz und Hypertonie. Trotz grosser Bemühungen zur Entwicklung von Inhibitoren konnte bis heute keine Substanz erfolgreich in der Klinik etabliert werden.

Die ubiquitär exprimierte GRK2 besteht aus drei Domänen mit unterschiedlichen Funktionen: der zentralen Kinasedomäne, welche das aktive Zentrum beherbergt; der aminoterminalen Domäne, welche Rezeptorsubstrate erkennt und bindet; und der carboxylterminalen Domäne (GRK2CTD), durch welche der Transport der Kinase zur Plasmamembran vermittelt wird. Eine Voraussetzung für diesen Schritt sowie die Aktivierung des Enzyms ist die Interaktion mit $G\beta\gamma$. Wird diese durch β ARKct, einem von der GRK2CTD abgeleitetem $G\beta\gamma$ -Scavengerpeptid, gestört, inhibiert dies die Aktivität von GRK2 und vermag das Auftreten von Herzinsuffizienz im Tiermodell zu verhindern. Da die übrigen GRK-Isoformen mittels alternativer Mechanismen zur Plasmamembran gelangen, ermöglicht die gezielte Störung der $G\beta\gamma$ -GRK2CTD-Bindung eine subtypspezifische Inhibierung. Analog dazu wird erwartet, dass Substanzen, welche selektiv mit der GRK2CTD interagieren, die Kinaseaktivität vermindern. Ein solcher Ansatz wurde jedoch nach unserem Wissen bisher noch nicht untersucht.

Zunächst wurden die drei GRK2-Domänen einzeln aus Bakterienkulturen aufgereinigt. In einem nächsten Schritt wurde ein Phagen-Display mit einer Peptidbibliothek durchgeführt. Dabei wurde GRK2CTD als Zielmolekül verwendet. Es wurden die folgenden, jeweils sieben Aminosäuren enthaltenden Sequenzen gefunden: ASTLIVF, IRYVPQT, HGGVRLY, HYTDFRW, IVSLQTP und HYIDFRW.

Mit den gefundenen Peptidsequenzen wurde eine Proteindatenbank durchsucht, um allfällige Homologien mit bekannten Proteinen zu erkennen. Dabei wurde eine teilweise Übereinstimmung der Peptidsequenz IVSLQTP mit NFAT, dem nuclear factor of activated T-cells, gefunden. Des Weiteren ist die Peptidsequenz ASTLIVF auch in WDR76, dem WD repeat-containing protein 76, enthalten. WDR76 weist eine ähnliche Struktur wie $G\beta\gamma$ auf, welches ebenfalls ein WD repeat-containing protein ist. Ausserdem ist $G\beta\gamma$, wie bereits erwähnt, verantwortlich für die Aktivierung von GRK2 und den Transport zur Plasmamembran in Richtung Rezeptorsubstrate. Deshalb wurde das ursprüngliche Peptid basierend auf der Proteinsequenz von WDR76 in Richtung Carboxylterminus (WD1) und Aminoterninus (WD3) verlängert. Die Peptide WD1 und WD3 wurden im Folgenden für weitere Experimente verwendet.

Für WD3 konnte die Interaktion mit der GRK2CTD mittels ELISA bestätigt werden, wo hingegen WD1 nicht signifikant mit der GRK2CTD interagiert.

Daraufhin wurde ein Inhibierungs-ELISA mit aus Bakterienkulturen aufgereinigtem G β 3 sowie GRK2CTD durchgeführt, um den Effekt der beiden Peptide WD1 und WD3 auf die G β γ -GRK2CTD-Interaktion zu untersuchen. Dabei konnte WD3 die G β 3-GRK2CTD Protein-Protein-Interaktion empfindlich stören. Im Gegensatz dazu beeinflusste WD1 die Bindung von GRK2CTD zu G β 3 nicht.

Neben der Phosphorylierung und Desensibilisierung von Rezeptoren kann GRK2 auch eine Reihe von zytosolischen Nichtrezeptorsubstraten phosphorylieren.

Ein solch lösliches Substrat wurde in einer *in vitro* Phosphorylierungsreaktion eingesetzt mit dem Ziel, den Effekt von WD1 und WD3 auf die Kinaseaktivität von GRK2 zu untersuchen. Dabei vermochte WD3 die GRK2-vermittelte Phosphorylierung dieses Nichtrezeptorsubstrates zu verhindern, während WD1 keinen Effekt zeigte.

Der Einfluss von WD1 und WD3 auf die Desensibilisierung eines G-protein-gekoppelten Rezeptors, d.h. des Bradykininrezeptors Typ 2, wurde *in vitro* in HEK-Zellen untersucht. Zusätzlich wurde ein weiteres Peptid (WD2) getestet, welches basierend auf der ursprünglichen Peptidsequenz in Richtung Amino- und Carboxylterminus verlängert worden war. Ausschliesslich WD3 erhöhte das Bradykinin-stimulierte Kalziumsignal, was auf eine reduzierte GRK2-vermittelte Rezeptordesensibilisierung hinweist.

Um die Eigenschaften von WD3 weiter *in vivo* zu untersuchen, wurde ein transgenes Mausmodell, welches die WD3-Peptidsequenz spezifisch im Herzen exprimiert, etabliert. WD3 verzögerte im Mausmodell das Auftreten von Herzinsuffizienzzeichen in einer durch chronische Hypertonie erzeugten kardialen Hypertrophie.

Zusammenfassend wird in dieser Arbeit eine modifizierte Version eines von einem Phagen-Display stammenden Peptids vorgestellt. Dieser Peptidprototyp zeigt *in vitro* und *in vivo* GRK2-inhibierende Eigenschaften. Dabei könnte insbesondere die Anwendung einer neuartigen Strategie, um GRK2 zu inhibieren, bedeuten, dass dieser Prototyp als Ausgangsstruktur zur Entwicklung eines Medikaments dienen könnte.

3 Abbreviations

6xHis	hexahistidine-tag/His-tag
7TM	seven-transmembrane
A	adenine
AAC	abdominal aortic constriction
ABTS	2,2'-azino-bis(3-ethylbenzothiazoline-6-sulphonic acid)
AGC	family of protein kinases A, G and C
APS	ammonium persulfate
AT1R	angiotensin II type-1 receptor
ATP	adenosine triphosphate
B2R	bradykinin receptor B2
BBS	BES-buffered saline
BES	<i>N,N</i> -bis[2-hydroxyethyl]-2-aminoethanesulfonic acid
βAR	β-adrenergic receptor
βARKct	amino acids 495-689 of GRK2
βARKnt	amino acids 1-14 of GRK2
βarr	β-arrestin
BLAST	Basic local alignment search tool
BSA	bovine serum albumin
C	cytosine (DNA) / carboxyl (amino acids)
CAMKIIδ	Ca ²⁺ /calmodulin-dependent kinase IIδ
cAMP	3',5'-cyclic adenosine monophosphate
cDNA	complementary DNA
DAG	diacylglycerol
DMEM	Dulbecco's modified eagle's medium
DMF	<i>N,N</i> -dimethyl formamide
DMSO	dimethyl sulfoxide
DNA	deoxyribonucleic acid
dNTPs	deoxynucleotides
ds	double-stranded
ECL	enhanced chemoluminescence
<i>E.coli</i>	<i>Escherichia coli</i>
EDTA	ethylenediaminetetraacetic acid
ELISA	enzyme-linked immunosorbent assay
eNOS	endothelial nitric oxide synthase
ERK	extracellular signal-regulated kinase
FBS	foetal bovine serum
Fura-2AM	Fura-2-acetoxymethyl ester
G	guanine

G protein	guanine nucleotide-binding protein
G418	Geneticin
GAP	GTPase-activating protein
G α	α -subunit of the heterotrimeric G protein
G β	β -subunit of the heterotrimeric G protein
G β 3	G protein subunit β -3, isoform 1
G β 3-s	G protein subunit β -3, isoform 2
G $\beta\gamma$	$\beta\gamma$ -complex of the heterotrimeric G protein
GDP	guanosine diphosphate
GEF	guanine nucleotide exchange factor
GIRK	G protein-gated inwardly rectifying potassium channel
GPCR	G protein-coupled receptor
GRAFS	glutamate, rhodopsin, adhesion, frizzled/taste2, secretin
GRK	G protein-coupled receptor kinase
GRK2CTD	carboxyl terminal domain of GRK2 (amino acids 454-689)
GRK2KD	kinase domain of GRK2 (amino acids 191-453)
GRK2NTD	amino terminal domain of GRK2 (amino acids 1-190)
GTP	guanosine triphosphate
GTPase	GTP-hydrolysing enzyme
HEK293A	cell line derived from human embryonic kidney cells
HEPES	4-(2-hydroxyethyl)-1-piperazineethanesulfonic acid
HRP	horseradish peroxidase
IP ₃	inositol-1,4,5-triphosphate
IPTG	isopropyl β -D-1-thiogalactopyranoside
I κ B α	nuclear factor of kappa light polypeptide gene enhancer in B-cells inhibitor, α
<i>lac</i>	lactose
LB	lysogeny broth
LDS	lithium dodecyl sulphate
mAB	monoclonal antibody
MAPK	mitogen-activated protein kinase
MEK	mitogen-activated protein kinase kinase
MHC	myosin heavy chain
miRNA	micro ribonucleic acid
MOPS	3-(<i>N</i> -morpholino)propanesulfonic acid
N	amino
NES	nuclear export signal
Ni-NTA	nickel-nitrilotriacetic acid
NLS	nuclear localization signal
NO	nitric oxide

OD	optical density
PAGE	polyacrylamide gel electrophoresis
PBS	phosphate buffered saline
PBST	PBS-Tween
PCR	polymerase chain reaction
PDC	phosducin
PEBP	phosphatidylethanolamine-binding protein
PEG	polyethylene glycol
Pfu	<i>Pyrococcus furiosus</i>
pfu	plaque forming units
PH	pleckstrin homology
pl	isoelectric point
PIP ₂	phosphatidylinositol-4,5-biphosphate
PKA	protein kinase A/cAMP-dependent protein kinase
PKC	protein kinase C
PLB	phospholamban
PLC β	β -isoform of phospholipase C
PMSF	phenylmethylsulfonyl fluoride
PPI	protein-protein interaction
PVDF	polyvinylidene difluoride
RAAS	renin-angiotensin-aldosterone system
RACK1	receptor for activated C kinase 1
RGS	regulator of G protein signalling
RH	regulator of G protein signalling homology
RhoGEF	Rho guanine nucleotide exchange factor
RKIP	Raf-1 kinase inhibitor protein
RS	arginine/serine
RT	room temperature (25 °C)
SDS	sodium dodecyl sulphate
SEM	standard error of the mean
Sf9	<i>Spodoptera frugiperda</i>
SIGK	SIGKAFKILGYPDYD
SIRK	SIRKALNILGYPDYD
SOB	super optimal broth
SOC	super optimal broth with catabolite repression
SRSF1	serine/arginine-rich splicing factor 1
ss	single-stranded
SSRI	selective serotonin reuptake inhibitor
T	thymine
TAE	Tris, acetic acid, EDTA

Taq	<i>Thermus aquaticus</i>
TBE	Tris, boric acid, EDTA
TBS	Tris-buffered saline
TBST	TBS-Tween
TE	Tris, EDTA
TEMED	tetramethylethylenediamine
Tris	Tris(hydroxymethyl) amino methane
TSB	transformation and storage buffer
WD	Tryptophan-Aspartic acid
WD1	ASTLIVGHWDGNMSLVDRRT
WD2	FLAEDASTLIVGHWDGNMSL
WD3	ERSSFSSFDLAEDASTLIVF
WDR	WD repeat-containing protein
WDR76	human WD repeat-containing protein 76
x-gal	5-bromo-4-chloro-3-indolyl- β -D-galactopyranoside

List of Figures

Figure 1: Agonist-binding of a GPCR initiates a downstream signalling network	11
Figure 2: Megaplex consisting of a GPCR simultaneously binding a G protein and β -arrestin	14
Figure 3: Arrestins adopt multiple functions	15
Figure 4: Structural characteristics of GRK isoforms	17
Figure 5: Domain-specific inhibition of GRK2	23
Figure 6: Schematic drawing of a phage display library screen	31
Figure 7: Vector map of pET-3d	38
Figure 8: Vector map of pcDNA3	40
Figure 9: Protein overexpression with the pET expression system	41
Figure 10: GRK2 is an enzyme with multiple domains	56
Figure 11: Cloning of C-terminally His-tagged GRK2NTD into pET-3d	57
Figure 12: Cloning of N-terminally (A) and C-terminally (B) His-tagged GRK2KD into pET-3d.....	57
Figure 13: Cloning of N-terminally (A) and C-terminally (B) His-tagged GRK2CTD into pET-3d.....	58
Figure 14: Protein expression of GRK2NTD6xCHis	59
Figure 15: GRK2NTD6xCHis was purified by Ni-NTA chromatography	60
Figure 16: GRK2KD was purified by Ni-NTA chromatography	61
Figure 17: Protein expression of GRK2CTD	62
Figure 18: GRK2CTD was purified by Ni-NTA chromatography	63
Figure 19: Evaluation of binding by a phage ELISA	64
Figure 20: Model of the crystal structure of GRK2 in complex with $G\beta\gamma$	66
Figure 21: GRK2CTD shows selective binding to WD3 in an ELISA	68
Figure 22: GRK2CTD binds $G\beta 3$ and $G\beta 3$ -s	69
Figure 23: WD3 interferes with the binding of GRK2CTD to $G\beta 3$ and $G\beta 3$ -s.....	70
Figure 24: WD3 inhibits the phosphorylation of SRSF1 by GRK2	71
Figure 25: An ELISA shows binding of SRSF1 to GRK2	72
Figure 26: WD3 sensitizes the bradykinin-stimulated Ca^{2+} signal of endogenously expressed B2R.....	74
Figure 27: Generation of a plasmid coding for WD3 under the control of the α -myosin heavy chain (α -MHC) promoter.....	75
Figure 28: Identification of the α -MHCWD3 transgene in the genomic DNA by PCR....	75
Figure 29: WD3 shows a cardioprotective effect in a pressure overload mouse model	76
Figure 30: Sequence and structure of WD repeat-containing proteins	80

4 Introduction

4.1 G protein-coupled receptor signalling

4.1.1 Characteristics of G protein-coupled receptors

The family of G protein-coupled receptors (GPCRs) comprises the largest and most diverse group of membrane receptors in the mammalian genome. Over 800 human genes encode these structurally highly conserved proteins with paramount importance in the field of pharmacotherapy (1,2).

Originally named for their interaction with heterotrimeric guanine nucleotide-binding proteins (G proteins), they are also known as seven-transmembrane (7TM) receptors owing to their unique characteristic motif of seven membrane-spanning α -helices. Other features include an N-terminal extracellular domain, a C-terminal intracellular tail, and loops on both sides of the cell membrane connecting the transmembrane helices (3,4). Understanding of GPCR functionality has tremendously increased with the availability of the first high-resolution crystal structure of rhodopsin in 2000 (5). In the last five years, the number of GPCR crystal structures has increased and more importantly, some receptors are available in multiple conformations (6).

The GRAFS classification system divides GPCRs based on sequence similarities into five families: glutamate, rhodopsin, adhesion, frizzled/taste2, secretin. The rhodopsin family is by far the largest family including around 700 receptors and can be classed into subgroups (α - δ) (7).

GPCRs activate a complex downstream signalling network

GPCRs take a prominent role in transmembrane signal transduction pathways and hence are involved in almost all physiological processes (8,9). They react to a variety of extracellular stimuli such as photons, peptides, proteins, small organic molecules, amino acids and ions (10).

According to the classical concept, the receptors elicit their diverse physiological functions upon stimulation by initiation of a signalling cascade involving heterotrimeric G proteins, second messenger molecules and a variety of effector proteins (11-13).

In recent years, growing evidence for arrestin-mediated G protein-independent signalling pathways has emerged. Classically, arrestins promote G protein-uncoupling following receptor phosphorylation by a G protein-coupled receptor kinase (homologous desensitization) (14). However, non-canonical functions for arrestins in scaffolding signal complexes initiating functions distinct from G protein-dependent processes have increasingly come into focus (15-17).

This led to a paradigm shift towards an extended model of more complex intracellular signalling networks initiated by 7TM receptors (Figure 1).

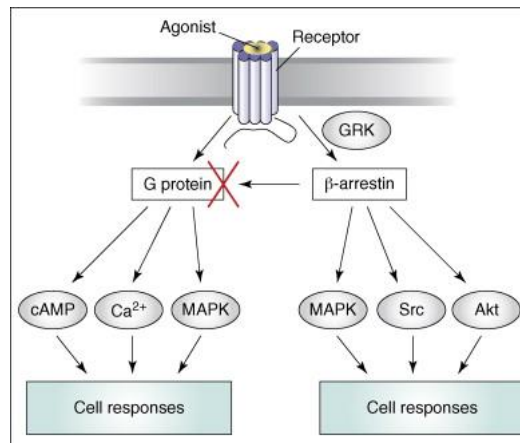


Figure 1: Agonist-binding of a GPCR initiates a downstream signalling network

Following agonist binding, GPCRs may activate G protein-dependent or β -arrestin-dependent (G protein-independent) pathways. Binding of β -arrestins to GPCRs phosphorylated by GRKs attenuates G protein-signalling (18).

4.1.2 Heterotrimeric G proteins are classical signal transducers

Heterotrimeric G proteins transmit receptor activation to intracellular second messengers (12). Mammalian heterotrimeric G proteins consist of three distinct subunits encoded by gene families: 21 α -subunits ($G\alpha$, 39-52 kDa) encoded by 16 genes, 6 β -subunits ($G\beta$, 36 kDa) encoded by 5 genes and 12 γ -subunits ($G\gamma$, 7-8 kDa) encoded by 12 genes (19). $G\alpha$, in its inactive state, is bound to GDP and forms a heterotrimer with $G\beta\gamma$. Upon ligand binding, the GPCR undergoes a conformational change and couples to the G protein. As guanine nucleotide exchange factors (GEF), GPCRs induce $G\alpha$ to exchange GDP for GTP, thereby activating it. The activated $G\alpha\cdot$ GTP then dissociates from $G\beta\gamma$. Both, $G\alpha\cdot$ GTP and $G\beta\gamma$ are thus free to interact with downstream effectors. Signal termination occurs through GTP-hydrolysis facilitated by the intrinsic GTPase activity of $G\alpha$ (11,20). Further, the family of regulator of G protein signalling (RGS) proteins were found to promote GTPase activity (21). Inactivation of $G\alpha$ enables re-association with $G\beta\gamma$ and thus prepares the G protein for a new cycle of activation (11,13).

4.1.2.1 The α -subunit of heterotrimeric G proteins

Based on sequence similarities, $G\alpha$ subunits have been divided into four canonical families: $G\alpha_s$, $G\alpha_{i/o}$, $G\alpha_{q/11}$ and $G\alpha_{12/13}$. The different subtypes display receptor specificity and a distinct pattern of effector activation (22).

Effectors of $G\alpha_s$

$G\alpha_s$ subunits stimulate adenylyl cyclase to convert adenosine triphosphate (ATP) to 3', 5'-cyclic adenosine monophosphate (cAMP) (23), a second messenger activating

protein kinase A (PKA) (24). This serine/threonine kinase, which belongs to the family of AGC kinases (protein kinases A, G and C), regulates a variety of physiological functions by direct activation of proteins by phosphorylation or alteration of gene transcription (25,26).

Effectors of $G\alpha_{i/o}$

Classically, $G\alpha_{i/o}$ subunits inhibit adenylyl cyclase, thus decreasing intracellular cAMP levels and reducing PKA activation (12,27).

Effectors of $G\alpha_{q/11}$ -subunits

$G\alpha_{q/11}$ activates the β -isoform of phospholipase C ($PLC\beta$), which converts phosphatidylinositol-4,5-biphosphate (PIP_2) into inositol-1,4,5-triphosphate (IP_3) and diacylglycerol (DAG). These second messengers increase intracellular Ca^{2+} by stimulating calcium release from the endoplasmic reticulum. DAG activates protein kinase C (PKC) (28,29).

In addition, $G\alpha_{q/11}$ directly interacts with G protein-coupled receptor kinase 2 (GRK2, originally named β -adrenergic receptor kinase (β ARK)). Via its N-terminal regulator of G protein signalling (RGS) homology (RH) domain, GRK2 rapidly inactivates $G\alpha_{q/11}$ in a phosphorylation-independent manner (30-32).

Effectors of $G\alpha_{12/13}$

The most recently discovered family of $G\alpha$ subunits ($G\alpha_{12/13}$) activates RhoGTPase nucleotide exchange factors (RhoGEF), which in turn promote nucleotide exchange on the small GTPase RhoA (33,34).

4.1.2.2 The $\beta\gamma$ -complex of heterotrimeric G proteins

The β - and γ -subunits of the heterotrimeric G protein act as a functional unit and co-expression is required for proper folding (35). $G\beta$ is a WD repeat-containing protein displaying a characteristic seven-bladed β -propeller-structure (36). $G\gamma$ conveys membrane attachment through isoprenylation at a C-terminal cysteine residue (35).

Downstream effectors of the $G\beta\gamma$ complex

Once dissociated from the $G\alpha$ subunit, $G\beta\gamma$ is free to interact with a variety of downstream effectors (37).

Kinases

In canonical GPCR signalling, $G\beta\gamma$ plays a pivotal role by activating and recruiting GRK2/3 to the plasma membrane, eventually promoting receptor desensitization and downregulation (38). Furthermore, $G\alpha_i$ -derived $G\beta\gamma$ can activate the mitogen-activated protein kinase (MAPK) pathway, which in turn is involved in cell cycle control (39,40).

Ion homeostasis

Additionally, Gβγ is involved in intracellular ion homeostasis by modulating the activity of a number of ion channels. It was found to modulate voltage-dependent N- and P/Q-type Ca²⁺-channels in neurons (41,42). Moreover, Gβγ is able to activate the G protein-gated inwardly rectifying potassium channel (GIRK) directly (43). Gβγ also stimulates PLCβ to release calcium from the endoplasmic reticulum (37).

Furthermore, Gβγ is involved in the regulation of adenylyl cyclase showing diverse effects depending on the isoforms (37,44).

4.1.2.3 Coupling specificity of GPCRs

Receptors are known to couple preferentially to specific Gα-subunits, thus eliciting a distinct cellular response. But it is also known that certain receptors are able to couple to multiple G proteins from different subclasses, simultaneously or successively (45).

In the case of the β-adrenergic receptor type 2 (β2AR), switching from canonical coupling to Gα_s to Gα_i is mediated by receptor phosphorylation through the second messenger-dependent kinase PKA (46).

4.1.3 Arrestins are mediators of GPCR signalling and desensitization

The family of arrestins consists of four members: the visual arrestins (arrestin-1 and arrestin-4) expressed in the retina (47,48), and the ubiquitously expressed arrestin-2 and -3 (β-arrestin 1 and 2) (49). β-arrestins were first described for dampening the β2-adrenergic response following agonist stimulation (50). The ~ 48-kDa proteins share ~70% sequence identity, but display distinct, albeit overlapping physiological roles (48,51).

Originally known for their role in “arresting” (52) GPCR signalling following phosphorylation by GRKs (14), arrestins are now increasingly recognized for also promoting G protein-independent receptor signal transduction (53,54).

4.1.3.1 Arrestins are signal transducers

A role for β-arrestins in GPCR signal transduction was first proposed for the stimulation of the mitogen-activated protein kinase (MAPK) pathway via activation of the non-receptor protein tyrosine kinase (Src) (15). Moreover, β-arrestin 2 was demonstrated to act as a scaffolding protein in the formation of stable signalling complexes containing the angiotensin II type-1 receptor (AT1R) and each of the component kinases of the extracellular signal-regulated kinase MAPK/ERK pathway (16). In addition, β-arrestins were found to be key players in endothelial growth factor receptor (EGFR) transactivation following agonist-stimulation of the β-adrenergic receptor type 1 (β1AR) (55).

Interestingly, arrestin-dependent receptor signalling is both spatially and temporally distinct from G protein-dependent signal transduction. Whereas e.g. G protein-dependent ERK1/2 activation is rapid, but transient and results in nuclear translocation of the kinase, β -arrestin-dependent ERK1/2 activation is slower, more persistent and often restricted to the cytosol (56). Thus, a time-course of a “first wave” of G protein-dependent signalling followed by a “second wave” of β -arrestin-dependent signalling could be established (56). Intriguingly, persisting β -arrestin-dependent signalling even after dissociation from the activating receptor could be demonstrated (57).

Recent data showing sustained G protein-dependent signalling by internalized GPCRs (58-61), however, challenges this model of G protein-dependent signalling switching to β -arrestin-dependent pathways. Only this year, Lefkowitz and co-workers proposed the formation of “megaplexes” composed of a single GPCR, β -arrestin and G protein (Figure 2). Simultaneous interaction of a GPCR with β -arrestin and G protein offers a possible explanation for the observation of sustained G protein-signalling after receptor internalization (62).

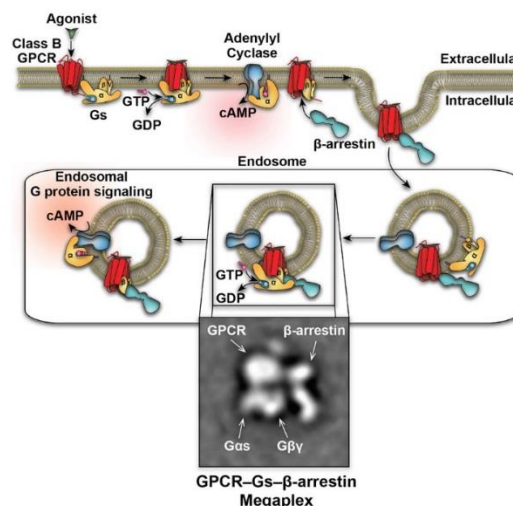


Figure 2: Megaplex consisting of a GPCR simultaneously binding a G protein and β -arrestin

Sustained G protein-signalling from within endosomes is explained by the formation of “megaplexes” containing a β 2V2R receptor chimera (i.e. a β 2AR (“class A” receptor) where the C-terminal tail was exchanged for the vasopressin type 2 receptor (“class B” receptor)) simultaneously engaged with a G protein and β -arrestin (62).

The formation of such “megaplexes” requires β -arrestin to interact with the receptor C-terminal tail rather than the core region, as the transmembrane core is occupied by the G protein (62). This “tail” conformation relies on a strong interaction of the receptor’s C-terminal tail with β -arrestin (62,63), which has been reported for “class B” GPCRs (e.g. AT1R) (64). “Class A” GPCRs (e.g. β 2AR), in contrast, lack the C-terminal

serine/threonine clusters necessary for the formation of a stable complex with β -arrestin and thus generally bind β -arrestins only transiently resulting in rapid recycling of receptors (65). Thus, the β -arrestin-GPCR interaction pattern confers a β -arrestin conformational signature (66), which in turn is linked to β -arrestin function.

4.1.3.2 Arrestins mediate GPCR sequestration

β -arrestins do not only act as scaffolding proteins in assembling signal complexes (16), but also with regard to the components of the endocytic machinery (67). Thus, they are critically involved in receptor sequestration following agonist-stimulation (Figure 3): (i) After phosphorylation by GRKs, arrestins bind to receptors leading to sterical uncoupling of receptors from their cognate G proteins and signal termination, i.e. desensitization of the receptors (14,50,68,69). (ii) Further, arrestin-binding may promote receptor internalization via clathrin-coated pits (67,70) or alternative pathways (71), eventually resulting in receptor degradation and downregulation (72). (iii) Alternatively, packing of receptors into endocytic vesicles can also be the first step in a recycling process back to the plasma membrane (resensitization) (73-75).

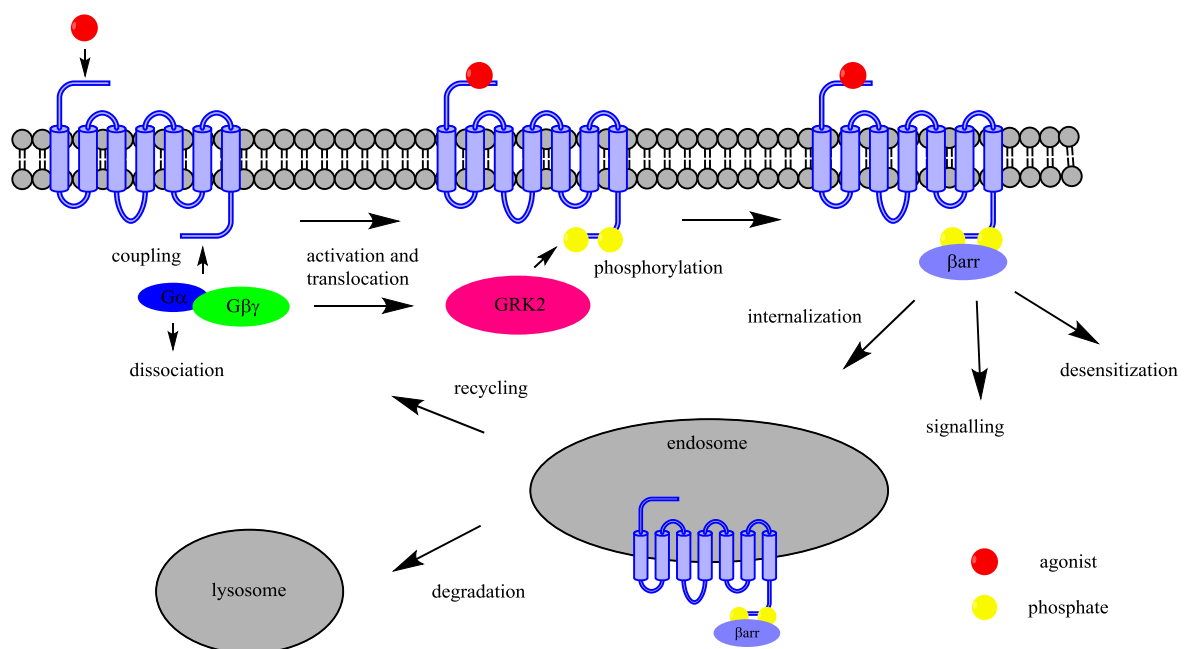


Figure 3: Arrestins adopt multiple functions

Canonical GPCR signalling involves activation of G proteins, which in turn activate distinct downstream effectors. Following phosphorylation of agonist-occupied receptors by GRKs, β -arrestin binds, which may lead to: (i) receptor desensitization through sterical uncoupling of G proteins, (ii) β -arrestin-dependent signalling events, (iii) internalization with subsequent recycling back to the plasma membrane, or lysosomal degradation. (adapted from (76) and (77)); abbreviation: β arr, β -arrestin

4.1.4 GPCR biased signalling

Whether β -arrestin predominantly partakes in signal activation or termination is linked to the conformational change induced upon receptor binding (66). Moreover, ligands may display bias by stabilizing receptor conformations (biased agonism), which favour activation of G protein-dependent or β -arrestin-dependent signalling pathways, as demonstrated for the β -blocking agent carvedilol, which blocks G protein-dependent signalling while stimulating β -arrestin-dependent activation of the MAPK pathway (78). Efforts towards therapeutic exploitation of biased agonism yielded a β -arrestin biased ligand (TRV120027) for AT1R, which promotes cardiac contractility and survival, while at the same time blocking deleterious hypertrophic signalling (79,80).

Furthermore, a role for GRKs in governing these distinct signalling patterns was suggested (81).

4.2 Physiological roles of G protein-coupled receptor kinases

G protein-coupled receptor kinases (GRK) are a family of AGC serine/threonine kinases (82), best known for orchestrating, in cooperation with arrestins, GPCR desensitization (83). They can be grouped into three subfamilies based on sequence similarities: the visual subfamily (GRK1, GRK7), the β ARK subfamily (GRK2, GRK3) named originally for their role in the regulation of β AR signalling and the GRK4 subfamily (GRK4-6) (84). Members of the visual subfamily of GRKs are solely expressed in rod and cone photoreceptors in the retina. GRK4 is expressed in neurons, kidneys and testes, where protein levels are highest. The other four GRK isoforms (GRK2, GRK3, GRK5, GRK6) are ubiquitously expressed (85).

4.2.1 GRKs are multi-domain kinases

Crystal structures from all three GRK subfamilies have been solved, revealing common structural features (86-90) (Figure 4).

GRKs (~62-80 kDa) are multi-domain proteins with a conserved N-terminal region unique to the GRK family followed by a regulator of G protein signalling (RGS) homology domain (RH) (~120 amino acids). The N-terminal domain (~55 amino acids) is critically involved in promoting receptor interaction (91,92). The central kinase domain (~270 amino acids) contains the active site with the adenosine triphosphate (ATP)-binding cleft, tailed with a short AGC kinase sequence (90,93). GRK C-termini, although sharing a common function of mediating cellular localization and membrane association, are structurally highly diverse and of variable length (~105-230 amino acids) (94,95).

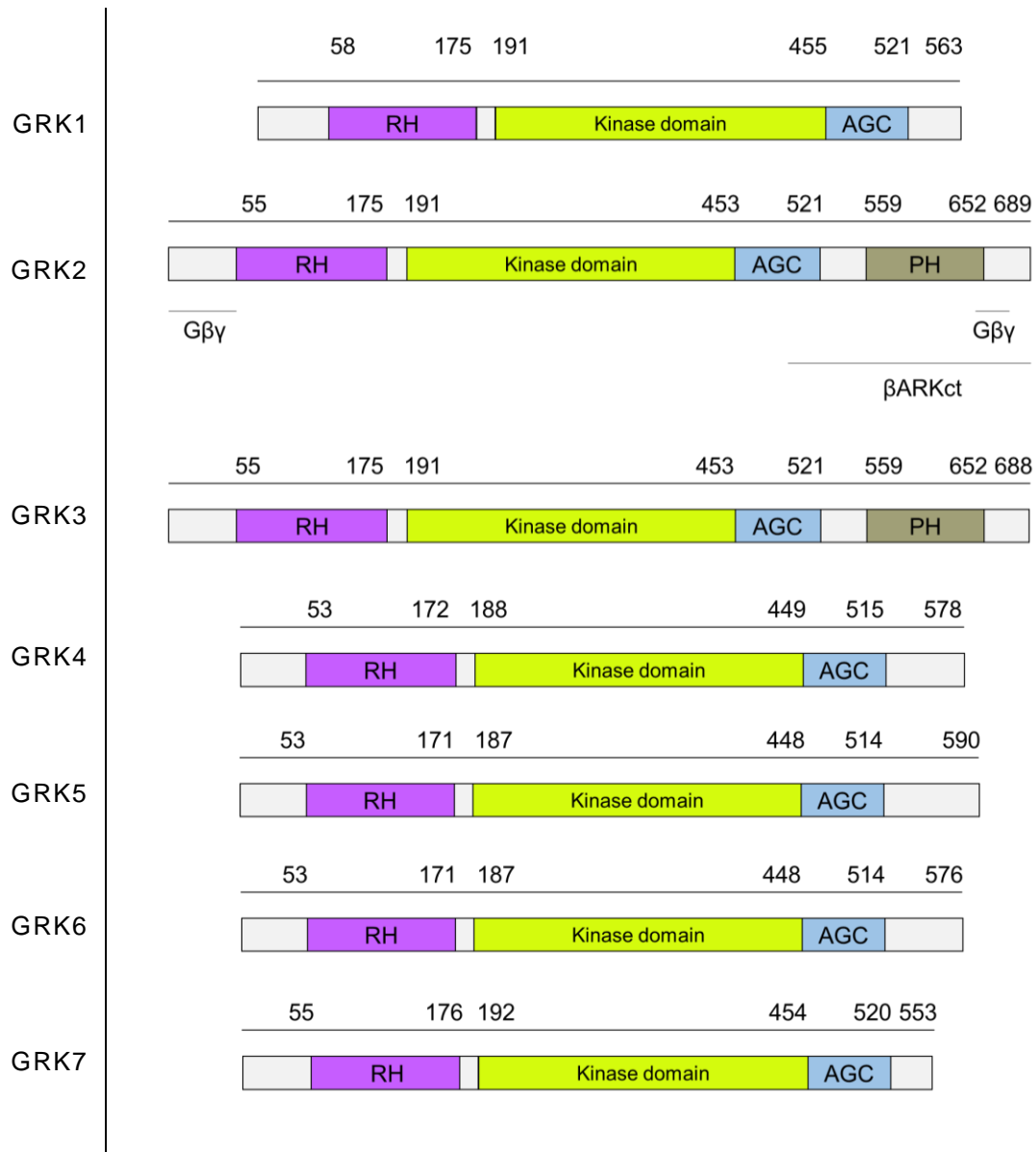


Figure 4: Structural characteristics of GRK isoforms

G protein-coupled receptors kinases are multi-domain proteins with structural variations between the different isoforms. (adapted from (96,97), includes information from the UniProt Knowledgebase); abbreviation: PH, pleckstrin homology

4.2.1.1 The visual subfamily

The visual GRKs are localized to the plasma membrane by lipid modifications. Whereas GRK1 is farnesylated, GRK7 is geranylgeranylated (98,99).

4.2.1.2 The βARK subfamily

The cytosolic proteins GRK2/3 contain a C-terminal pleckstrin homology (PH) domain enabling binding to Gβγ and subsequent membrane-translocation and PIP₂-binding (38,100-102). This mechanism of activation is unique to the βARK subfamily members

(103). Additionally, G $\beta\gamma$ contributes to GRK2 activity by interacting with its N-terminal domain (104). Furthermore, a role for membrane lipids in activating GRK2 was reported (105).

4.2.1.3 The GRK4 subfamily

The N-terminal domain of the GRK4 subfamily members has been shown to interact with PIP₂ thereby increasing the catalytic activity (101). GRK5 also binds to the plasma membrane via an amphipathic helix located in its C-terminal domain (106). Furthermore, GRK5 contains a nuclear localization signal (NLS) and a nuclear export signal (NES) (107). Post-translational C-terminal palmitoylation of GRK4 and GRK6 enhances lipid binding and localization to the plasma membrane (108,109).

4.2.2 GRKs are multifunctional proteins

GRKs are able to phosphorylate a number of both receptor and non-receptor substrates, and exert kinase-independent functions.

4.2.2.1 Receptor desensitization

GRKs were first described for playing a role in receptor desensitization by phosphorylating serine/threonine residues on the C-terminal tail and intracellular loops of agonist-occupied GPCRs (110,111). Phosphorylation subsequently promotes arrestin binding and G protein uncoupling by sterical hindrance, thus dampening G protein-dependent cellular responses (50,112). In addition to GRKs promoting homologous receptor desensitization, i.e. only activated agonist-occupied receptors are affected, second messenger-dependent protein kinases A (PKA) and C (PKC) are involved in heterologous desensitization, which is directed towards both inactive and active receptors (113,114).

It is noteworthy that only seven GRKs regulate over 800 GPCRs indicating that the kinases are highly promiscuous. Remarkably, GRKs may contribute to functional selectivity of receptors. The distinct phosphorylation patterns (“barcodes”) of GRK2/3 and GRK5/6 affect GPCR signalling (111). This barcode hypothesis is in line with data showing that GRK2-phosphorylation of β 2AR primarily leads to internalization, whereas phosphorylation by GRK6 favours the β -arrestin-mediated pathway of MAPK activation. At the same time, both GRKs contribute to receptor desensitization (115,116).

4.2.2.2 Phosphorylation of non-receptor substrates

On top of its role in regulating GPCR signalling via phosphorylation, GRK2 phosphorylates a number of cytosolic non-receptor substrates (85).

A linker role for GRK2 between GPCR activation and cytoskeletal remodelling has been suggested. GRK2 phosphorylates several members of the cytoskeleton, such as tubulin (117) or radixin (118) and ezrin (119) of the radixin/ezrin/moesin protein family.

Moreover, phosphocannin was reported as a substrate of GRK2 (120). Phosphocannin is a cytosolic protein known to interact with G $\beta\gamma$ and thereby may compete with GRK2 for G $\beta\gamma$ (121). Phosphorylation by GRK2 significantly diminishes this interaction (120).

Synucleins were also identified as GRK2-substrates, although the implications are not clear (122).

In macrophages, GRK2 was reported to mediate TNF α (tumour necrosis factor α)-induced NF- κ B (nuclear factor κ B)-dependent gene transcription by phosphorylation of I κ B α (inhibitory κ B) (123).

Moreover, GRK2 is able to phosphorylate and desensitize non-GPCR membrane receptors, as e.g. the platelet-derived growth factor receptor- β (PDGFR β) (124).

4.2.2.3 Kinase-independent functions of GRK2

GRK2 has been demonstrated to interact with G $\alpha_{q/11}$ via its N-terminal RH domain. Whereas GTPase activity is modest in comparison to other RGS proteins, G α sequestration bears a certain importance (30). Moreover, GRK2 may block G α_q -mediated activation of PLC β by competitive binding (30,125). The RH domain located in the N-terminal domain seems only to be active in the β ARK subfamily and shows specific GTPase-activating protein-activity exclusively towards G α_q (30,126).

In a similar fashion, GRK2, via its C-terminal PH domain, scavenges G $\beta\gamma$ thereby interfering with downstream effector functions (39). An additional G $\beta\gamma$ interaction site is located in the N-terminal domain of GRK2, which is also capable of interrupting G $\beta\gamma$ signalling (104).

Moreover, GRK2 is able to modulate receptor internalization in a kinase-independent manner by recruiting phosphoinositide 3-kinase (127) or the GRK-interacting protein GIT1 (128) to the plasma membrane. GRK2 also directly interacts with clathrin via its C-terminal domain (129).

4.3 Pathophysiological roles of GRK2

A pathophysiological role for GRK2 was first proposed for heart failure more than 20 years ago (130). The number of diseases connected to impaired GRK2 function has been increasing ever since (131).

4.3.1 Heart failure

Heart failure is a clinical syndrome defined by structural and/or functional abnormalities of the heart leading to reduced cardiac performance (132). In heart failure patients, GRK2

expression levels are upregulated and activity is heightened (130). GRK2 dysregulation is thought to be deleterious in several ways.

GRK2 upregulation leads to a state of chronic desensitization and consequently impaired β -adrenergic responsiveness (130). Moreover, the β 1/ β 2AR ratio of 80:20 in the healthy heart is changed to 60:40 in the failing heart due to selective downregulation of β 1AR (133,134). Although this change is considered adaptive, as β 2AR displays anti-apoptotic effects via $G\alpha_i$ -coupling, whereas $G\alpha_s$ signalling increases myocyte apoptosis (135).

In addition, under conditions of oxidative stress, ERK-mediated phosphorylation at Ser670 of GRK2 promotes the binding of the mitochondrial chaperone heat-shock protein 90 (Hsp90). This leads to mitochondrial accumulation of GRK2 and consequently the promotion of pro-death signalling (136).

GRK2 upregulation in the adrenal glands is involved in the desensitization of the α -adrenergic receptor type 2 (α 2AR)-mediated feedback inhibition of catecholamine release, which is thought to be deleterious to cardiac function. Hence, GRK2 contributes to the vicious cycle of enhanced activation of the sympathetic nervous system and chronic GPCR desensitization observed in heart failure (137).

Moreover, several studies point towards a beneficial role for GRK2-inhibition in heart failure.

Mice hemizygous for GRK2 gene ablation (GRK2^{+/-}) have 50% reduced GRK2 expression levels and present with a phenotype characterized by improved cardiac contractility and relaxation (138).

Moreover, GRK2-inhibition, subsequent normalization of β AR levels and resensitization of endogenous β AR signalling shows a cardioprotective effect in several animal models including a large animal model mimicking human physiology (139-141). Some of the beneficial effects observed under β -blocker treatment can be attributed to reduced sympathetic drive and consequential normalization of elevated GRK2 levels (142).

There is also support for a beneficial effect of GRK2-inhibition on the disturbed substrate metabolism in late-stage heart failure (143).

Intriguingly, myocardial GRK2 gene ablation after myocardial infarction was able to stop adverse remodelling (144).

Taken together, reduction of GRK2 activity in the heart is a well-studied approach to target the structural and physiological alterations, which accompany heart failure development.

4.3.2 Hypertension

A role for GRK2 in hypertension was suggested, because expression and activity of the kinase are enhanced in circulating lymphocytes of hypertensive individuals (145). Enhanced GRK2 expression levels could underlie the impaired β -adrenergic function

present in hypertension (145). Moreover, GRK2 inhibits protein kinase B-mediated activation of the endothelial nitric oxide synthase (eNOS) and thus, reduces NO production (146). This might explain the increased vasodilatory response observed in GRK2^{+/-} mice (147).

However, vascular tone is a result of a careful balance between vasodilatory and vasoconstrictory pathways, both of which are in part GPCR-mediated. Global GRK2 knockout was found to increase both opposing pathways and eventually, resulted in spontaneous hypertension (148). GRK2^{+/-} mice, in contrast, are resistant to the deleterious effects of angiotensin II on vascular structure and functionality (147). In agreement with the elevated GRK2 levels found in patients with hypertension, GRK2 overexpression led to a hypertensive state in mice (149). Therefore, GRK2 deserves further investigation as a target for hypertension, although physiological outcomes have to be carefully monitored.

4.3.3 Diabetes mellitus

A number of studies support a role for GRK2 as an inhibitor in insulin signalling. GRK2 levels were found to be upregulated in blood mononuclear cells from insulin-resistant patients and in different models of insulin resistance (150). Moreover, applying models of insulin-resistance, GRK2^{+/-} mice are protected from developing impaired insulin sensitivity (150) and induced GRK2 ablation improves insulin sensitivity (151). In addition, GRK2-inhibition could ameliorate glucose homeostasis (152).

The mechanisms at a molecular level are not entirely clear yet. GRK2 interferes with β -adrenergic signalling, which plays a role in the development of insulin resistance (153). GRK2 also negatively regulates insulin-stimulated glucose transport in a kinase-independent manner via interaction with $G\alpha_{q/11}$ or by direct interaction with the insulin receptor substrate 1 (IRS1) (150,154,155).

4.3.4 Obesity

A role for GRK2 in age- and diet-induced adiposity was implied (150). In GRK2^{+/-} mice on a high-fat diet, adiposity was lowered (150) and induced gene ablation prevented further body weight gain and the development of adiposity (151).

Given the scale of the obesity epidemic and the lack of adequate pharmacological treatment options, further research into GRK2 seems worthwhile.

4.3.5 Osteoporosis

The GPCR calcium-sensing receptor (CaR), which negatively regulates parathyroid hormone (PTH) secretion, is investigated as a potential drug target in osteoporosis (156,157). Sustained elevated levels of parathyroid hormone (PTH) increase bone loss, whereas intermittent pulses increase bone mass (158). Stimulation of the CaR by

increased extracellular calcium levels, leads to reduced PTH secretion (159) and is in part attenuated in a kinase-independent manner by GRK2 (160).

4.3.6 Cancer

A role for GRK2 in cell differentiation and survival arose from the observation of embryonic lethality in global GRK2^{-/-} mice (161). This is likely due to a more general role in embryogenesis rather than a cardiac-specific function, because GRK2 knockout restricted to the heart produced viable offspring with normal heart structure and function (162).

Interestingly, GRK2 upregulation was reported for thyroid cancers, where it showed an antiproliferative effect (163). A similar effect could be observed in hepatocellular carcinoma, where GRK2 overexpression decreased cell proliferation and tumour growth. Mechanistically, a role for GRK2 in the cell cycle arrest during G2/M transition was proposed (164). In line with a role for GRK2 in cell cycle control is the finding, that transient downregulation of the kinase during G2/M transition is crucial for cell cycle progression (165).

GRK2 protein levels are also upregulated in a number of breast cancer cells lines. However, these data support a tumour-promoting role for GRK2, with elevated levels stimulating mitogenic ERK1/2 signalling and pro-survival (166).

Overall, this indicates, that further research into the underlying mechanisms of the role of GRK2 in cancer development is needed.

4.3.7 Potential of a GRK2-inhibitor

In conclusion, GRK2 has been implicated as a drug target for a variety of different conditions. Research into the pathophysiology of GRK2 has focused on heart failure, where there is still an urgent need for new medications (167).

As detailed in the next chapter, several compounds with a GRK2-inhibitory effect have been described and characterized, but to date none has reached clinical trials or market approval.

4.4 Approaches to GRK2-inhibition

The tri-domain structure of GRK2, with every domain contributing to activity, allows for a range of approaches to inhibit GRK2 effector functions (Figure 5).

Firstly, compounds interacting with the N-terminal domain of GRK2 may hinder the binding of receptor substrates. Moreover, G α_q -mediated kinase-independent effector functions can be blocked. Secondly, targeting the enzyme active site provides a more general way to prevent kinase activity, but is unlikely to interfere with kinase-independent functions. Thirdly, intervening with the G $\beta\gamma$ -mediated GRK2 activation and membrane

translocation provides a route to inhibit both the phosphorylation of GPCR-substrates, as well as soluble substrates. To what extent kinase-independent effects are affected, however, is unclear.

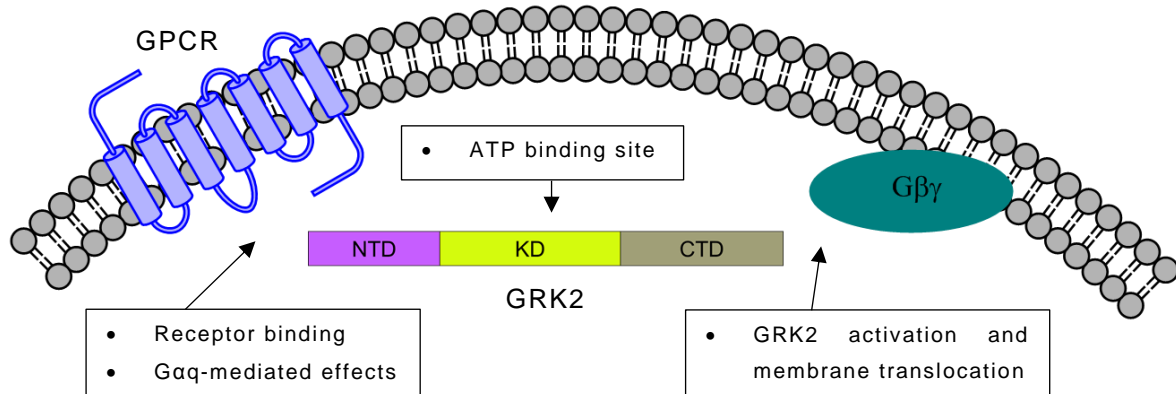


Figure 5: Domain-specific inhibition of GRK2

The multi-domain structure of GRK2 allows for multiple routes of inhibiting kinase-dependent and -independent effects (adapted from (131)).

In addition to different target sites and blocking specific effector functions, inhibitors also vary in their biochemical nature (small molecules, peptides, and proteins), potency and the selectivity they display for the seven GRK isoforms.

4.4.1 GRK2-inhibition via the N-terminal domain

RKIP is a dual-specific inhibitor of Raf-1 and GRK2

The Raf-1 kinase inhibitor protein (RKIP) is a member of the family of phosphatidylethanolamine-binding proteins (PEBP), with the capacity to inhibit both GRK2 (168) and the serine/threonine kinase Raf-1, thus inhibiting the Raf-MEK-ERK1/2-pathway by competitive inhibition of MEK phosphorylation (169). Phosphorylation of the amino acid Ser153 by the second-messenger dependent kinase PKC mediates a target switch from Raf-1 to GRK2 (168,170). RKIP is thought to interact with the N-terminus of GRK2, thereby interfering with receptor substrate binding (91,168). RKIP also shows inhibitory activity against several serine proteases (171).

RKIP is upregulated under cardiac stress and some evidence supports the notion of an adaptive role mediating cardioprotection, which is in line with the beneficial effects seen under GRK2-inhibition (172). However, RKIP, possibly by inhibiting the cardioprotective MAPK-pathway, interferes with survival pathways and plays a role in apoptosis. Another study showed that cardiac overexpression of RKIP representing levels seen under cardiac stress led to increased heart dilatation, cardiac dysfunction, upregulation of the

cardiac lipid gene metabolism and cardiomyocyte death indicating transition to heart failure (173).

Thus, RKIP is an effective GRK2-inhibitor with specificity towards receptor substrates, by targeting the receptor interaction site located in the N-terminal domain. RKIP, however, also shows cardiotoxic side effects mediated by its Raf-1 inhibitory property (173).

The amino terminal GRK2 inhibitor peptide (β ARKnt)

A peptide covering the extreme N-terminus of GRK2, that is the first 14 amino acids (MADLEAVLADVYSL), inhibits β 2AR-phosphorylation after stimulation with the β -adrenergic agonist isoproterenol, but it does not affect phosphorylation of the soluble substrate tubulin (174).

The extreme N-terminus of GRKs, which forms an amphipathic helix, displays significant sequence conservation. Moreover, it selectively enhances the catalytic activity towards receptor substrates, possibly by simultaneously binding phospholipids through its hydrophobic side and facilitating an intramolecular interaction with the kinase domain through its polar side (174).

The therapeutic potential of this peptide, to our knowledge, has not been further investigated.

4.4.2 Targeting the central kinase domain

An RNA-aptamer selectively inhibits GRK2

An RNA-aptamer (C13) found via an *in vitro* selection process is a potent inhibitor of GRK2-mediated phosphorylation of bovine rhodopsin. Moreover, it shows specificity for members of the GRK family (175). C13 is thought to target the kinase domain and interfere with phosphorylation by stabilizing a unique inactive conformation through interactions within and outside of the ATP binding pocket (176). Aptamers are not generally suitable for therapeutic application, but may be used in displacement assays to identify small molecule inhibitors (177). Paroxetine, a market-approved selective serotonin-reuptake inhibitor (SSRI), was identified as a selective GRK2-inhibitor through its ability to displace C13 from GRK2 (178).

Paroxetine is a GRK2 inhibitor

Paroxetine has been revealed as a GRK2-inhibitor with selectivity over other GRK subfamilies. The crystal structure shows paroxetine fitting into the enzyme active site, thus stabilizing an inactive conformation (178). Isoproterenol-stimulation in paroxetine-treated mice leads to increased myocardial contractility and enhanced inotropic response. Moreover, paroxetine treatment in a myocardial infarction-induced heart failure mouse model results in enhanced ejection fraction, fractional shortening and improved

contractility. It limits adverse ventricular remodelling and preserves structural integrity of the myocardium. GRK2-inhibition with paroxetine also normalized β -adrenergic signalling as indicated by reduced serum catecholamine levels, restored β AR density and decreased myocardial GRK2 upregulation (179).

Interestingly, paroxetine, in contrast to the β -blocker metoprolol, prevents induction of the foetal gene expression program, thus delivering improvements on top of those observed with β -blocker treatment (179).

Nevertheless, a compound approved for the treatment of psychiatric disorders is not an ideal GRK2-inhibitor. Moreover, improved selectivity and potency would be desirable. A derivative, synthesized with the desire to tackle these concerns, exhibited less activity regarding serotonin reuptake. Unfortunately, it also enhanced inhibition of other AGC kinases (93).

Protein kinase inhibitors

There are known serine/threonine kinase inhibitors, which were tested for their GRK2-inhibitory potential.

One of them, balanol, inhibits members of the AGC kinase family (180) and displays some selectivity for GRK2 over other GRKs (87). Balanol has been reported as a potent inhibitor of GRK2-mediated phosphorylation of the soluble substrate tubulin. Balanol interferes with GRK2 activity by stabilization of an inactive enzyme conformation (87).

Takeda Pharmaceutical Company Limited developed a number of compounds with a heterocyclic structure similar to balanol (181). These compounds selectively inhibit GRK2 through stabilization of the inactive conformation, as revealed from crystal structures (182). However, for reasons unknown, none of the compounds has proceeded to clinical trials.

Furthermore, one group screened an assembly of known kinase inhibitors for their selective targeting of either GRK2 or GRK5. The most potent candidate was co-crystallized with GRK2 and $G\beta\gamma$ to gain further insight into the structure-activity relationship (88).

4.4.3 Targeting the C-terminal interaction with $G\beta\gamma$

The carboxyl terminal GRK2 inhibitor peptide (β ARKct)

β ARKct is a peptide consisting of the C-terminal amino acids 495-689 of GRK2 covering the $G\beta\gamma$ -binding site, interaction with which is crucial in activating and translocating GRK2 to the plasma membrane towards receptor substrates (139). Therefore, β ARKct

acts as a competitive inhibitor of GRK2 by scavenging G $\beta\gamma$ -subunits and interfering with membrane translocation.

Cardiac-specific overexpression of β ARKct in a transgenic heart failure model, protected animals from heart failure development. G $\beta\gamma$ sequestration as a mechanism of action led to less cardiac dilation, enhanced heart function and prolonged survival (183). In another transgenic mouse model with GRK2 overexpression to levels found in human heart failure (3-fold increase), cardiac-specific expression of β ARKct led to a normalization of the β AR-stimulated contractility (184).

Adenoviral-mediated gene delivery of β ARKct was performed in several animal models of heart failure. In a clinically relevant large animal model (porcine) of post-myocardial heart failure, gene delivery resulted in improved contractile function, decreased plasma catecholamine levels, and subsequent reversal of cardiac remodelling and foetal gene expression (141). In cardiomyocytes from end-stage heart failure patients undergoing heart transplantation, β ARKct was able to improve the β AR-stimulated contractile response, further supporting the maladaptive nature of GRK2 upregulation in heart failure (185).

However, the restoration of adrenergic responsiveness observed with β ARKct cannot be solely attributed to GRK2-inhibition. In the context of its role in G $\beta\gamma$ -sequestration, β ARKct has been reported to improve cardiac contractility by increasing the L-type Ca²⁺-channel current (186).

Hence, the molecular mechanisms underlying β ARKct-mediated cardiac effects are not fully elucidated yet. At the same time, this finding shed light on a novel potential target for heart failure treatment (186).

Peptides and small molecules targeting G $\beta\gamma$

Studies towards interrupting the G $\beta\gamma$ -GRK2 interaction have yielded several GRK2-inhibitory peptides and small molecules.

A shorter GRK2CTD-derived peptide (amino acids 643-670) corresponding to the 'G $\beta\gamma$ binding domain' (187), inhibits GRK2-activity and phosphorylation of rhodopsin. Interestingly, one group used a phage display library screen with G $\beta\gamma$ as bait to elucidate requirements for binding partners and identified a protein-protein interaction "hot spot" on G $\beta\gamma$ (188). A mutated form (SIGK) (189), of the peptide with the highest affinity for G $\beta\gamma$ (SIRK) inhibited certain G $\beta\gamma$ effector functions, while leaving others unaffected (190). Based on the identified "hot spot", a virtual docking of a small molecule library yielded one compound (M119), which selectively interfered with G $\beta\gamma$ -protein interactions (191). In an animal model of heart failure, both M119 and a closely related analogue, gallein, prevented heart failure progression and improved cardiac function.

These data indicate that small molecule disruption of the G $\beta\gamma$ -GRK2 interaction is feasible and effective in ameliorating heart failure symptoms (192).

A phosducin-derived peptide

Phosducin (PDC), a cytosolic protein mainly expressed in retinal photoreceptor cells and the pineal gland, has been shown to inhibit G $\beta\gamma$ -mediated effector functions. Moreover, a PDC-derived peptide (amino acids 215-232) containing a high-affinity G $\beta\gamma$ -binding site showed a moderate inhibitory effect on GRK2-mediated phosphorylation of rhodopsin (193).

4.4.4 Peptide GRK2-inhibitors

Receptor-derived peptides

A peptide comprising the first intracellular loop (amino acids 56-74) of the hamster β 2AR inhibits receptor phosphorylation by GRK2, but does not show inhibitory activity towards non-receptor substrates (194).

Modification of this peptide by adding charged amino acids and truncation yielded a 40-fold more potent peptide-inhibitor (PepInh, AKFERLQTVTNYFITSE), which displayed activity towards rhodopsin (195). However, it does not interfere with GRK2-mediated phosphorylation of a peptide substrate indicating a mechanism of action differing from competition with ATP or the substrate (195). Moreover, PepInh displays specificity, as it does not interfere with activity of PKA or PKC, but only modest selectivity within the GRK family (195). In a pressure overload mouse model, the peptide retarded signs of heart failure (143).

Peptides derived from a substrate-binding site of GRK2

Peptides (KRX-683₁₀₇, KRX-683₁₂₄ and ³⁸³⁻³⁹⁰HJ loop) derived from a kinase-substrate interaction site of GRK2 have been reported to inhibit GRK2 activity *in vitro* and show favourable effects on glucose homeostasis in an animal model (152,196,197).

4.4.5 Other GRK2-inhibitors

Polyanionic compounds have been the first reported inhibitors of GRK2-mediated receptor phosphorylation, with heparin and dextran sulphate showing the highest potency (198). In addition, heparin also blocks agonist-induced phosphorylation of β AR in permeabilized cells (199). However, polyanionic compounds are inherently highly charged and as such membrane-impermeable. Furthermore, the molecular weight of both heparin and dextran sulphate impedes their clinical use.

Recently, α -hederin has been shown to block GRK2-mediated phosphorylation of the β 2AR. α -hederin is a component of the dry extract of *Hedera helix*, which is used in the treatment of diseases of the respiratory tract for its secretolytic and bronchospasmolytic effects. Inhibition of GRK2 is in line with the observed increase in adrenergic responsiveness of the airways (200).

In conclusion, a number of GRK2 inhibitors have already been identified and characterized. They differ in their mechanism of action, the specific effector functions they block and their biochemical composition. Many of the described compounds are peptides or proteins (RKIP, β ARKnt, β ARKct, PepInh), which indicates a potential for amino acid-based structures in targeting GRK2.

4.5 The therapeutic potential of peptide drugs

The number of therapeutic peptides entering clinical trials has been exponentially increasing over the last 30 years. Whereas the majority binds extracellular targets, around 15% are directed towards targets within the cell (201).

In recent years, peptides have been increasingly recognized for their pharmacological potential. Not complying with Lipinski's rule of five (202), such polyamides were thought largely unfit for the development into pharmaceuticals. However, their distinct physicochemical properties combine some of the advantages of both larger proteins and small molecules, thus potentially filling a niche in the space of drug candidates (203).

4.5.1 Characteristics of peptides

Peptides, short proteins of less than 50 amino acids, comprise a promising class of current and future therapeutics (201,204). Peptides might prove especially valuable for modulating intracellular protein-protein interactions (PPI), which have been notoriously difficult to target. Small molecules, although suitable for fitting into binding pockets restricted in size as e.g. enzyme active sites, are usually too small to interfere successfully with the larger interfaces of PPIs. Monoclonal antibodies (mAB) and peptides both provide larger surface areas and can thus effectively complement PPIs, with the latter having better access to intracellular targets (201).

In addition, peptides demonstrate high target specificity and affinity comparable to larger proteins, but generally require lower production costs than mABs due to standard synthetic procedures. As peptides are degraded to amino acids, they exhibit a favourable toxicity profile (204). Immunogenicity is less of a risk in comparison to larger proteins such as mAB. In addition, owing to their smaller size, peptides are potentially membrane permeable, therefore offering the possibility of reaching intracellular targets, and possess better tissue penetration (203).

However, there are considerable challenges to be overcome when exploiting peptides for therapeutic application. Peptides show an overall unfavourable pharmacokinetic profile and generally poor oral bioavailability. Solubility is variable and dependent on hydrophilicity. Hydrophilicity and molecular mass may limit the membrane permeability (204). Furthermore, susceptibility to proteolytic cleavage, hydrolysis and oxidation pose challenges in terms of stability and rapid renal and hepatic clearance shortens their

plasma half-life to minutes (201,203) Conformational flexibility often limits affinity and selectivity (201).

Some of these shortcomings may be overcome by chemical modification, as outlined below.

4.5.2 Modifications

Currently, subcutaneous injection is the most common route for administration of peptide therapeutics, although alternative delivery systems are increasingly recognized (204). Nonetheless, oral application is desirable, but generally requires chemical modifications or formulation efforts (204,205).

Methods to increase the proteolytic stability include cyclisation, introduction of unnatural amino acids, N-methylation and establishment of intramolecular hydrogen bonds (206,207). The plasma half-life can be prolonged by promoting binding to serum albumin or attachment of polymeric molecules such as e.g. polyethylene glycol (PEG) (203). The membrane permeability may be enhanced by addition of lipid groups (e.g. myristoylation) (152,208). Moreover, amino acid side chains can be replaced by specific functional groups towards the development of a small molecule analogue (209).

4.5.3 Displacement assay

Alternatively, a displacement assay could be performed. This may lead to the identification of small molecules, which compete with a peptide for a common interaction partner. Such an approach was taken in the discovery of the kinase-inhibitor paroxetine, which displaced the RNA-aptamer C13 from GRK2 (178).

4.5.4 Gene therapy

Taking into account the difficulties with regard to oral delivery of peptide drugs, alternative routes of administration have to be considered. One possible technology is gene transfer therapy, i.e. introduction of recombinant DNA through viral or non-viral delivery (210,211).

Recently, a heart failure study aiming at delivering the sarco(endo)plasmic reticulum Ca^{2+} -ATPase (SERCA2a) using an adeno-associated virus for delivery has advanced to Phase IIb clinical trials, where unfortunately the promising results from earlier studies could not be confirmed (212).

Nevertheless, these studies are in support of the potential of gene transfer therapy for heart failure treatment. Moreover, there is ample data supporting a gene therapy approach for GRK2-inhibition from studies using β ARKct (185,210,213).

Taken together, peptides represent a viable class of therapeutics with specific advantages compared to small molecules or biomacromolecules. A promising approach

for the identification of candidate peptide drugs is e.g. a phage display library screen, as outlined in the next chapter.

4.6 Peptide phage display library screen for candidate drugs

4.6.1 Principle of a phage display library screen

First described in 1985 by Smith and co-workers, phage display technology has since become a widely applied method in drug discovery (214-216).

Peptides or proteins are displayed fused to bacteriophage coat proteins, thus directly linking phenotype to genotype. Non-lytic filamentous phage, such as e.g. M13, which infect F plasmid-containing gram-negative bacteria (usually *E.coli* strains) are used most commonly (217). M13 contains two coat proteins suitable for peptide fusion expression: (i) the minor coat protein pIII, of which five copies are expressed and (ii) the major coat protein pVIII, of which several thousand copies cover the length of the bacteriophage (218). Thus, libraries of displayed amino acid sequences can be screened for high affinity binding to target proteins.

In a process termed bio panning (Figure 6), the target compound (bait), immobilized directly or via an affinity tag, is exposed to the phage library. After removal of unbound phages by washing, the bound phages are eluted. Thereby, because of the stability of filamentous phage towards pH, denaturants and ionic strength, a variety of unspecific methods may be applied (e.g. acid, high salt concentration). Alternatively, a known interaction partner may be used for a more specific competitive elution (214,218). Following amplification of the eluted phages in *E. coli*, another round of bio panning can be performed. Finally, sequencing of the extracted DNA provides the peptide sequence (219).

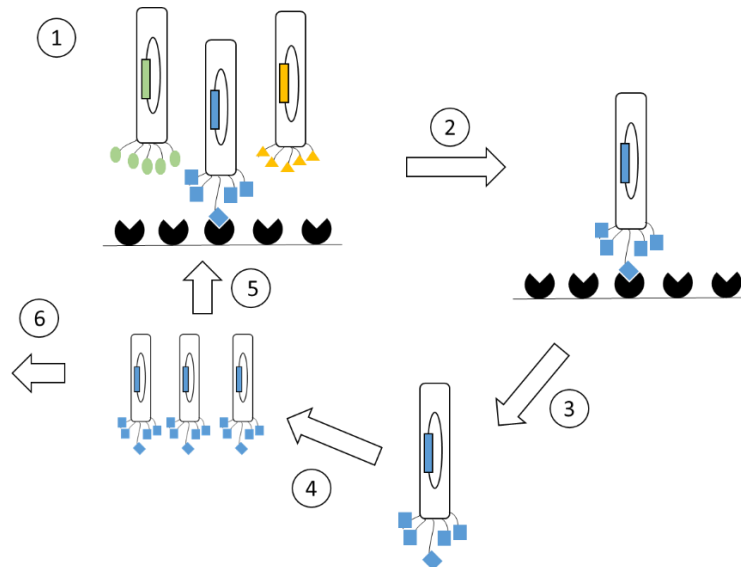


Figure 6: Schematic drawing of a phage display library screen

1. A peptide-displaying phage library is exposed to a bait-coated plate. 2. The unbound phages are removed by washing. 3. The bound phages are eluted. 4. The eluted phages are amplified. 5. The amplified phages are exposed to a bait-coated plate starting a new selection round. 6. After three rounds of panning, enriched phages may be isolated and sequenced. (adapted from (219))

4.6.2 Peptide libraries

Libraries may vary with regard to the peptides they display. Linear peptides of variable length have been used (218,220), allowing screening of ligands for targets with continuous interaction sites or residues, which are widely apart (218).

Linear peptides tend to exhibit conformational flexibility, which can reduce their affinity. In contrast, libraries displaying cyclic peptides, which are conformationally more constrained, may be more successful in the finding of high affinity ligands (221).

4.6.3 Applications of phage display technology

Intriguingly, phage display library screens yield peptides, which largely target biologically relevant sites. Hence, they often have the capacity to modulate the activity of the target protein, be it orthosterically or allosterically.

Phage display as a method may be employed in numerous scientific fields, including analysis of protein-protein interactions (218), identification of novel protein interactions partners or inhibitors (222,223), search for enzyme substrates and/or inhibitors (218,219) and target validation (215).

Commercially available peptide libraries have also successfully been employed in the search for enzyme inhibitors (219,224).

Interestingly, phage display library screening has already been used in the search for a GRK2-inhibitor.

Peptides selected from phage display libraries using G β γ subunits as baits interfered with specific G β γ effector functions (225). The search for small molecule inhibitors of G β γ effector functions employing one such peptide yielded the compound M119, which blocks G β γ -mediated GRK2 activation (191). Another prominent example of a phage display-derived GRK2-inhibitor is the RNA-aptamer C13 (175). In a displacement assay with this aptamer, paroxetine was identified as a GRK2-inhibitor (178).

These two examples underline the potential of phage display technique for the identification of potent modulators of protein function.

4.7 Aim

GRK2 is a ubiquitously expressed protein, which has been implicated in a variety of conditions. However, to date no GRK2-inhibitor has reached clinical approval.

GRK2 has been successfully inhibited by targeting the N-terminal domain thereby interfering with substrate recognition, by blocking the enzyme active site located in the central kinase domain or by preventing enzyme activation and membrane translocation mediated by G β γ -interaction with the C-terminal domain. The latter approach has been extensively studied with the help of the β ARKct peptide and proven beneficial in several heart failure animal models. Nevertheless, there is still no compound available, which interferes with the G β γ -GRK2 interaction by directly targeting the C-terminal domain of the kinase.

Thus, the aim of this project is to find and characterize peptides, which selectively interact with the C-terminal domain of GRK2.

5 Materials and Methods

Chemicals, which were not specified otherwise, were obtained from Merck (Zug, Switzerland).

5.1 Molecular cloning

Polymerase chain reaction

Amplification of cDNA fragments for cloning was performed using 1 U/reaction *Pfu* DNA polymerase (Promega AG, Dübendorf, Switzerland) in *Pfu* DNA polymerase buffer (Promega AG, Dübendorf, Switzerland). Single colony screening of bacterial clones was performed using 1 U/reaction *Taq* DNA polymerase (Sigma-Aldrich Chemie GmbH, Buchs SG, Switzerland) in the supplied buffer. Primers (Microsynth AG, Balgach, Switzerland) were used at 0.4 μ M, dNTPs (New England BioLabs, Bioconcept, Allschwil, Switzerland) at 200 μ M and 0.1-10 ng of DNA as template. The DNA was amplified with a standard program (Table 1) using a Thermocycler 3000 (Biometra, Göttingen, Germany):

Step	Temperature	Time
1	94 °C	5 min
2	94 °C	30 s
3	50-65 °C	40 s
4	72 °C	120 s/1000 bp (<i>Pfu</i> DNA polymerase) 60 s/1000 bp (<i>Taq</i> DNA polymerase)
5	72 °C	10 min

25-30 cycles

Table 1: Standard PCR program

After initial melting of the dsDNA (step 1), 25-30 cycles of melting of dsDNA (step 2), followed by annealing (step 3) and elongation (step 4) of the primers were run. A final elongation step (step 5) was added.

The PCR products were separated by agarose gel electrophoresis.

DNA concentration measurement

The concentration of dsDNA was determined by appropriate dilution in 10 mM Tris, pH 6.8 and measurement of the absorbance at 260 nm (Biophotometer, Eppendorf, Germany). An extinction coefficient of 0.020 (μ g/ml)⁻¹ cm⁻¹ was used for the calculation of the concentration (226).

Annealing of single-stranded oligonucleotides

Single-stranded oligonucleotides were annealed using 25 µM top and bottom strand oligonucleotide, respectively, in oligonucleotide annealing buffer supplemented with 1-3% (v/v) DMSO (Sigma-Aldrich Chemie GmbH, Buchs SG, Switzerland) by incubation at 95 °C for 4 min, at 40 °C for 10 min and at RT for 30 min (Thermocycler 3000). Annealed oligonucleotides were detected by agarose gel electrophoresis.

Oligonucleotide annealing buffer

The oligonucleotide annealing buffer contained 1 mM EDTA and 100 mM NaCl in 10 mM Tris, pH 8.0.

Agarose gel electrophoresis

DNA fragments were separated by agarose gel electrophoresis using 1-2% (w/v) agarose gels (Agarose MP, Roche, Sigma-Aldrich Chemie GmbH, Buchs SG, Switzerland) with 5 µl/100ml 1% (w/v) ethidium bromide for visualisation. Gels were prepared with TAE or TBE buffer and run with 100 V. For identification of the fragment size, a DNA ladder (GeneRuler 1kb DNA Ladder (Thermo Fisher Scientific AG, Reinach, Switzerland) or Low molecular weight DNA ladder (New England BioLabs, Bioconcept, Allschwil, Switzerland)) was run in parallel with the samples. DNA was visualised with UV-light (312 nm) using Intas Gel Capture software.

TAE buffer (1 x)

The TAE buffer was prepared with 40 mM Tris, 20 mM acetic acid, and 2 mM EDTA.

TBE buffer (1 x)

The TBE buffer was prepared by dissolving 89 mM Tris, 89 mM boric acid, and 2 mM EDTA in water.

Enzyme restriction digestion

Restriction digestion of the DNA was performed with suitable enzymes (New England BioLabs, Bioconcept, Allschwil, Switzerland) in the supplied buffers under conditions according to the manufacturer's instructions.

DNA gel extraction

DNA was excised under UV-light (365 nm) from agarose gels, extracted using the QIAquick Gel Extraction Kit (QIAGEN, Hombrechtikon Switzerland) according to the manufacturer's protocol and eluted with 30-50 µl water or 10 mM TE buffer, pH 8 (Invitrogen, Thermo Fisher Scientific AG, Reinach, Switzerland).

Ligation

DNA fragments were ligated with T4 DNA ligase (New England BioLabs, Bioconcept, Allschwil, Switzerland) in T4 DNA Ligase Reaction Buffer (New England BioLabs, Bioconcept, Allschwil, Switzerland) at 16 °C for 2-4 h or at 20 °C overnight. The concentrations of vector and fragment solutions were estimated by separation of different volumes (2, 5 and 10 µl) of 1/10 dilutions in an agarose gel. Ligation reactions were performed using 200 ng of the vector backbone and four times as many molecules of the fragment.

Heat-shock transformation

For plasmid DNA-preparation, competent *E. coli* XL1 blue (Stratagene, Agilent Technologies AG, Basel, Switzerland) were thawed on ice and, in a pre-chilled 15 ml reaction tube, 100 µl were mixed with 10 µl ligation mixture or 1 µl DNA-Midi/Maxi-Preparation, respectively, and further incubated on ice for 20 min. The bacteria-DNA mixture was heat-shocked at 42 °C for 45 s and subsequently incubated on ice for 2 min. After addition of 900 µl pre-warmed (42 °C) SOC, the mixture was incubated at 37 °C and 200 rpm for 30 min. Selective LB agar plates were pre-warmed at 37 °C, streaked with 10-100 µl of the bacteria-DNA mixture and incubated overnight at 37 °C. The next day, single colonies were used for inoculating 2 ml of selective LB medium and grown at 37 °C and 200 rpm for 3-4 h. The bacteria were pelleted by centrifuging 1 ml of the culture at 16'000 x g for 1 min. Then, the pelleted bacteria were lysed with 100 µl water and 5 µl were used as template for a single colony screening PCR.

SOC

To prepare 50 ml of SOC, 48 ml of SOB, 0.5 ml of 1 M MgCl₂, 0.5 ml of 1 M MgSO₄, and 1 ml of 20% (w/v) D(+)-glucose monohydrate were mixed.

SOB

For 200 ml SOB, 4 g of bacto-tryptone (Becton Dickinson AG, Allschwil, Switzerland), 1 g of bacto-yeast extract (Becton Dickinson AG, Allschwil, Switzerland), and 0.1 g NaCl were dissolved in water and sterilized.

LB medium

LB medium was prepared by dissolving 1% (w/v) bacto-tryptone, 0.5% bacto-yeast extract, and 1% (w/v) NaCl in water.

LB agar plates

LB agar plates contained 1.5% (w/v) bacto-agar (Becton Dickinson AG, Allschwil, Switzerland) in LB medium.

Preparation of competent bacteria

E.coli were spread on LB agar plates and incubated overnight at 37 °C. Next, a single colony was cultivated overnight in 5 ml of LB medium at 37 °C and 200 rpm. An aliquot (1 ml) of the overnight-culture was diluted in 120 ml of LB medium and grown to mid-log phase ($OD_{600\text{ nm}}=0.4-0.6$). The bacteria were pelleted by centrifugation at 3000 rpm at 4°C for 10 min. Thereafter, the bacterial pellet was resuspended in 12 ml of TSB on ice. Aliquots were flash frozen with liquid nitrogen and stored at -80 °C.

TSB

To prepare 100 ml of TSB, 10 g PEG 3000 were dissolved in 40 ml of LB medium and the pH was adjusted to 6.1. Thereafter, 5 ml of DMSO, 2 ml of 1 M $MgSO_4$, and 2 ml of 1 M $MgCl_2$ were added. LB medium was added to a final volume of 100 ml.

Midi/Maxi-Preparations of plasmid DNA

Plasmid DNA was extracted from bacterial cultures using the Invitrogen PureLink HiPure Plasmid Purification Kit (Thermo Fisher Scientific AG, Reinach, Switzerland) according to the manufacturer's protocol. For Midi-Preparations 25 ml and for Maxi-Preparations 200 ml of bacterial overnight-culture were used. The extracted DNA was dissolved in 100-400 μ l TE and stored at -20 °C.

Sequencing

Sequencing reactions were performed by Microsynth AG, Balgach, Switzerland according to the company's instructions.

Primers

The primers were purchased from Microsynth AG, Balgach, Switzerland.

The following primers were used for cloning of hexahistidine-tagged GRK2-domains into the pET-3d vector (Figure 7) (the tag-sequence is underlined):

GRK2seq16	C-terminal hexahistidine tagged GRK2NTD forward
	5'-TAT AAT CC ATG GCC GCG GAC CTG GAG GCG GTG CTG GCC GAC GTG AGC TAC CTG ATG GCG ATG GAG-3'
GRK2seq17	C-terminal hexahistidine tagged GRK2NTD reverse
	5'-TAT AAT GGA TCC TTA <u>ATG GTG ATG GTG ATG GTG</u> GTC ATT CAT GGT CAG GTG GAT GTT GAG CTC CAC ATT C-3'
GRK2seq19	N-terminal hexahistidine-tagged GRK2KD forward
	5'-TAT AAT CC ATG GCC <u>CAT CAC CAT CAC CAT CAC</u> TTC AGC GTG CAT CGC ATC ATT GGG CGC GGG-3'
GRK2seq20	N-terminal hexahistidine-tagged GRK2KD reverse
	5'-AAT GGA TCC TTA GAA AAA GGG GCT CTC TTT CAC CTC CTG-3'
GRK2seq34	C-terminal hexahistidine-tagged GRK2KD forward
	5'-TAT AAT CC ATG GCC TTC AGC GTG CAT CGC ATG ATT GGG CGC-3'
GRK2seq35	C-terminal hexahistidine-tagged GRK2KD reverse
	5'-AAT GGA TCC TTA <u>ATG GTG ATG GTG ATG GTG</u> GAA AAA GGG GCT CTC TTT CAC CTC CTG-3'
GRK2seq24	N-terminal hexahistidine-tagged GRK2CTD forward
	5'-AAT TAT AAT TC ATG ACC <u>CAT CAC CAT CAC CAT CAC</u> CGC TCC CTG GAC TGG CAG ATG GTC TTC TTG-3'
GRK2seq25	N-terminal hexahistidine-tagged GRK2CTD reverse
	5'-AAT GGA TCC TCA GAG GCC GTT GGC ACT GCC GCG CTG GAC-3'
GRK2seq32	C-terminal hexahistidine-tagged GRK2CTD forward
	5'-TAT AAT TAT AAT TC ATG ACC CGC TCC CTG GAC TGG CAG ATG GTC-3'
GRK2seq33	C-terminal hexahistidine-tagged GRK2CTD reverse
	5'-AAT GGA TCC TCA <u>ATG GTG ATG GTG ATG GTG</u> GAG GCC GTT GGC ACT GCC GCG CTG GAC-3'

Table 2: Primers for cloning of the His-tagged GRK2 domains into pET-3d

pET-3a sequence landmarks	
T7 promoter	615-631
T7 transcription start	614
T7-Tag coding sequence	519-551
T7 terminator	404-450
pBR322 origin	2814
<i>bla</i> coding sequence	3575-4432

The maps for pET-3b, pET-3c and pET-3d are the same as pET-3a (shown) with the following exceptions: pET-3b is a 4639bp plasmid; subtract 1bp from each site beyond *Bam*HI at 510. pET-3c is a 4638bp plasmid; subtract 2bp from each site beyond *Bam*HI at 510. pET-3d is a 4637bp plasmid; the *Bam*HI site is in the same reading frame as in pET-3c. An *Nco*I site is substituted for the *Nde*I site with a net 1bp deletion at position 550 of pET-3c. As a result, *Nco*I cuts pET-3d at 546. For the rest of the sites, subtract 3bp from each site beyond position 551 in pET-3a. *Nde*I does not cut pET-3d.

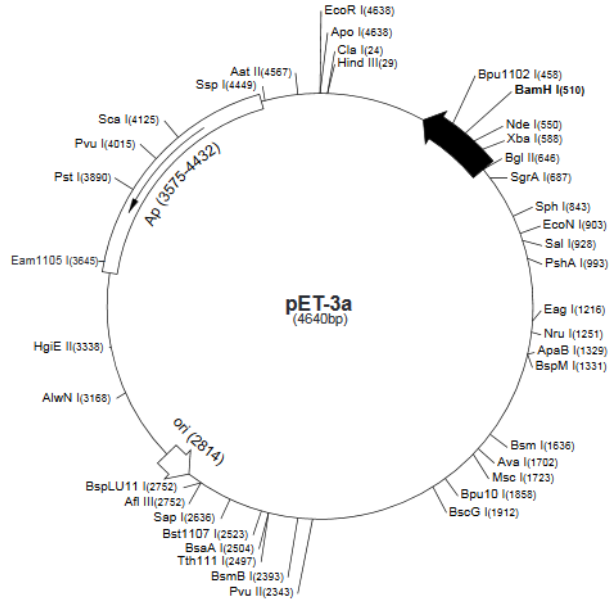


Figure 7: Vector map of pET-3d

The vector map of pET-3d (Novagen) shows a multiple cloning site and the T7 promoter.

Single-stranded oligonucleotides

Single-stranded oligonucleotides were obtained from Microsynth AG, Balgach, Switzerland.

The following single-stranded oligonucleotides were used for the generation of the WD-peptide containing plasmids (pcDNA3, Figure 8):

WD1	upper strand
5'-GTC CAA TAC GGA TCC ATG GCC AGC ACC CTG ATC GTG GGC CAC TGG GAC GGC AAC ATG AGC CTG GTG GAC AGG AGG ACC TGA CTC GAG GTA TTG GAC-3'	
WD1	lower strand
5'-GTC CAA TAC CTC GAG TCA GGT CCT CCT GTC CAC CAG GCT CAT GTT GCC GTC CCA GTG GCC CAC GAT CAG GGT GCT GGC CAT GGA TCC GTA TTG GAC-3'	
WD2	upper strand
5'-GTC CAA TAC GGA TCC ATG TTC CTG GCC GAG GAC GCC AGC ACC CTG ATC GTG GGC CAC TGG GAC GGC AAC ATG AGC CTG TGA CTC GAG GTA TTG GAC-3'	
WD2	lower strand
5'-GTC CAA TAC CTC GAG TCA CAG GCT CAT GTT GCC GTC CCA GTG GCC CAC GAT CAG GGT GCT GGC GTC CTC GGT CAG GAA CAT GGA TCC GTA TTG GAC-3'	
WD3	upper strand
5'-GTC CAA TAC GGA TCC ATG GAG AGG AGC AGC TTC AGC AGC TTC GAC TTC CTG GCC GAG GAC GCC AGC ACC CTG ATC GTG TTC TGA CTC GAG GTA TTG GAC-3'	
WD3	lower strand
5'-GTC CAA TAC CTC GAG TCA GAA CAC GAT CAG GGT GCT GGC GTC CTC GGC CAG GAA GTC GAA GCT GCT GAA GCT GCT CCT CTC CAT GGA TCC GTA TTG GAC-3'	

Table 3: Single-stranded oligonucleotides for the cloning of the WD-Peptides into pcDNA3

Comments for pcDNA3:
 5446 nucleotides
 CMV promoter: bases 209-863
 T7 promoter: bases 864-882
 Polylinker: bases 889-954
 Sp6 promoter: bases 959-1016
 BGH poly A: bases 1018-1249
 SV40 promoter: bases 1790-2115
 SV40 origin of replication: bases 1984-2069
 Neomycin ORF: bases 2151-2945
 SV40 poly A: bases 3000-3372
 ColE1 origin: bases 3632-4305
 Ampicillin ORF: bases 4450-5310

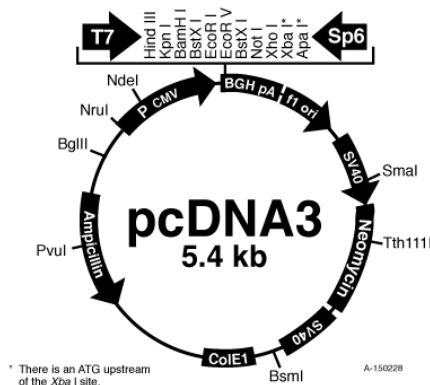


Figure 8: Vector map of pcDNA3

The vector map of pcDNA3 (Invitrogen) shows a multiple cloning site, promoters and bacterial resistance genes.

The following single-stranded oligonucleotides were used for cloning of the WD3 peptide sequence into the α -myosin heavy chain (α -MHC) vector:

WD3	upper strand
	5'-GTC CAA TAC GTC GAC ATG GAG AGG AGC AGC TTC AGC AGC TTC GAC TTC CTG GCC GAG GAC GCC AGC ACC CTG ATC GTG TTC TGA AAG CTT GTA TTG GAC-3'
WD3	lower strand
	5'-GTC CAA TAC AAG CTT TCA GAA CAC GAT CAG GGT GCT GGC GTC CTC GGC CAG GAA GTC GAA GCT GCT GAA GCT GCT CCT CTC CAT GTC GAC GTA TTG GAC-3'

Table 4: Single-stranded oligonucleotides for cloning of the WD3-Peptide into α -MHC

5.2 Protein procedures

Expression of recombinant proteins using the pET expression system

The cDNA of proteins to be overexpressed was cloned into the bacterial expression vector pET-3d (Novagen, Merck KGaA, Darmstadt, Germany), which contains the bacteriophage-derived T7 promoter under the control of the *lac* operon (227). *E.coli* BL21(DE3)pLysS were used as a host strain. The pLysS plasmid constitutively expresses

low levels of T7 lysozyme. Therefore, it represses basal protein expression by inhibition of basal levels of T7 RNA polymerase. Moreover, basal protein expression is repressed by the *lac* repressor, which upon addition of isopropyl β -D-1-thiogalactopyranoside (IPTG, Sigma-Aldrich Chemie GmbH, Buchs SG, Switzerland) is inactivated. This leads to the transcription of the T7 RNA polymerase gene under the control of the *lac* promoter. Thereafter, T7 RNA polymerase starts the transcription of the gene sequences under the control of the T7 promoter in the pET-3d plasmids. Thus, proteins of interest are selectively overexpressed following the addition of IPTG (Figure 9).

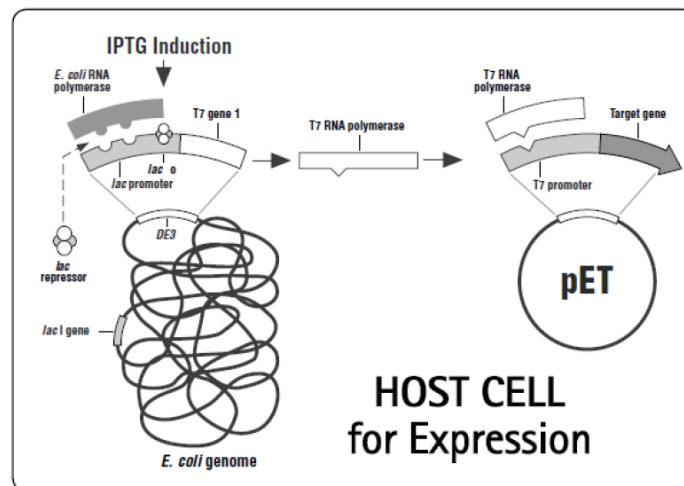


Figure 9: Protein overexpression with the pET expression system

This schema illustrates how addition of IPTG releases the *lac* repressor, thereby allowing the transcription of the T7 RNA polymerase gene. The T7 RNA polymerase in turn transcribes the target gene inserted into the pET expression vector. (pET System Manual, 11th edition, Novagen)

Single use competent BL21(DE3)pLysS (Promega AG, Dübendorf, Switzerland) were transformed by heat-shock transformation and spread on selective LB agar plates. Single colonies were picked and cultivated overnight at 37 °C and 200 rpm in 10 ml of selective LB medium. The overnight cultures were diluted 1/20 in 200 ml of selective LB medium and grown to mid-log phase under the same conditions. As an uninduced control, a sample of 10 ml of the bacterial culture was centrifuged at 4000 x g at RT for 10 min (Rotanta 460R, Hettich Laborapparate, Bäch, Switzerland). The supernatant was disposed of and the bacterial cell-pellet was flash frozen in liquid nitrogen and subsequently stored at -80 °C. Thereafter, the protein expression was induced with 1 mM IPTG for 3-4 h at 37 °C and 200 rpm. Hourly samples were taken for time-course analysis of the protein expression and treated as above. Finally, the bacterial culture was centrifuged at 4000 x g at RT for 10 min, the supernatant disposed of and the bacterial pellet stored at -20 °C until purification.

For SDS-PAGE analysis or immunoblotting, the samples taken before and after induction of the protein expression were thawed on ice, resuspended in 200 μ l freshly prepared 8 M urea and incubated at RT for 30 min. The viscosity of the suspension was reduced by sonication on ice (HD2200, 2-3 x 3 sec with 30% cycle and 70% power; UW2200; MS73; BANDELIN electronic GmbH & Co.KG, Berlin, Germany). After addition of 50 μ l of 5 x SDS sample buffer and 25 μ l of β -mercaptoethanol (Sigma-Aldrich Chemie GmbH, Buchs SG, Switzerland), the samples were incubated at RT for 1 h and subsequently stored at -20 $^{\circ}$ C.

SDS sample buffer (5 x)

To prepare 5 x SDS sample buffer, 5% (w/v) SDS (Bio-Rad Laboratories AG, Cressier, Switzerland) and 10% (v/v) glycerol were dissolved in 250 mM Tris, pH 6.8. A tiny amount of bromophenol blue was added.

Optical density measurement

The growth of bacterial cultures was monitored by measuring the optical density (OD) at 600 nm (Biophotometer, Eppendorf, Germany).

Purification of His-tagged proteins by metal affinity chromatography

Ni-NTA affinity chromatography allows the purification of recombinant proteins with a polyhistidine tag, which can be introduced by standard molecular cloning techniques.

The column was prepared by equilibrating 1-2 ml of 50% Ni-NTA slurry (QIAGEN, Hombrechtikon, Switzerland) with 10-20 ml of lysis buffer. Then, the bacterial cell pellet of a 50 ml or 200 ml culture was thawed on ice and resuspended in 10 or 20 ml of lysis buffer, respectively. The viscosity of the bacterial suspension was reduced by sonication on ice (HD2200, 5-10 x 3 sec with 30% cycle and 70% power; UW2200; MS73; BANDELIN electronic GmbH & Co.KG, Berlin, Germany). Next, the suspension was cleared by centrifugation at 4000 x g at 4 $^{\circ}$ C for 15 min (Sorvall RC 6 Plus, Thermo Electron Corporation, Rotor SLA 3000). The supernatant was incubated on the equilibrated Ni-NTA resin at 4 $^{\circ}$ C with agitation for 1 h to overnight, followed by removal of unspecifically bound proteins by washing with 20 x resin volumes of wash buffer. Thereafter, the bound proteins were eluted with 10 ml of elution buffer and collected in 2 ml aliquots. Aliquots of the flow-through, the washing step and the eluates were mixed with appropriate amounts of 5 x SDS sample buffer and analysed by SDS-PAGE or immunoblotting.

The Ni-NTA resin was regenerated by incubation with 0.5 M NaOH for 30 min and subsequently stored in 30% (v/v) ethanol at 4 $^{\circ}$ C. Thus, packed columns were used up to five times for purification of the same protein.

Lysis buffer

The lysis buffer contained 8 M urea, 100 mM NaH₂PO₄, 10 mM Tris, and 100 mM β-mercaptoethanol. The pH was adjusted to 8.0.

Wash buffer

The wash buffer was prepared as the lysis buffer, but the pH was adjusted to 6.3.

Elution buffer

The elution buffer was prepared as the lysis buffer, only the pH was adjusted to 4.3.

Protein separation by SDS-PAGE

Protein samples mixed with the appropriate volume of 5 x SDS sample buffer were separated by SDS-PAGE. Gels consisted of an upper stacking gel and a lower separation gel. Polymerisation of the stacking gel was initiated with 1 µl/ml TEMED (Carl Roth GmbH + Co. KG, Karlsruhe, Germany) and 0.1% (w/v) APS (Bio-Rad Laboratories AG, Cressier, Switzerland). For starting the polymerisation of the separation gel, 0.5 µl/ml TEMED and 0.325% (w/v) APS were used. The proteins were resolved at 80-120 V in SDS running buffer for approximately 2-2 ½ h. A protein weight marker (PageRuler Plus Prestained Protein Ladder, Thermo Fisher Scientific AG, Reinach, Switzerland) was run in parallel with the samples. The stacking gels were removed with a scalpel and the separation gels were either directly stained with Coomassie brilliant blue or blotted by semi-dry blotting technique and subsequently stained and destained.

Stacking gel

Stacking gels (3.75%) were prepared with 0.125 ml/ml of 30% (w/v) acrylamide/bis-acrylamide solution (29:1, 3.3% crosslinker, Bio-Rad Laboratories AG, Cressier, Switzerland), and 0.1% (w/v) SDS in 125 mM Tris, pH 6.8.

Separation gel

Separation gels were prepared with appropriate amounts of 30% (w/v) acrylamide/bis-acrylamide solution and 0.1% (w/v) SDS in 375 mM Tris, pH 8.8.

SDS running buffer

For the preparation of the SDS running buffer, 192 mM glycine, 25 mM Tris, and 0.2% (w/v) SDS were dissolved in water.

Staining solution

The staining solution was prepared with 10% (v/v) acetic acid, 20% (v/v) methanol and 0.05% (w/v) Coomassie brilliant blue R 250.

Destaining solution

The destaining solution contained 10% (v/v) acetic acid and 20% (v/v) methanol.

Immunoblot detection of proteins

After separation by SDS-PAGE and removal of the stacking gel, the separation gel was incubated with transfer buffer for 45 min with agitation. A PVDF membrane (Immobilon-P, 0.45 µm, Merck & Cie, Schaffhausen, Switzerland) was activated in methanol for 7 min and subsequently equilibrated in transfer buffer for 30 min. In addition, two filter papers (Extra thick blot paper, Bio-Rad Laboratories, Cressier, Switzerland) were equilibrated in transfer buffer for 30 min. The separated proteins were transferred to the membrane by semi-dry blotting technique with 20 V and 0.04 A for 40 min (Trans-Blot SD semi-dry Transercell, Bio-Rad Laboratories AG, Cressier, Switzerland). The membranes were washed five times with water to remove residual methanol and incubated overnight in PBS at 4° C. Then, the membranes were blocked with 20 ml of blocking buffer for 1 h at RT with agitation, followed by incubation with an appropriate primary antibody diluted in blocking buffer for 1 h at RT with agitation. After washing 4 x 5 min with PBST 0.05%, the membranes were incubated with enzyme-conjugated secondary antibody diluted in blocking buffer for 30 min at RT with agitation. Next, the membranes were washed 6 x 5 min with PBST 0.05% and 4 x 5 min with PBS to remove residual detergent. The visualization was performed with ECL Western Blotting detection reagent (Amersham, GE Healthcare, Sigma-Aldrich Chemie GmbH, Buchs SG, Switzerland) according to the manufacturer's instructions. X-ray films (Super RX, Fuji Medical x-ray film, Schenk, Röntgenbedarf AG, Hettlingen, Switzerland) were exposed for 20 s to 2 min, developed (Tetenal, Roentoroll HC, Tetenal AG & Co, Germany) and fixed (Tetenal Superfix MRP, Tetenal AG & Co, Germany)

Transfer buffer

The transfer buffer contained 192 mM glycine, 25 mM Tris, 0.2% (w/v) SDS and 20% (v/v) methanol.

PBS

PBS was prepared by dissolving 137 mM NaCl, 2.7 mM KCl, 6.5 mM Na₂HPO₄ and 1.5 mM KH₂PO₄ in water.

Blocking buffer

The blocking buffer was prepared by dissolving 5% (w/v) BSA (Sigma-Aldrich Chemie GmbH, Buchs SG, Switzerland) in PBST 0.05% (PBS with 0.5% (v/v) Tween 20).

Antibodies

The following primary antibodies were used for immunoblot detection of proteins or ELISAs:

anti-GRK2 antibodies were raised in rabbit against purified recombinant GRK2 expressed in Sf9 cells (173); anti-GRK2CTD antibody is a mouse monoclonal antibody raised against amino acids 468-689 of human GRK2 (sc-13143, Santa Cruz Biotechnology, LabForce AG, Muttenz, Switzerland); HRP-conjugated anti-M13 antibody is a monoclonal antibody purified from mouse ascites fluid, which reacts specifically with the bacteriophage M13 major coat protein product of gene VIII (27-9421-01, Amersham, GE Healthcare, Sigma-Aldrich Chemie GmbH, Buchs SG, Switzerland); anti-SRSF1 antibody is a mouse monoclonal antibody epitope mapping near the N-terminus of the SF2/ASF protein (sc-33652, Santa Cruz Biotechnology, LabForce AG, Muttenz, Switzerland); anti-WDR76 antibodies were produced in rabbit against an antigen sequence containing the WD3 sequence (HPA040626, Sigma-Aldrich Chemie GmbH, Buchs SG, Switzerland).

The following secondary antibodies were used for immunoblot detection of proteins or ELISAs:

Peroxidase-conjugated AffiniPure F(ab')₂ Fragment Goat-Anti-Rabbit (111-036-046)/goat anti-mouse (115-036-071) IgG, Fc Fragment Specific (Jackson ImmunoResearch Laboratories, USA) as applicable.

Acetone precipitation

Proteins were precipitated by mixing 0.5 ml of protein solution with 1 ml ice-cold (-20 °C) acetone and centrifugation at 13'200 x g for 20 s. The supernatant was disposed of and the protein pellet dissolved in 1 x SDS sample buffer. The samples were sonicated on ice (HD2200, 3-5 x 3 sec with 30% cycle and 10% power; UW2200; MS73; BANDELIN electronic GmbH & Co.KG, Berlin, Germany) and separated by SDS-PAGE.

SDS sample buffer (1 x)

To prepare the 1 x SDS sample buffer, 2% (w/v) SDS, 10% (v/v) glycerol and 300 mM β-mercaptoethanol were dissolved in 62.5 mM Tris, pH 6.8. A tiny amount of bromophenol blue was added.

Desalting columns (PD-10)

Buffer exchange of protein solutions with PD-10 desalting columns (GE Healthcare, Glattbrugg, Switzerland) was performed according to the manufacturer's instructions. The proteins were eluted with the desired buffer in aliquots of 1 ml.

Protein Concentration measurement

The protein concentration was quantified by Bradford's assay (228) using Roti-Quant reagent (Carl Roth GmbH + Co. KG, Karlsruhe, Germany). The assay was performed in 96-well plates (F8 Maxisorp Nunc-Immuno Module, Thermo Fisher Scientific AG, Reinach, Switzerland) according to the manufacturer's protocol. The absorbance was read at 595 nm with a microplate reader (VersaMax ELISA Microplate Reader, Molecular Devices, Sunnyvale CA, USA) and evaluated using SoftMax Pro 5.4.5 software.

ELISA procedure

Peptides or proteins were coated onto 96-well plates in carbonate buffer (pH: 1-2 units above the pI of the peptide or protein) and incubated overnight at 4 °C. Subsequent incubation steps were carried out at RT with agitation. The plates were blocked with ELISA blocking buffer for 1-2 h. The washing steps were carried out with TBST 0.05%. Interaction partners or antibodies were added in blocking buffer and incubated for 1 h. The ABTS detection reaction was prepared freshly by adding 36 µl of 30% H₂O₂ to 21 ml ABTS-Stock solution and 100 µl were added to each well. The substrate reaction was allowed to proceed for 30 min before the absorbance was read at 410 nm (VersaMax ELISA Microplate Reader, Molecular Devices, Sunnyvale CA, USA). The data were evaluated with SoftMax Pro 5.4.5 software.

Peptides were obtained from EMC microcollections GmbH, Tübingen, Germany and were N-terminally acetylated in order to increase stability.

Carbonate buffer

The carbonate buffer contained 100 mM NaHCO₃.

ELISA blocking buffer

The ELISA blocking buffer contained 2% (w/v) BSA in TBST 0.05% or alternatively 0.1-0.2% milk (frema Reform Instant-Magermilchpulver, Granovita GmbH, Heimertingen, Germany) in TBST 0.05%.

TBST 0.05%

To prepare TBST 0.05%, 150 mM NaCl and 50 mM Tris were dissolved and the pH was adjusted to 7.5. Thereafter, 0.05% (v/v) Tween 20 were added.

ABTS-Stock solution

The ABTS-Stock solution was prepared by dissolving 22 mg ABTS in 100 ml of 50 mM sodium citrate solution, pH 4.0.

5.3 Peptide phage display library screening

For the phage display peptide library screening, the Ph.D.-7 library (New England BioLabs, Bioconcept, Allschwil, Switzerland) was used, which displays linear heptapeptides.

Peptides interacting with the target protein were selected in three consecutive rounds of panning. Thereby, the eluted phages from earlier rounds were amplified and used as input phage for the next round. The eluted phages from the third round were amplified individually. Next, the interaction with the target protein was assessed with an ELISA and the peptide sequences of the phages showing the strongest binding were determined.

Surface panning

For coating of the bait-protein, wells (F8 Maxisorp Nunc Immuno-Module, Thermo Fisher Scientific AG, Reinach, Switzerland) received 10-100 µg/ml of bait-protein in carbonate buffer and were incubated at 4 °C with gentle agitation in a humidified container overnight. Streptavidin (New England BioLabs, Bioconcept, Allschwil, Switzerland) was used in parallel as a positive control. The next day, the coating solution was poured off and wells were blocked for 2 h at 4°C. Wells were washed six times with TBST 0.1% (v/v) Tween 20 for the first round of panning and 0.5% (v/v) Tween 20 for the second and third round of panning using a wash bottle. A 100-fold representation of the library (10^{11} plaque forming units (pfu)) was diluted with 100 µl of TBST 0.01% or 0.05%, respectively, added to the coated wells and gently rocked at RT for 60 min. Unbound phages were removed by washing ten times with TBST and bound phages were eluted with 100 µl of phage display elution buffer by rocking gently for 10-20 min. The eluate was neutralized with 15 µl of 1 M Tris, pH 9.1 and stored at 4 °C until amplification. For the streptavidin control experiment, the bound phages were eluted by gently rocking with 0.1 mM biotin (New England BioLabs, Bioconcept, Allschwil, Switzerland) in TBS for 30 min.

Carbonate buffer

The carbonate buffer contained 100 mM NaHCO₃ and the pH was adjusted to 8.6.

Phage display blocking buffer

The phage display blocking buffer was prepared by dissolving 0.5% (w/v) BSA in carbonate buffer. The buffer for the streptavidin control experiment was supplemented with 0.1 µg/ml streptavidin.

Phage Display elution buffer

For the phage display elution buffer, 0.1% (w/v) BSA were dissolved in 0.2 M glycine, pH 2.2.

Phage precipitation

E. coli ER2738 (New England BioLabs, Bioconcept, Allschwil, Switzerland) were streaked on selective (20 µg/ml tetracycline (Sigma-Aldrich Chemie GmbH, Buchs SG, Switzerland) in 1:1 ethanol/water) LB agar plates and incubated at 37 °C overnight. Next, a single colony was used to inoculate 20 ml of selective LB medium. The culture was grown to early-log phase ($OD_{600\text{ nm}}=0.01-0.05$) at 200 rpm at 37 °C. Eluted phages from the first and second round were amplified by infection of the early-log phase culture and incubation at 37 °C and 200 rpm for 4.5 h. Third round eluates were not amplified, but directly used for ELISA or sequencing. The cultures were centrifuged with 12'000 x g at 4 °C for 10 min (Sorvall RC 6 Plus, Thermo Electron Corporation, Rotor SS34). After re-centrifuging the supernatant, the phages were precipitated at 4 °C overnight by adding 2.7 ml of precipitation buffer to 16 ml of the supernatant. The precipitated phages were pelleted by centrifugation at 12'000 x g at 4 °C for 15 min. The supernatant was decanted and the phage pellet re-centrifuged for 3 min. After removal of the residual supernatant, the phage pellet was resuspended in 1 ml of TBS and incubated at RT for 60 min. The phage suspension was transferred to a fresh tube, followed by centrifugation at 14'000 rpm for 5 min. Thereafter, the supernatant was transferred to a fresh tube and the phages were re-precipitated by addition of 167 µl of precipitation buffer and incubation on ice for 60 min. The phage suspension was centrifuged at 14'000 rpm and 4 °C for 10 min. Next, the supernatant was discarded and the pellet re-centrifuged for 90 s. The residual supernatant was removed, the phages were resuspended in 200 µl TBS, incubated at RT for 60 min and centrifuged at 14'000 rpm for 1 min. The supernatant containing the amplified phages to be used for subsequent panning rounds, was transferred to a fresh tube, incubated at 65 °C for 15 min to kill residual bacteria and stored at 4 °C.

Precipitation buffer

The precipitation buffer contained 20% (w/v) PEG 8000 (Sigma-Aldrich Chemie GmbH, Buchs SG, Switzerland) in a 2.5 M NaCl solution.

Determination of the phage eluate titer

For the determination of the phage titer, serial dilutions of the eluted phages (10^8-10^{11} for the amplified first and second round eluates, 10^4-10^7 for the unamplified third round eluates) in LB medium were prepared and 10 µl were used to infect 200 µl of *E.coli* ER2738 mid-log culture. After vortexing for 10 s and incubation at RT for 1-5 min, the infected bacteria were transferred to 3 ml of previously melted Top Agar, immediately vortexed and spread on selective LB agar plates for blue/white screening. The plates were allowed to cool down for 5-10 min and incubated at 37 °C overnight. A phage titer, determined by counting blue plaques only, of $\sim 10^{13-14}$ pfu/ml was expected. For the second and third round panning experiments, a volume corresponding to 10^9-10^{11} pfu was used as input phage.

Top Agar

For the preparation of Top Agar, 1% (w/v) bacto-tryptone, 0.5% (w/v) bacto-yeast extract, 0.5% (w/v) NaCl, and 0.7% (w/v) bacto-agar were dissolved in water.

LB agar plates for blue/white screening

The LB agar plates were prepared by adding IPTG (50 µg/ml in DMF) and x-gal (40 µg/ml in DMF) to selective LB medium supplemented with 1.5% (w/v) bacto-agar.

Amplification of single plaques

Blue plaques (around 10-20) from a freshly titered plate (<1-3 days, <100 plaques) were amplified in 1 ml of a 1/100 dilution of an *E.coli* ER2738 overnight culture at 37 °C and 200 rpm for 4.5-5 h. The cultures were pelleted at 14'000 rpm for 30 s. Whereas the bacterial pellet was stored at -20 °C for subsequent alkaline lysis and sequencing, the supernatant was re-centrifuged in a fresh tube. The upper 80% of the phage-containing supernatant were transferred to a fresh tube and incubated at 65 °C for 15 min to kill residual bacteria. Finally, the amplified phage stock was stored at 4 °C.

Phage ELISA

Multi-well plates were coated with 10-100 µg/ml of target protein dissolved in 100 µl of carbonate buffer or streptavidin control at 4 °C overnight with gentle agitation in a humidified container. Control wells received 100 µl incubation buffer without target protein. The wells were blocked with 0.5% (w/v) BSA in carbonate buffer at 4 °C for 2 h. Then, wells were washed six times with TBST 0.5%. The amplified phage stock from the third panning round was diluted 1:1 with blocking buffer, and 100 µl were added to a well coated with target protein and a control well, respectively, and incubated at RT for 2 h with agitation. Unbound phages were removed by washing six times with TBST 0.5%. Bound phages were detected by addition of an M13-specific antibody-conjugate diluted in blocking solution (1/5000) at RT for 1 h with agitation. After removal of unbound antibody-conjugate by washing six times with TBST 0.5%, the ABTS substrate was added. The absorbance was read at 415 nm after 10, 30 and 45 min (Bio-Rad Model 680 Microplate Reader, Microplate Manager 5.2 Software).

Alkaline lysis for preparation of DNA

The DNA was isolated from bacterial pellets by alkaline lysis. To this end, the pellets from bacteria infected with a single phage each, were resuspended in 100 µl of Buffer R3 (Pure link HiPure Plasmid Filter Purification Kit, Invitrogen) and incubated at RT for 5 min. The bacterial cells were lysed by incubation with 200 µl of Buffer L7 (Pure link HiPure Plasmid Filter Purification Kit, Invitrogen) on ice for 5 min. The suspension was mixed with 150 µl of Buffer N3 (Pure link HiPure Plasmid Filter Purification Kit, Invitrogen), briefly vortexed and incubated on ice for 15 min. The mixture was centrifuged

at 16'000 x g for 5 min. The supernatant was transferred to a fresh tube and DNA was precipitated by the addition of 1 ml of 100% ice-cold ethanol, followed by vortexing and incubation at -20 °C for 5 min. The precipitated DNA was pelleted by centrifugation at 16'000 x g for 5 min. Thereafter, the pellet was resuspended in 250 µl of 0.3 M sodium acetate, pH 4.8, mixed with 700 µl of 100% ice-cold ethanol, vortexed and centrifuged at 16'000 x g for 5 min. The DNA pellet was dried and resuspended in 20 µl water and dissolved by incubation for 30 min at RT. The plasmid DNA (1.2 µg) was sequenced with primer -96 gIII (5'-CCC TCA TAG TTA GCG TAA CG-3'). Experiments yielding the consensus site (His-Pro-Gln) for the streptavidin control were considered successful.

Protein database search of identified peptides for sequence similarities

A basic local alignment search tool (BLAST) search of the NCBI protein database was performed to search for sequence similarity with known human proteins (taxid: 9606) (229). The non-redundant protein sequences database was searched with the blastp (protein-protein BLAST) algorithm. Search parameters were adjusted to search for a short input sequence by default.

5.4 *In vitro* phosphorylation assay

Expression and purification of His-tagged proteins from Sf9 insect cells

Proteins of interest were expressed using the Bac-to-Bac Baculovirus Expression System (Invitrogen, Thermo Fisher Scientific AG, Reinach, Switzerland) according to the manufacturer's instructions. For protein purification, the insect cells were washed once with 10 ml of ice-cold PBS, followed by resuspension of the pellet with 10 ml of lysis buffer. The cell suspension was sonicated (3 x 3 sec with 30% cycle and 33% power) and centrifuged at 4700 x g at 4 °C for 30 min. The supernatant was incubated with 0.5 ml equilibrated Ni-NTA resin for 1 h on ice. Unbound proteins were removed by washing with 20 ml of wash buffer, after which the bound proteins were eluted with 5 ml of elution buffer.

Protein expression and purification from Sf9 insect cells were performed in the Molecular Pharmacology Unit, ETH Zurich, Switzerland by Stefan Wolf.

Lysis buffer

The lysis buffer contained 300 mM NaCl and 50 mM HEPES supplemented with 1% (v/v) IGEPAL CA-630 (Sigma-Aldrich Chemie GmbH, Buchs SG, Switzerland), 1 mM PMSF (Sigma-Aldrich Chemie GmbH, Buchs SG, Switzerland) and 100 µl Protease Inhibitor Cocktail (P8340, Sigma-Aldrich Chemie GmbH, Buchs SG, Switzerland). The pH was adjusted to 7.5.

Wash buffer

To prepare the wash buffer, 300 mM NaCl and 50 mM HEPES were dissolved in water and supplemented with 30 mM imidazole (Sigma-Aldrich Chemie GmbH, Buchs SG, Switzerland). The pH was adjusted to 7.5.

Elution buffer

For the elution buffer, 300 mM NaCl, 50 mM HEPES, and 300 mM imidazole were dissolved in water and the pH was adjusted to 7.5.

Phosphorylation reaction

To assess the GRK2-inhibitory activity of the peptides, a kinase assay was performed. The phosphorylation was performed in a reaction mixture of 50 μ l containing 130 nM of His-tagged GRK2 purified from Sf9 cells infected with a recombinant baculovirus, 300 nM of His-tagged protein substrate purified from bacterial culture and the compound of interest at different concentrations in DMSO at a final concentration of 2% in assay buffer. After incubation on ice for 30 minutes, the reaction was started by addition of 5 μ l of ATP ((Sigma-Aldrich Chemie GmbH, Buchs SG, Switzerland)/ γ^{32} P-ATP (10 μ Ci/ml, PerkinElmer Inc., Germany)) to give a final volume of 50 μ l. The reaction took place at 30 °C. After 30 min, the reaction was stopped by the addition of 20 μ l Bolt 4x LDS sample buffer (Invitrogen, Thermo Fisher Scientific AG, Reinach, Switzerland) and 8 μ l of Bolt 10 x sample reducing agent (Invitrogen, Thermo Fisher Scientific AG, Reinach, Switzerland). After an incubation at 70 °C for 10 minutes, phosphorylated proteins were separated by SDS-PAGE at 165 V using 12% Bolt Bis-Tris Plus gels (Invitrogen, Thermo Fisher Scientific AG, Reinach, Switzerland) and MOPS SDS running buffer.

Assay buffer

The assay buffer contained 20 mM Tris, 5 mM MgCl₂, and 2 mM EDTA dissolved in water. The pH was adjusted to 7.5.

Detection of phosphorylated proteins by autoradiography

X-ray films (Amersham Hyperfilm ECL, GE Healthcare, Sigma-Aldrich Chemie GmbH, Buchs SG, Switzerland) were exposed to the acrylamide gels for a couple of hours to overnight at -80 °C and developed as described earlier. Subsequently, exposed films were analysed using Image J software and GraphPad Prism for statistical analysis.

5.5 Cell culture

Cell thawing

A frozen aliquot of HEK293A cells (3×10^6 cells, Invitrogen, Thermo Fisher Scientific AG, Reinach, Switzerland) was removed from liquid nitrogen storage, thawed in a 37 °C water bath and slowly added to 10 ml complete medium. The cell suspension was centrifuged at 300 rpm at RT for 5 min. Next, the cell pellet was resuspended in 10 ml of complete medium. One third and two thirds, respectively, of the cell suspension were cultivated in 10 ml of complete medium on a culture dish (TPP tissue culture dish 60 cm², TPP Techno Plastic Products AG, Trasadingen, Switzerland) at 37 °C under 5% CO₂ in a humidified incubator.

Complete medium

The complete medium contained DMEM (D6429, Sigma-Aldrich Chemie GmbH, Buchs SG, Switzerland) supplemented with 10% (v/v) FBS (Hyclone, Lot RZG35920, Thermo Fisher Scientific AG, Reinach, Switzerland) and 100 U/ml penicillin/100 µg/ml streptomycin (Sigma-Aldrich Chemie GmbH, Buchs SG, Switzerland).

Cell cultivation

Adherent HEK293A cells were cultured in complete medium at 37 °C and 5% CO₂ in a humidified incubator. Cell culture medium was changed at least every three days.

Cell splitting

Adherent cells were washed with PBS (Dulbecco's phosphate buffered saline, Sigma-Aldrich Chemie GmbH, Buchs SG, Switzerland) and trypsinized with 0.05% Trypsin-EDTA (Sigma-Aldrich Chemie GmbH, Buchs SG, Switzerland) for 2-3 min. Trypsin was inactivated by the addition of 10% FBS-containing medium (three volumes).

Determination of the cell number

For determination of the cell number, the cell suspension was mixed with an equal volume of 0.4% (w/v) Trypan Blue (Sigma-Aldrich Chemie GmbH, Buchs SG, Switzerland) in PBS. The cells were counted using a Neubauer hemocytometer (LO-Laboroptik GmbH, Bad Homburg, Germany) according to the manufacturer's instructions. After applying 10 µl of the 1:1 diluted cell suspension, the number of living cells in four squares was counted. The cell concentration (cells/ml) was calculated with the following formula:

$$\text{concentration} = \frac{\text{number of cells} \times 10'000}{\text{number of squares}} \times \text{dilution factor} \times 100$$

Calcium phosphate transfection

Adherent cells, which had been cultured to 80-90% confluency, were transiently transfected using the calcium phosphate transfection method. The cells were split 1:3 and incubated for 3-4 h at 37 °C in a humidified incubator under 5% CO₂.

The following reaction mixture was prepared:

1	plasmid DNA	20 µg
2	water	to a volume of 450 µl
3	2.5 M CaCl ₂ · 2 H ₂ O	50 µl

Table 5: Reaction mixture for the calcium phosphate transfection

The plasmid DNA was diluted in water to a volume of 450 µl and 50 µl of 2.5 M CaCl₂ were added.

This mixture (Table 5) was added dropwise to 500 µl of 2 x BBS while vortexing. After an incubation of 20 min at RT, the transfection mixture was added dropwise to the previously split cells. After 12-16 hours, cells were washed with PBS and supplied with new complete medium.

BBS (2 x)

To prepare 2 x BBS, 280 mM NaCl, 1.5 mM Na₂HPO₄, and 50 mM BES (Sigma-Aldrich Chemie GmbH, Buchs SG, Switzerland) were dissolved in water and the pH was adjusted to 6.95.

Measurement of the intracellular free calcium concentration with FURA-2 (230)

Measurements were performed 36-48 h after the transfection. The adherent cells were washed with PBS, trypsinized and centrifuged at 300 rpm for 5 min at RT. The cells were loaded with FURA-2 by resuspension in 2.5 ml of complete medium supplemented with 2.5 µl of 1 mM FURA-2AM (dissolved in DMSO), followed by incubation at 37 °C under 5% CO₂ for 30 min. After centrifugation of the cells, FURA-2AM was deesterified by an incubation with 10 ml of Fura Buffer for 30 min at RT in the dark. For the measurement, the cells (1-2 x 10⁶) were centrifuged and resuspended in 2 ml of Fura Buffer. The samples were alternatively excited at intervals of 0.08 s at 340 and 380 nm and the emission was recorded at 509 nm. The measurement was performed using a Perkin Elmer LS 55 Fluorescence Spectrometer and FLWinLab software.

Fura Buffer

The Fura buffer was prepared by dissolving 138 mM NaCl, 5 mM KCl, 1 mM MgCl₂, 1.6 mM CaCl₂, 1 g/l D(+)-glucose monohydrate and 20 mM Na⁺-HEPES in water and adjusting the pH to 7.3.

5.6 Establishment of transgenic mouse lines

All animal experiments were performed in accordance with National Institutes of Health guidelines, and approved by the local committee on animal care and use (University of Zurich).

Preparation of linearized plasmid DNA for generation of transgenic mouse lines

Plasmid DNA for generation of transgenic mouse lines was prepared using the EndoFree Plasmid Maxi Kit (QIAGEN, Hombrechtikon, Switzerland) according to the manufacturer's protocol. To this end, 100 ml of bacterial culture were used and DNA was dissolved in 200 µl of endofree TE-Buffer. Plasmid DNA sequences were removed by restriction digestion with NotI. After purification by agarose gel electrophoresis, linearized DNA was diluted to 2 ng/µl.

Transgene introduction

Transgenic mice were generated in the Molecular Pharmacology Unit, ETH Zurich, Switzerland by Dr. Joshua AbdAlla as previously described (173).

Preparation of genomic DNA from mouse biopsies for the genotyping PCR

Ear-punch biopsies were digested overnight at 57 °C and 1000 rpm in 200-220 µl of Lysis buffer supplemented with 10 µl of proteinase K solution (20 mg/ml, Roche Proteinase K, Sigma-Aldrich Chemie GmbH, Buchs SG, Switzerland). The reaction was stopped by incubation for 20 min at 99 °C in a thermomixer (Eppendorf, Schönenbach, Switzerland). Samples were centrifuged at 23000 x g at 4 °C for 5 min. The supernatant containing the genomic mouse DNA was used as a template for the genotyping PCR.

Lysis buffer

The lysis buffer contained 2.5 ml of 10% sodium lauroyl sarcosinate (Sigma-Aldrich Chemie GmbH, Buchs SG, Switzerland), 1 ml of 5 M NaCl, and 2.5 g Chelex-100 (Bio-Rad Laboratories AG, Cressier, Switzerland) in a total volume of 50 ml.

Genotyping PCR

The PCR reaction was performed using *Taq* Polymerase in the supplied buffer supplemented with 50 µg/ml BSA (New England BioLabs, Bioconcept, Allschwil, Switzerland), 250 µM MgCl₂ (Promega AG, Dübendorf, Switzerland), and 100 µM dNTPs.

Primers specific for the α -MHC-vector were used at 0.625 μ M, namely MHC2 (5'-AGG ACT TCA CAT AGA AGC CTA GCC CAC ACC-3') as a forward primer and HGH2 (5'- ATT AGG ACA AGG CTG GTG GGC ACT GGA GTG-3') as a reverse primer. The PCR reaction was carried out in a reaction volume of 40 μ l with 1.5 μ l of genomic mouse DNA prepared as described above. Amplifications were performed with a standard program using a Thermocycler 3000 (Biometra, Göttingen, Germany):

Step	Temperature	Time
1	95 °C	2 min
2	95 °C	45 s
3	60 °C	60 s
4	72 °C	60 s
5	72 °C	10 min

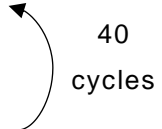


Table 6: Standard PCR program for the genotyping of transgenic mice

An initial melting step (step 1) at 95 °C for 2 min was followed by 40 cycles of melting of dsDNA at 95 °C for 45 s (step 2), annealing of the primers at 60 °C for 60 s (step 3) and elongation of the primers at 72 °C for 60 s (step 4). A final elongation step (step 5) at 72 °C for 10 min was added and samples were subsequently cooled down to 4 °C.

The amplified fragments were mixed with 5x Green GoTaq Flexi Buffer (Promega AG, Dübendorf, Switzerland) and separated by agarose gel electrophoresis in 2% (w/v) agarose gels prepared with 10 μ l/100 ml 1% (w/v) ethidium bromide for visualization.

Abdominal aortic constriction

Abdominal aortic constriction was performed in the Molecular Pharmacology Unit, ETH Zurich, Switzerland, essentially as described (143,231).

5.7 Statistical analysis

Data were analysed using GraphPad Prism 6 software. Groups were analysed using two-tailed student's t-test and p-values < 0.05 were considered significant. Results are given as mean \pm SEM.

6 Results

6.1 Cloning, protein expression and purification of GRK2 domains

GRK2 is a drug target for a variety of pathologies (4.3). Inhibition of the multi-domain kinase can be achieved by targeting any of the three domains (Figure 10).

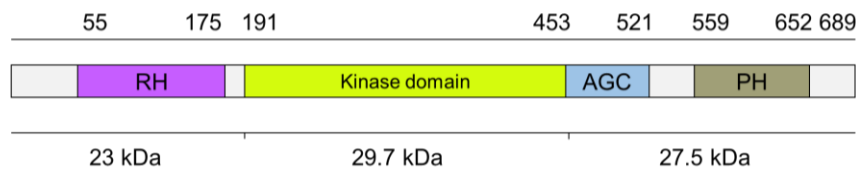


Figure 10: GRK2 is an enzyme with multiple domains

GRK2 consists of three distinct domains: The kinase domain containing the catalytically active site, flanked by the N-terminal domain mediating the interaction with the receptor and the C-terminal domain, which upon activation by the $G\beta\gamma$ -complex ($G\beta\gamma$) facilitates translocation to the cell membrane (90-95).

To screen a phage display peptide library for domain-specific interaction partners, the different GRK2 domains were overexpressed individually in the pET bacterial expression system, which allows expression of a given protein under the control of the T7 promoter. A hexahistidine tag was attached to each domain to enable protein purification by Ni-NTA chromatography.

To this end, plasmids for bacterial expression containing the corresponding cDNA sequences for the three GRK2 domains were generated.

6.1.1 Generation of GRK2 domain-containing plasmids

For the N-terminal domain of GRK2 (GRK2NTD), the cDNA corresponding to the first 190 amino acids of GRK2 was amplified by PCR using suitable primers (GRK2seq16/17) for introduction of a His-tag C-terminally. The PCR also introduced the NcoI/BamHI recognition sites for restriction endonucleases. After PCR, the amplified fragments were cut by restriction digestion with NcoI and BamHI and inserted into the NcoI/BamHI cut pET-3d plasmid.

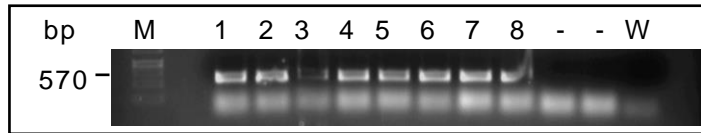


Figure 11: Cloning of C-terminally His-tagged GRK2NTD into pET-3d

Single colony screening PCR of bacterial clones: Separation by agarose gel electrophoresis showed the amplification of an approximately 570 bp fragment for clones 1-8. Control clones (-) and water control (W) were negative.

Single colony screening (Figure 11) showed that all eight colonies were positive for the GRK2NTD. Clone 6 was chosen for DNA sequencing, which confirmed the identity of the DNA and its correct insertion into pET-3d (13.1).

For cloning of the central kinase domain (GRK2KD), the cDNA coding for amino acids 191-453 of GRK2 was amplified introducing His-tags N-terminally or C-terminally, respectively, with suitable primers (GRK2seq19/20, GRK2seq34/35) (Figure 12). After introduction of the NcoI/BamHI recognition sites for restriction endonucleases by PCR, the amplified fragments were cut and inserted into the NcoI/BamHI cut pET-3d plasmid.

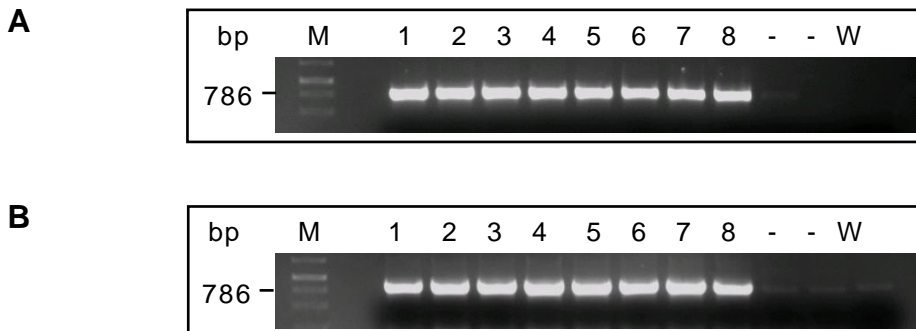


Figure 12: Cloning of N-terminally (A) and C-terminally (B) His-tagged GRK2KD into pET-3d

Single colony screening PCR of bacterial clones: Separation by agarose gel electrophoresis showed the amplification of an approximately 786 bp fragment for clones 1-8 (A and B). Control clones (-) and water controls showed only a slight or no signal.

Again, almost all bacterial colonies were positive for the DNA of interest (Figure 12). Clones 2 (6xNHisGRK2KD) and 1 (GRK2KD6xCHis) were chosen for DNA sequencing, which confirmed the identity of the DNA and its correct insertion into pET-3d (13.2, 13.3).

Cloning of the C-terminal domain was carried out by amplification of the cDNA encoding for amino acids 454-689 of GRK2 with primers (GRK2seq24/25, GRK2seq32/33) introducing His-tags N- or C-terminally, respectively (Figure 13). Recognition sites for the BspHI and BamHI restriction endonucleases were also inserted by PCR. After cutting the amplified fragments with BspHI and BamHI, they were inserted into the NcoI/BamHI cut pET-3d plasmid. This was possible, because BspHI and NcoI produce the same overhang (5'-CATG).

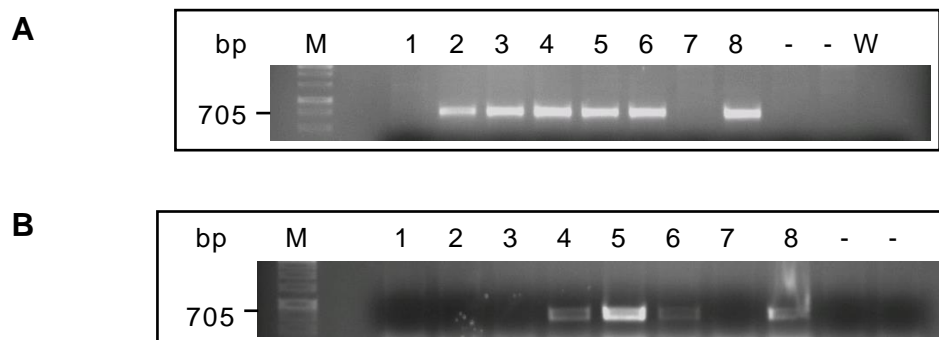


Figure 13: Cloning of N-terminally (A) and C-terminally (B) His-tagged GRK2CTD into pET-3d

Single colony screening PCR of bacterial clones: Separation by agarose gel electrophoresis showed the amplification of an approximately 705 bp fragment for clones 4-6 and 8 (A) and 2-6 and 8 (B). Control clones (-) and water control (W) were both negative.

Single colony screening showed that six out of eight colonies were positive for the N-terminally His-tagged and four out of eight for the C-terminally His-tagged GRK2CTD (Figure 13). For DNA sequencing, clones 2 (6xNHisGRK2CTD) and 4 (GRK2CTD6xCHis) were chosen, which confirmed the identity of the DNA and its correct insertion into pET-3d (13.4, 13.5).

6.1.2 Protein expression and purification of GRK2 domains

The generated pET-3d plasmids were used for the expression of His-tagged GRK2 domains in *E.coli* BL21(DE3)pLysS.

Protein expression and purification of GRK2NTD

The plasmid coding for C-terminally His-tagged GRK2NTD (GRK2NTD6xCHis) was transformed into *E.coli* BL21(DE3)pLysS and protein expression was induced with 1 mM IPTG. Uninduced controls plus samples isolated 1, 2 and 3 h after IPTG-induction were separated by SDS-PAGE. A band of 24 kDa was induced in the GRK2NTD samples, but was absent in the controls. The relative molecular mass of ~24 kDa corresponds well with the expected mass of GRK2NTD6xCHis. Immunoblot detection with a polyclonal

GRK2-specific antibody (1/2000) confirmed the identity of the IPTG-induced 24-kDa protein as GRK2NTD in samples 1, 2 and 3. Maximum induction of GRK2NTD was already achieved after 1 h of induction.

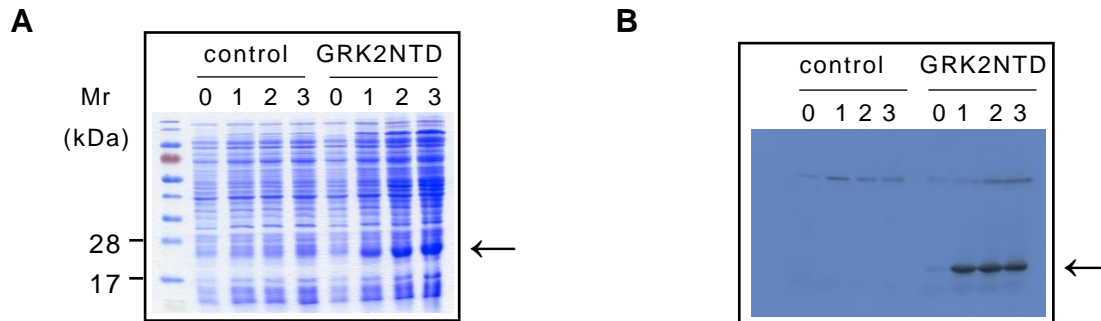


Figure 14: Protein expression of GRK2NTD6xCHis

Aliquots before (0) and 1, 2 and 3 hours (1-3) after IPTG-induced protein expression were resolved by SDS-PAGE followed by Coomassie brilliant blue staining (A) or detected by immunoblotting with a polyclonal GRK2-specific antibody (B).

Next, the GRK2NTD6xCHis was purified by Ni-NTA chromatography. To this end, pelleted bacteria from 50 ml of culture were resuspended with 10 ml of lysis buffer. After reduction of the viscosity by sonication, the suspension was centrifuged and the cleared supernatant incubated with 2 ml equilibrated Ni-NTA resin overnight. Unbound proteins were removed by washing with 30 ml of wash buffer, followed by elution of the bound proteins with 1.5 ml of elution buffer, pH 5.9 and subsequently 1.5 ml of elution buffer, pH 4.3. The purified protein was collected in four aliquots of 0.75 ml each. The overall yield of the purified protein was only 3 mg from 200 ml of bacterial culture.

The Coomassie brilliant blue staining of the flow-through, washes and eluates separated by SDS-PAGE showed no band with the expected size of ~24 kDa (data not shown), probably due to the low amount of the target protein (GRK2NTD6xCHis). Thus, eluates E1-E3 were precipitated with acetone to concentrate the purified protein. Separation of the acetone-precipitated eluates E1-E3 by SDS-PAGE revealed a weak band in all eluates (Figure 15, A). Immunoblot detection with a polyclonal GRK2-specific antibody showed equal amounts of purified protein in eluates E1-E3 (Figure 15, B).

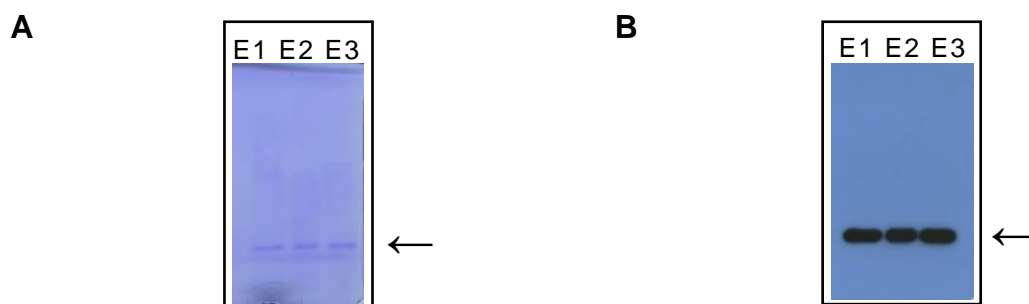


Figure 15: GRK2NTD6xCHis was purified by Ni-NTA chromatography

Eluates E1-E3 from the protein purification of GRK2NTD6xCHis were resolved by SDS-PAGE (A). Proteins were stained with Coomassie brilliant blue (A) and GRK2NTD was detected by immunoblotting with a polyclonal GRK2-specific antibody (B).

Protein expression and purification of GRK2KD

The plasmid coding for the N-terminally or C-terminally His-tagged GRK2KD, respectively, (6xNHisGRK2KD, GRK2KD6xCHis) was transformed into *E.coli* BL21(DE3)pLysS and protein expression was induced with 1 mM IPTG. Separation of the proteins from uninduced samples and samples after hours 1-3 by SDS-PAGE revealed no expression of the C-terminally His-tagged protein (data not shown). For the N-terminally His-tagged protein, by contrast, analysis by SDS-PAGE showed the strong induction of a protein of ~28 kDa in samples 1, 2 and 3 increasing over time (Figure 16, A). The relative molecular mass of 6xNHisGRK2KD is ~30 kDa. Thus, GRK2KD runs slightly lower in the SDS-PAGE gel than expected. This effect might be a result of the basic character of the protein ($pI=8.6$) or of the N-terminal position of the His-tag, which can result in the purification of an incompletely translated or a degraded protein.

For the purification of 6xNHisGRK2KD, bacteria from a 200 ml bacterial expression culture were resuspended with 20 ml of lysis buffer, sonicated and centrifuged. The cleared supernatant was incubated with 2 ml of Ni-NTA resin overnight with agitation. After washing with 40 ml of wash buffer, the purified protein was eluted at pH 4.3 and collected in five 2 ml aliquots. From 200 ml of bacterial culture, up to 8 mg protein could be purified.

Aliquots taken during the purification steps were resolved by SDS-PAGE (Figure 16, B). Coomassie blue staining showed reasonable purification of a ~ 28-kDa protein.

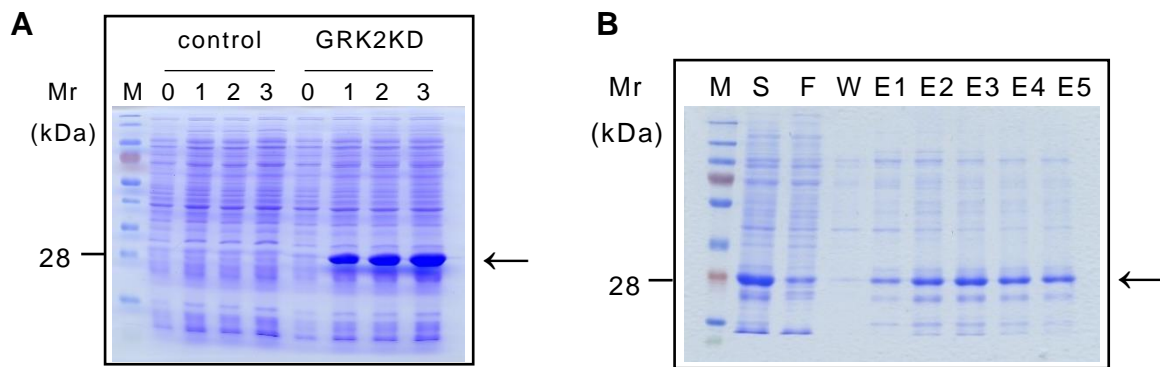


Figure 16: GRK2KD was purified by Ni-NTA chromatography

Aliquots taken before (0) and 1, 2 and 3 hours after (1-3) IPTG-induced protein expression were resolved by SDS-PAGE (A).

Aliquots from the supernatant (S), flow-through (F), wash (W) and eluates (E1-E5) from the purification of 6xNHisGRK2KD were resolved by SDS-PAGE. Proteins were stained with Coomassie brilliant blue. M, Marker

Protein expression and purification of GRK2CTD

E.coli BL21(DE3)pLysS were transformed with the plasmid coding for N-terminally or C-terminally His-tagged GRK2CTD, respectively, (6xNHisGRK2CTD, GRK2CTD6xCHis). Samples before and 1, 2 and 3 h after induction of protein expression with 1 mM IPTG were resolved by SDS-PAGE. Coomassie brilliant blue staining showed the strong induction of a protein of ~30 kDa, which increased during the 3 h induction period (Figure 17). As the relative molecular mass of His-tagged GRK2CTD is ~28 kDa, GRK2CTD runs slightly higher in the SDS-PAGE gel than expected.

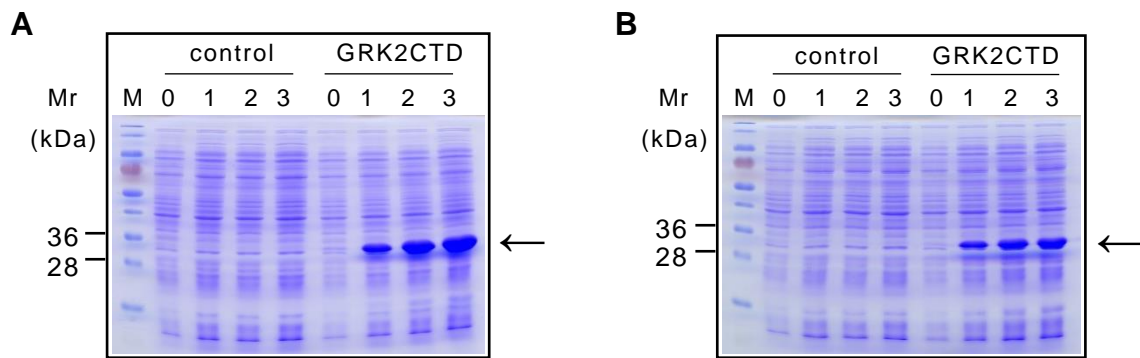


Figure 17: Protein expression of GRK2CTD

Aliquots before (0) and after 1, 2 and 3 hours (1-3) of IPTG-induced protein expression of N-terminally (A) and C-terminally (B) His-tagged GRK2CTD were resolved by SDS-PAGE. Proteins were stained with Coomassie brilliant blue. M, Marker

For purification, 200 ml of bacterial expression culture were pelleted, followed by resuspension with 20 ml of lysis buffer. After sonication and centrifugation, the cleared supernatant was incubated with 2 ml of Ni-NTA resin overnight with agitation. After removal of unbound protein by washing with 40 ml of wash buffer, the purified protein was eluted at pH 4.3 and collected in five 2 ml aliquots. Up to 15 mg of purified protein could be obtained from 200 ml of bacterial culture.

Aliquots of the purification procedure were resolved by SDS-PAGE (Figure 18). Coomassie brilliant blue staining showed the enrichment of a ~ 30-kDa protein. Again, the band is slightly higher than expected for the His-tagged GRK2CTD with a relative molecular mass of ~28 kDa.

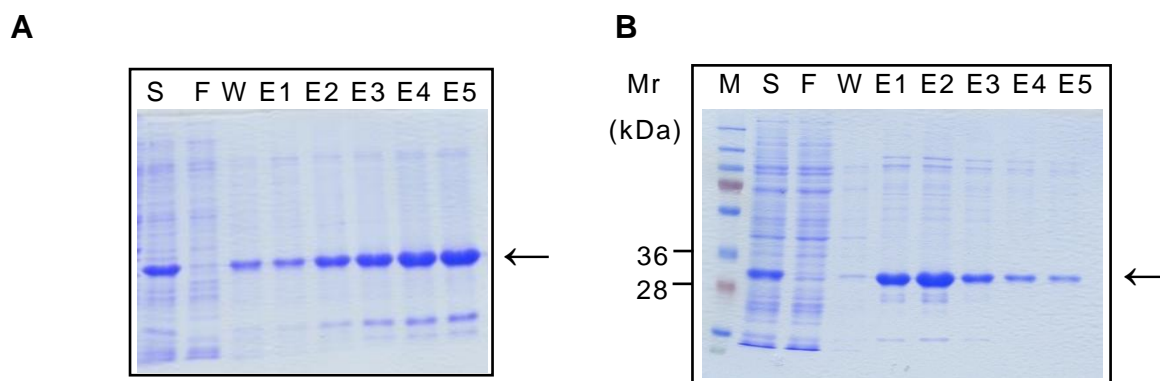


Figure 18: GRK2CTD was purified by Ni-NTA chromatography

Aliquots from the supernatant (S), flow-through (F), wash (W) and eluates (E1-E5) of the purification of 6xNHisGRK2CTD (A) and GRK2CTD6xCHis (B) were resolved by SDS-PAGE. Proteins were stained with Coomassie brilliant blue. M, Marker

6.2 Peptide phage display library screening with GRK2CTD as bait

6.2.1 Panning procedure

After purification of the recombinant GRK2CTD6xCHis in high amounts, it was used as a bait in three rounds of panning with a library displaying 1×10^9 different heptapeptides as described in chapter 5.3. A control experiment used streptavidin.

For the first round of panning, one well of a 96-well plate was coated overnight at 4 °C with 125 μ l of purified GRK2CTD (35 μ g/ml) in carbonate buffer (pH 8.6) and, as a control, one well was coated with 125 μ l streptavidin (100 μ g/ml) in carbonate buffer. The phage titer of the amplified eluates was determined by streaking dilutions (10^8 - 10^{11}) on selective LB agar plates. Counting of the phage plaques yielded a phage titer of $8.6 \cdot 10^{12}$ pfu/ml for GRK2CTD and $1.25 \cdot 10^{12}$ pfu/ml for the streptavidin control experiment, respectively. Consequently, input phage volumes corresponding to 10^{11} pfu for the second round of panning were calculated to be 12 μ l (GRK2CTD) and 80 μ l (streptavidin control experiment), respectively. The amplified eluate was applied onto the plate coated with GRK2CTD in a total volume of 150 μ l.

The second round of panning used wells coated with 125 μ l of protein solution (100 μ g/ml each) in carbonate buffer. The phage titer of the amplified eluates was determined to be approximately 10^{13} pfu/ml for both GRK2CTD and the streptavidin control experiment.

For the third round of panning, 10 μ l of amplified eluates corresponding to approximately 10^{11} pfu were diluted with 140 μ l TBS and used as input phage.

For the third round of panning, wells were again coated with 125 μl of protein solution (100 $\mu\text{g}/\text{ml}$ each) in carbonate buffer. In contrast to the first two rounds, eluates were not amplified, but rather diluted (10^4 - 10^7) and titered directly. The phage titer was determined to be approximately 10^7 pfu/ml for both GRK2CTD and streptavidin.

Amplified phage stocks were prepared for 11 clones from the last titering steps for both GRK2CTD and the streptavidin control experiment.

6.2.2 Phage ELISA

An ELISA was performed to evaluate binding of the eluted phages to purified GRK2CTD6xCHis. To this end, wells were coated overnight at 4 $^\circ\text{C}$ with 125 μl of GRK2CTD6xCHis solution (125 $\mu\text{g}/\text{ml}$) in carbonate buffer (pH 8.6) or empty buffer as a control. For the streptavidin control experiment, streptavidin was used instead of purified GRK2CTD6xCHis. After blocking with carbonate buffer supplemented with 0.5 % BSA for 2 h at 4 $^\circ\text{C}$, wells were washed six times with TBST 0.5%. Thereafter, 100 μl of amplified phage stocks 1:1 diluted with blocking buffer were added to the protein-coated wells or control wells. After incubation for 2 h at RT with shaking, wells were washed as above and 200 μl of M13-specific monoclonal antibody (1/5000 in blocking buffer) were added. After incubation for 1 h at RT with shaking, wells were washed again as above and 200 μl of freshly prepared ABTS-substrate solution were added to each well. After allowing the substrate reaction to proceed for 30 min, the absorbance was read at 415 nm. Phages showing the strongest signal in this assay (Figure 19) were sequenced.

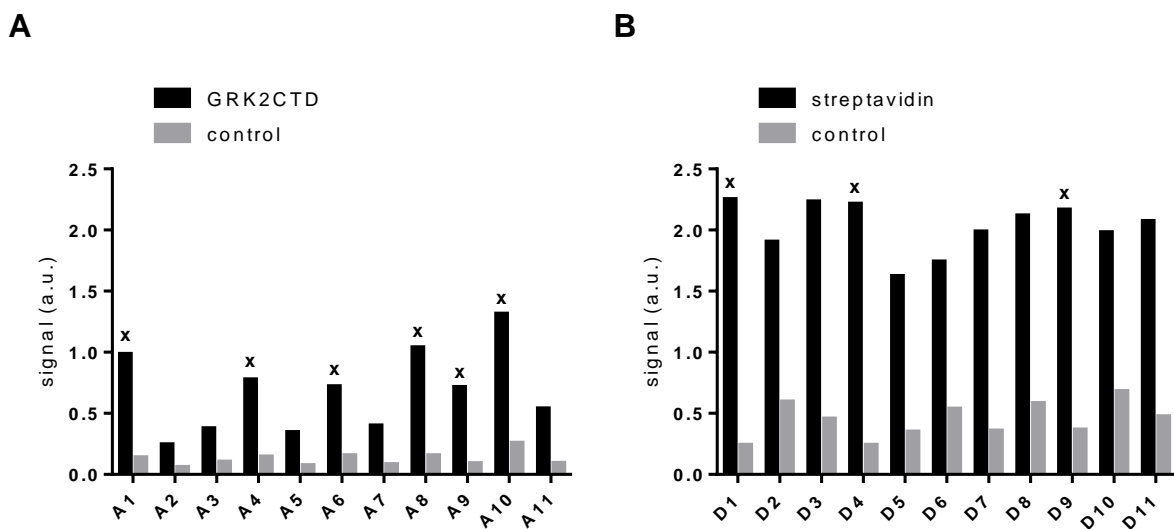


Figure 19: Evaluation of binding by a phage ELISA

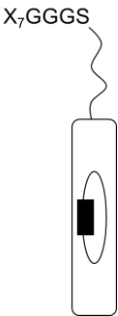
(A) Binding of eluted phages to GRK2CTD. (B) Binding of eluted phages from the streptavidin control experiment to streptavidin.

6.2.3 Peptide results

The DNA for sequencing was prepared by alkaline lysis for clones A1, A4, A6, A8, A9 and A10 and resuspended with 20 µl of water. For the sequencing, 1.2 µg DNA and 4 pmol of the primer -96gIII were used. The results are displayed in Table 7.

Clones D1, D4 and D9 of the streptavidin control experiment were also sequenced. They all yielded the expected consensus sequence site (WLFNHPQ) (232).

A



B

Clone	Sequence
A1	ASTLIVEF
A4	IRYVPQT
A6	HGGVRLY
A8	HYTDFRW
A9	IVSLQTP
A10	HYIDFRW

Table 7: Peptide sequences

(A) Schematic drawing of a phage displaying a random peptide sequence with a GGGs-linker. (B) Peptide sequences of eluted phages.

6.3 Development of a GRK2-interacting peptide based on the panning results

6.3.1 BLAST sequence analysis

Phage display technology may be utilized as a source to identify novel interaction partners for a specific bait-protein (233,234). Therefore, the NCBI protein database was searched for sequence similarity of the phage display-derived heptapeptides with known human proteins. Agreement in at least six continuous amino acids was considered as a hit (Table 8).

Protein	Sequence	Protein sequence
WDR76	ASTLIVF	...SFSSFDFLAED ASTLIV GHWDGNMSL...
Cadherin 20	IRYVPQT	...MLPEIESL FRYVPQT CAVNS...
-	HGGVRLY	-
-	HYTDFRW	-
NFATc2	IVSLQTP	...PESSGR IVSLQT ASNPIECS...
-	HYIDFRW	-

Table 8: Peptide sequence homology with known proteins

A BLAST search of the NCBI protein database identified sequence homology (i.e. at least six continuous amino acids in common) with known proteins for three of the six phage display-derived peptides.

The peptide sequence ASTLIVF showed homology with the WD repeat-containing protein 76 (WDR76), IRYVPQT with cadherin 20 and IVSLQTP with the nuclear factor of activated T-cells (NFAT).

WD repeat-containing proteins are abundant in the mammalian proteome (235). Intriguingly, G β is a prominent member of this protein family and displays the characteristic seven-bladed propeller structure (Figure 20).

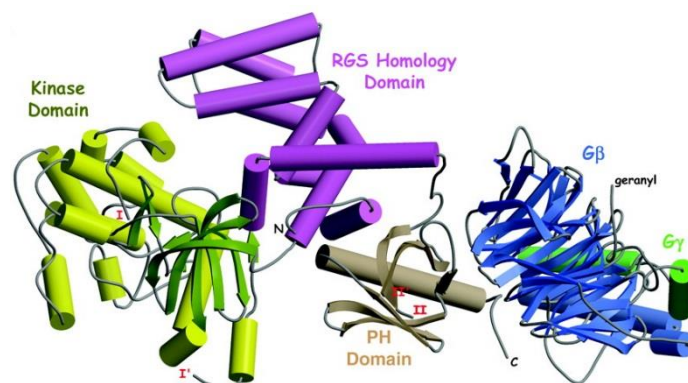


Figure 20: Model of the crystal structure of GRK2 in complex with G β γ

The crystal structure of bovine GRK2 with G β 1 γ 2 shows the characteristic WD domain structure of G β γ interacting with the C-terminal domain of the kinase (236).

With regard to the known interaction of the WD repeat-containing protein G β with GRK2CTD, this peptide (ASTLIVF) was considered the most promising one for further investigation.

6.3.2 Sequence elongation based on WDR76

Thus, the original phage display-derived peptide (ASTLIVF) was elongated based on the sequence of WDR76 (Table 9).

original peptide	ASTLIVF
WDR76	...RNERSSFSSFDFLAED ASTLIV GHWDGNMSLVDRRTPGTSY...
WD1 peptide	ASTLIV GHWDGNMSLVDRRT
WD2 peptide	FLAED ASTLIV GHWDGNMSL
WD3 peptide	ERSSFSSFDFLAED ASTLIV F

Table 9: Sequence elongation of WD-peptides

The original peptide from the peptide phage display library screen was elongated C-terminally (WD1), N-terminally (WD3) or in both directions (WD2) to a length of ~20 amino acids.

The longer peptides (WD1 and WD3) were subsequently characterized for their potential to interact with GRK2. WD2 showed strong aggregation and therefore could not be tested.

6.3.3 An ELISA shows selective binding of GRK2CTD to WD3

To investigate the interaction of the WD1 and WD3 peptides with GRK2CTD, an ELISA binding experiment was performed by coating WD1 or WD3, respectively, at increasing concentrations. To enhance coating efficiency, BSA was added to a total protein concentration of 4 µg/ml (237). GRK2CTD was added at a constant concentration of 2 µg/ml. Bound GRK2CTD was detected using a primary GRK2CTD-specific polyclonal antibody (1/300) and a secondary HRP-conjugated antibody (1/4000). The substrate reaction was allowed to proceed for 30 min, after which the absorbance was read at 410 nm.

GRK2CTD shows concentration-dependent binding to WD3 (Figure 21). For WD1, in contrast, a concentration-dependent increase in GRK2CTD-binding cannot be observed. Although at 10 µg/ml, WD1 shows a significant interaction with GRK2CTD, WD1 shows no concentration-dependent interaction as can be seen for WD3.

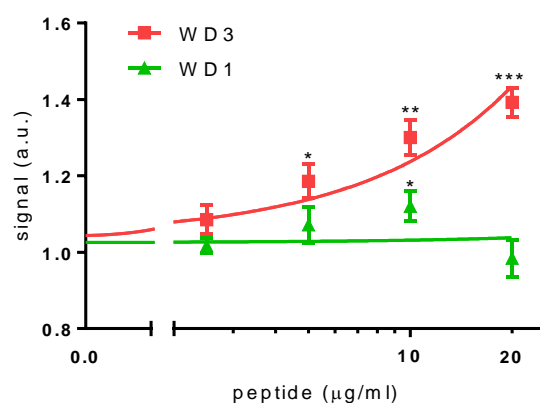


Figure 21: GRK2CTD shows selective binding to WD3 in an ELISA

Wells coated with increasing amounts (2.5, 5, 10 and 20 µg) of the elongated peptides WD1 and WD3, respectively, were exposed to GRK2CTD at a constant concentration of 2 µg/ml.

Data of four experiments are displayed as mean ± SEM. Statistical analysis was performed using an unpaired student's t-test. Linear curve fitting was performed using GraphPad Prism 6.

6.4 The GRK2-interacting peptide shows GRK2-inhibitory features

6.4.1 WD3 interferes with the binding of GRK2CTD to Gβ3

Blockade of the Gβγ-binding to GRK2 via its C-terminal domain confers kinase inhibition (191,192), as Gβγ subunits are essential for kinase activation and targeting to the plasma membrane (38). Similarly, a compound interacting with the GRK2CTD could inhibit GRK2 function by interfering with this protein-protein interaction. Thus, the effect of the peptides WD1 and WD3, respectively, on the Gβ-GRK2CTD interaction was examined in an inhibition ELISA. The Gβ-subunit directly interacts with GRK2 (238,239), whereas the Gγ-subunit mediates membrane anchoring of the Gβγ-GRK2-complex via its prenylation site (240). Thus, the assay was performed using only Gβ-subunits. More specifically, Gβ3 and a shorter splice variant, Gβ3-s, were used.

6.4.1.1 GRK2CTD binds to Gβ3 and Gβ3-s

To verify the interaction of Gβ3 and Gβ3-s with GRK2CTD, a direct binding ELISA was performed using recombinant His-tagged proteins purified from bacterial cultures. Gβ3 and Gβ3-s, respectively, were coated at different concentrations ($6 \cdot 10^{-7}$ M, $3 \cdot 10^{-7}$ M,

1.5·10⁻⁷ M, 7.5·10⁻⁸ M, 3.75·10⁻⁸ M, 1.88·10⁻⁸ M, 9·10⁻⁹ M) and GRK2CTD was added at a constant concentration of 6 µg/ml. As a control, wells were coated with BSA. A polyclonal GRK2-specific antibody (1/300) was used as a primary and a HRP-conjugated antibody (1/10'000) as a secondary antibody. Absorbance was read at 410 nm 30 min after addition of the substrate ABTS.

Whereas GRK2CTD did not interact with BSA, GRK2CTD interacted with both Gβ3 and Gβ3-s in a concentration-dependent manner (Figure 22).

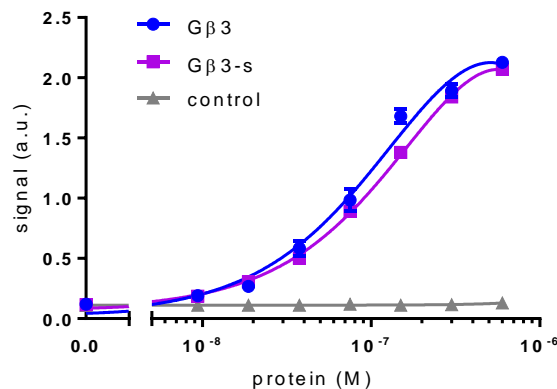


Figure 22: GRK2CTD binds Gβ3 and Gβ3-s

Binding of GRK2CTD to Gβ3 and Gβ3-s, respectively, was determined by ELISA. BSA was used as a control.

Data of three independent experiments are displayed as mean ± SEM.

6.4.1.2 WD3 inhibits the binding of GRK2CTD to Gβ3

Based on the binding assay described above, an inhibition ELISA was performed by coating with a constant concentration (6·10⁻⁷ M) of Gβ3 and Gβ3-s, respectively. After removal of unbound protein by washing steps, GRK2CTD was added at a constant concentration (6 µg/ml) and pre-mixed with increasing amounts of the elongated peptides WD1 and WD3, respectively. For detection, a primary polyclonal GRK2CTD-specific antibody (1/300) and a secondary HRP-conjugated antibody (1/4000) were used. Absorbance was read at 410 nm 30 minutes after addition of the substrate.

The results show that WD3 significantly interfered with the binding of GRK2CTD to Gβ3. WD3 also showed a tendency to inhibit the interaction of GRK2CTD with Gβ3-s. In contrast, WD1 did not affect the interaction of GRK2CTD with Gβ3 or Gβ3-s at concentrations up to 100 µg/ml (Figure 23: A, B).

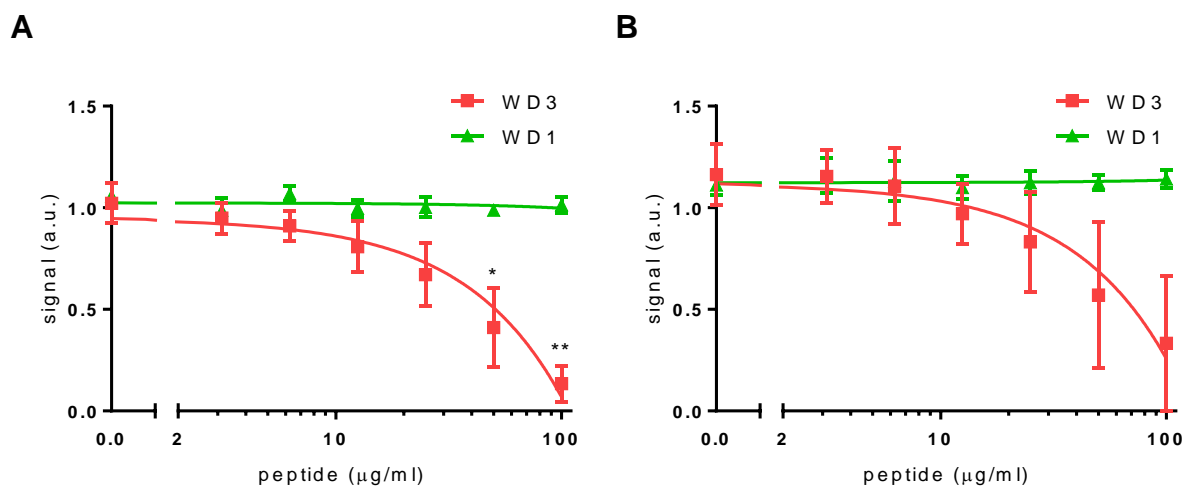


Figure 23: WD3 interferes with the binding of GRK2CTD to Gβ3 and Gβ3-s
 Binding of GRK2CTD to Gβ3 (A) and Gβ3-s (B), in the presence of different concentrations of WD1 and WD3 was assessed in an ELISA. Data of three independent experiments are displayed as mean ± SEM. Statistical analysis was performed using an unpaired student's t-test.

6.4.2 Assessment of kinase activity

To evaluate the effect of the peptides, WD1 and WD3, on the kinase activity of GRK2 a phosphorylation assay using a soluble substrate of GRK2 was performed.

6.4.2.1 WD3 inhibits the phosphorylation of the splicing factor SRSF1 by GRK2

The serine/arginine-rich splicing factor 1 (SRSF1) regulates splicing of cardiac Ca²⁺/calmodulin-dependent kinase IIδ (CAMKIIδ), thereby participating in the functional transition from juvenile-to-adult heart characterized by increased workload (241). The cytoplasmic splicing variant CAMKIIδC phosphorylates phospholamban (PLB), thereby accelerating Ca²⁺-reuptake into the sarcoplasmic reticulum and consequently increasing the rate of relaxation following contraction (242). Overexpression of CAMKIIδC results in a heart failure phenotype with disturbed Ca²⁺-handling (243).

SRSF1 contains several phosphorylation sites, including a cluster located in the C-terminal arginine/serine-rich (RS) domain (UniProt Knowledgebase). SRSF1 has recently been identified as a novel substrate of GRK2 (Quitterer, U., unpublished data).

Phosphorylation was performed using 130 nM of recombinant GRK2 purified from Sf9 insect cells infected with a baculovirus encoding for GRK2 and 300 nM of recombinant SRSF1 purified from *E.coli* as a substrate. Compounds under investigation were added at increasing concentrations dissolved in DMSO yielding a final concentration of 2% total DMSO. The GRK2-stimulated incorporation of phosphate into the SRSF1 substrate was

detected by the addition of [γ - 32 P]-labelled ATP (10 μ Ci/ml, total ATP 5 μ M). After separation by SDS-PAGE, gels were exposed to X-ray films for autoradiography. The control in the absence of peptide was set to 100% and values were calculated accordingly.

Whereas WD3 successfully inhibited the phosphorylation of SRSF1 by GRK2 ($59 \pm 9\%$, $p=0.0087$, $n=3$, Figure 24: A, C), WD1 did not lead to a reduced signal ($102 \pm 4\%$, $p=0.6126$, $n=3$, Figure 24: B, C).

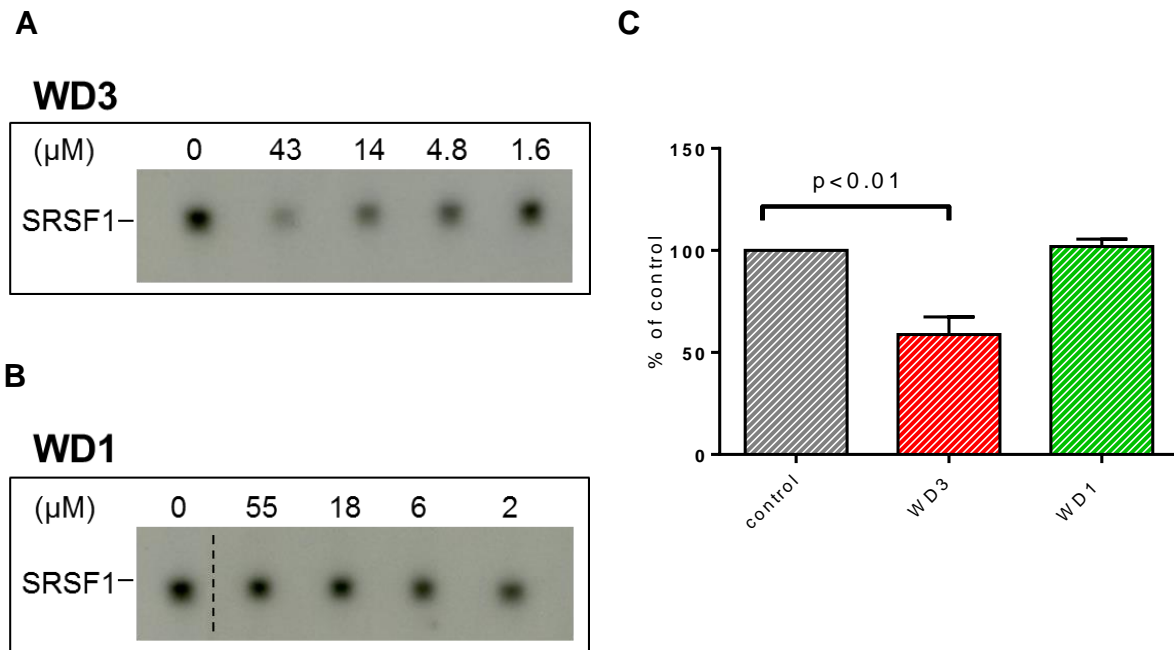


Figure 24: WD3 inhibits the phosphorylation of SRSF1 by GRK2

WD1 and WD3 were tested at different concentrations in phosphorylation assays using GRK2 and SRSF1 as a substrate.

Representative autoradiograms showing phosphorylation of SRSF1 in the presence of different concentrations of WD3 (A) and WD1 (B). (C) Statistical analysis of three independent experiments (WD3: 43 μ M, WD1: 55 μ M), (unpaired student's t-test).

6.4.2.2 An ELISA shows binding of SRSF1 to GRK2

Since SRSF1 is a novel substrate for GRK2 phosphorylation, the GRK2-SRSF1 protein interaction was investigated by ELISA technique. To this end, GRK2 purified from Sf9 cells infected with a GRK2-expressing baculovirus was coated at different concentrations and subsequently SRSF1 purified from bacterial culture was added at a constant concentration of 5 μ g/ml. BSA was used as a control. Detection was performed using a primary mouse monoclonal antibody against SRSF1 (1/300) and a secondary

HRP-conjugated goat anti-mouse antibody (1/4000). The substrate reaction was allowed to proceed for 30 min, before the absorbance was read at 410 nm.

The results of the ELISA showed that SRSF1 shows a concentration-dependent interaction with GRK, whereas SRSF1 does not interact with BSA, which was used as a control protein.

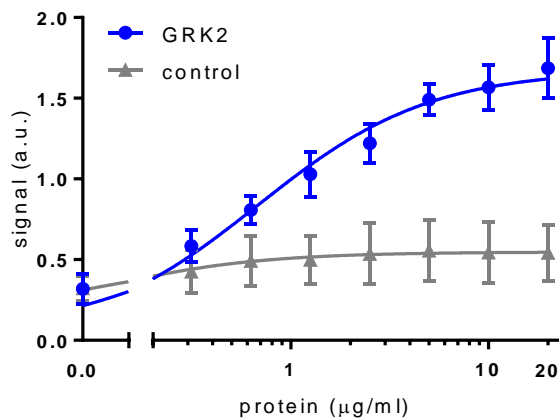


Figure 25: An ELISA shows binding of SRSF1 to GRK2

Binding of SRSF1 (5 µg/ml) to GRK2 or BSA, which was used as a control. Data of three independent experiments are displayed as mean ± SEM.

6.4.3 Inhibition of GRK2-mediated receptor desensitization

The bradykinin receptor B2 (B2R) is a ubiquitously expressed GPCR with roles in the cardiovascular system, pain modulation and airway function (244). In the renin-angiotensin-aldosterone system (RAAS), B2R plays an important counterpart to AT1R by acting as a vasodepressor through stimulation of NO release by eNOS (245).

Upon binding of the endogenous peptide-agonist bradykinin, B2R couples most prominently to $G\alpha_q$, thus eliciting a rise in the intracellular free Ca^{2+} concentration. Moreover, B2R has been also shown to couple to $G\alpha_i$ and $G\alpha_{12/13}$ (244).

Homologous desensitization of B2R may be initiated by various GRKs including GRK2 and GRK5 (246).

Fura-2 is a fluorescent dye used for measuring Ca^{2+} levels photospectrometrically (230). The acetoxymethylester derivative (Fura-2AM) is able to permeate the cell membrane. Intracellular esterases hydrolyse it to the membrane-impermeable Ca^{2+} -sensitive carboxylic form, Fura-2. Whereas the free dye shows an absorbance maximum at ~340 nm, binding of Ca^{2+} shifts it to ~380 nm (emission: 509 nm). Thus, alternating excitation at 340 nm and 380 nm allows the determination of the ratio between calcium-

free and calcium-bound Fura-2, thereby correcting for differences in dye concentration or loading efficiency (247).

6.4.3.1 Generation of plasmids expressing WD-Peptides

The WD-Peptides (WD1-3) were cloned by annealing of single-stranded oligonucleotides into pcDNA3 for expression in mammalian HEK293A cells. The identity and its correct insertion into pcDNA3 was confirmed by DNA sequencing (13.6, 13.7, and 13.8).

6.4.3.2 WD3 increases the bradykinin-stimulated Ca²⁺-signal in HEK293A cells

HEK293A cells were transiently transfected with 20 µg of plasmid DNA coding for WD1, WD2 or WD3, respectively. Cells transfected with pcDNA3 were used as a negative control and cells transfected with pcDNA3RKIP were used as a positive control (248).

The rise in the free intracellular calcium concentration, [Ca²⁺]_i, after stimulation of the endogenously expressed B2R with 100 nM bradykinin (Sigma-Aldrich Chemie GmbH, Buchs SG, Switzerland) was measured with Fura-2 and was expressed as fluorescence ratio at 340 nm and 380 nm. The maximum response after stimulation with bradykinin (as indicated by ΔI) was statistically analysed in comparison to the control (pcDNA3, ΔI=0.43 ± 0.06).

Whereas expression of WD1 and WD2 showed no effect on the bradykinin-stimulated intracellular free Ca²⁺ concentration (ΔI=0.49 ± 0.11, p=0.2112, n=4, Figure 26: A, D; 0.41 ± 0.12, p=0.6155, n=4, Figure 26: B, D) relative to the control, the expression of WD3 led to a significant increase in the bradykinin-stimulated intracellular [Ca²⁺]_i (ΔI=0.59 ± 0.10, p=0.0159, n=4, Figure 26: C, D). As a positive control, the dual-specific GRK2 and Raf-1 kinase inhibitor, RKIP, was used. The expression of RKIP also led to a significant enhancement of the bradykinin-stimulated Ca²⁺-signal (ΔI=0.51 ± 0.05, p=0.0081, n=4, Figure 26: D).

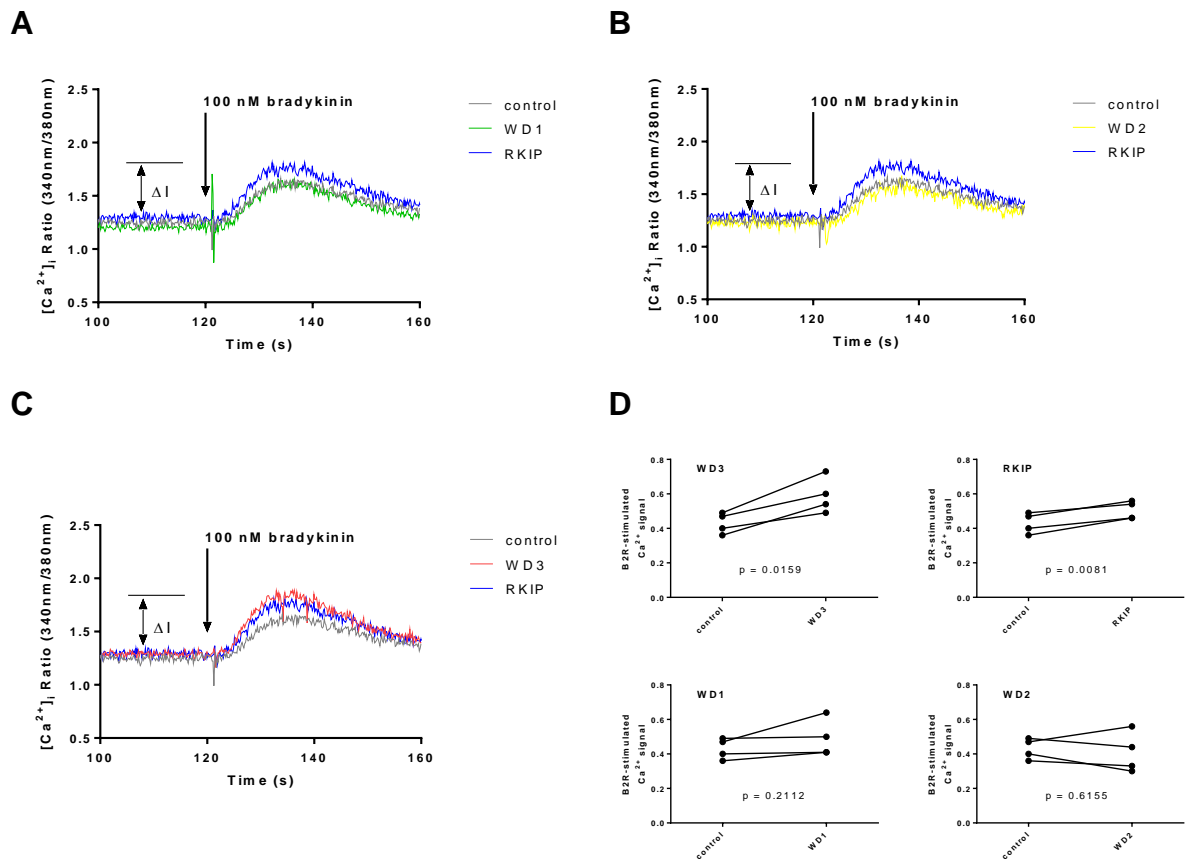


Figure 26: WD3 sensitizes the bradykinin-stimulated Ca^{2+} signal of endogenously expressed B2R

HEK293A cells were transiently transfected with plasmid DNA encoding WD1, WD2 or WD3 and stimulated with 100 nM of bradykinin. Cells transfected with pcDNA3 were used as a negative and cells transfected with pcDNA3RKIP as a positive control. (A-C) Representative calcium measurements of WD-expressing cells. (D) Statistical analysis of the maximum $[Ca^{2+}]_i$ peak (ΔI) of four independent experiments (paired student's t-test).

6.5 In vivo characterization of the GRK2-inhibitory peptide

6.5.1 Generation of a plasmid for cardiac-specific expression of WD3

For the generation of a transgenic mouse model with cardiac-specific expression of the WD3 peptide, the corresponding DNA was cloned into a vector containing the α -myosin heavy chain promoter, thereby restricting protein expression to cardiac tissue (249).

To this end, annealing of single-stranded oligonucleotides was performed and inserted into the Sall/HindIII cut α -MHC plasmid by a ligation reaction. Bacterial clones were screened by PCR using vector-specific primers (HGH2 and MHC2).

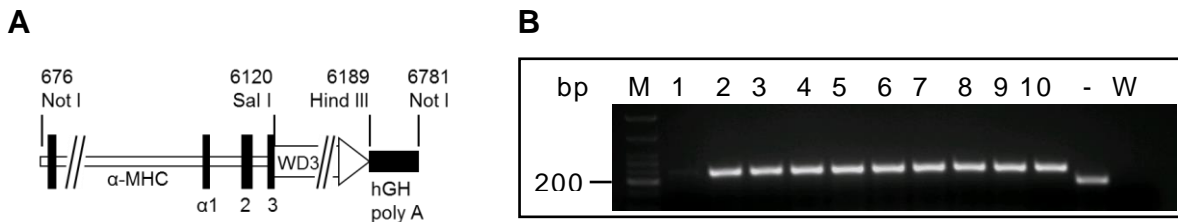


Figure 27: Generation of a plasmid coding for WD3 under the control of the α -myosin heavy chain (α -MHC) promoter

Schematic drawing of the vector construct (A). Single colony screening PCR shows the amplification of a ~250 bp fragment for samples 2-10, whereas the negative control (-) shows the amplification of an only ~130 bp long fragment (B). The observed difference reflects the amplification of the vector sequence without insert, which corresponds well with the fragment size of approximately 100 bp. The water control (W) is negative. M, Marker

The DNA was sequenced (13.9) and endotoxin-free DNA was prepared from clone 2 (Figure 27) and subsequently linearized by restriction digestion with NotI.

6.5.2 Establishment of a transgenic mouse model

Introduction of the transgene into the mouse strain C57BL/6J was performed in the Molecular Pharmacology Unit of ETH Zurich, Switzerland by Dr. Joshua Abd Alla according to a method described elsewhere (173).

6.5.3 Genotyping of transgenic animals by PCR

Animals were genotyped by PCR using genomic DNA isolated from ear punch biopsies as template and vector-specific primers (HGH2 and MHC2). Mice were born at mendelian frequency (Figure 28).

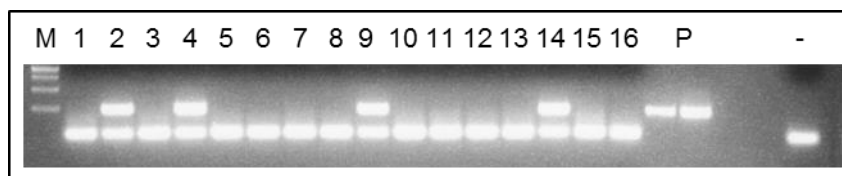


Figure 28: Identification of the α -MHCWD3 transgene in the genomic DNA by PCR

Isolated genomic DNA was amplified with vector-specific primers (HGH2 and MHC2) and separated on an agarose gel. M, Marker; P, positive control; -, negative control

6.5.4 The GRK2-inhibitory peptide shows a cardioprotective effect *in vivo*

To study the effect of WD3 on the development of cardiac hypertrophy, a model of chronic pressure overload induced by abdominal aortic constriction (AAC) was applied (250). In this model, pressure overload is induced by ligation of the aorta above the renal arteries (Figure 29, lower right panel), which leads to increased blood pressure proximal to the constriction and consequently chronic pressure overload-induced hypertrophy (Figure 29, lower left panel) (250). GRK2-inhibition has been shown to reduce the development of signs of cardiac dysfunction and heart failure after AAC (143).

Cardiac-specific expression of WD3 retarded the development of cardiac hypertrophy after AAC in comparison to a non-transgenic wild-type mouse (Figure 29, upper panel). This finding presents the first evidence of a cardioprotective effect of WD3 *in vivo*.

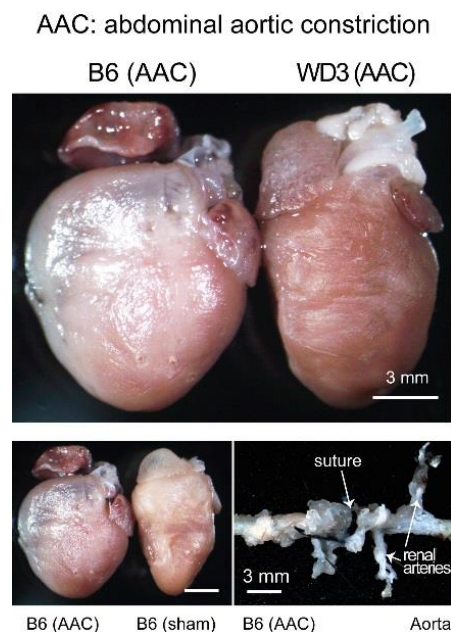


Figure 29: WD3 shows a cardioprotective effect in a pressure overload mouse model

WD3 retards AAC-induced cardiac hypertrophy compared to a wild-type control mouse (B6), upper panel. AAC induces chronic pressure overload and cardiac hypertrophy compared to sham-operated animals (sham), lower left panel. Suprarenal suture of the aorta, lower right panel. The aorta was dissected two weeks after ligation of the aorta above the suprarenal arteries.

7 Discussion

The ubiquitously expressed serine/threonine kinase GRK2 is a key player in many physiological processes (4.2.2). Particularly, GRK2 has been extensively studied for its role in phosphorylating GPCRs and thereby attenuating signalling events in cooperation with arrestins (14,110). Recently, GRK2 phosphorylation of cytosolic non-receptor substrates as well as kinase-independent functions have gained increasing attention (251). Furthermore, GRK2 has been implicated in such varied conditions as heart failure, diabetes, inflammation and cancer (131). Although efforts towards the finding of a GRK2-inhibitor have been ongoing for more than 25 years (198) and, in the case of heart failure, progressed as far as studying the effects in a large animal model (141), no compound has reached clinical trials yet. Thus, there is still a need for new inhibitors.

The modular structure of GRK2 allows for inhibition by targeting any of the three domains. However, the diverse GRK2 effector roles are affected differently depending on the approach chosen. Firstly, for the N-terminal domain containing the receptor recognition site, RKIP has been shown to interfere with the phosphorylation of receptor substrates (168,170). Secondly, kinase domain inhibitors such as paroxetine are expected to prevent phosphorylation of all GRK2 substrates. Thirdly, the GRK2-inhibitory potential of interfering with the G $\beta\gamma$ -mediated GRK2 activation and membrane translocation has been extensively studied with the help of the GRK2-derived peptide β ARKct (183,184,239). Nevertheless, the mechanism of action is probably more accurately described as an inhibition of G $\beta\gamma$ effector functions, one of which is the said activity towards GRK2. It has to be remembered, however, that some of the beneficial effects observed with β ARKct are thought to be GRK2-independent (186,238). It follows, that β ARKct and small molecules employing the same inhibitory mechanism (192), are inadequate for studying the outcome of targeting the C-terminal domain of GRK2 with regard to substrate-specificity and kinase-independent effects. Still, inhibiting the G $\beta\gamma$ -GRK2CTD interaction is a well-established approach to GRK2-inhibition. Moreover, it confers specificity towards members of the β ARK-subfamily, as membrane localization for the other isoforms employs different mechanisms (98,106,108,109).

In the presented study, direct targeting of GRK2CTD was investigated as a hitherto unexplored approach to GRK2-inhibition. More specifically, peptides interacting with GRK2CTD were sought for subsequent characterization of their inhibitory properties.

Small molecules have historically been preferred as pharmacologically active substances due to their advantageous pharmacokinetic features, good oral availability and the ease of formulation. However, a substantial proportion of the GRK2-inhibitors studied so far are peptides or proteins (RKIP, β ARKct, the various peptide inhibitors described in

chapter 4.4.4) indicating that this could be a promising approach. In addition, interfering with G β γ -mediated kinase activation requires targeting of a protein-protein interaction site, which is known as a challenging task (252). Peptides are considered to have the potential for effectively blocking protein-protein interactions (PPIs) (201,207,253). PPI interfaces are characterized by a wider contact area compared to protein-small molecule interfaces. These generally contain so-called “hot spots”, which are characterized by facilitating high-affinity interactions (254). Intriguingly, phage display library screening has been reported to preferentially identify these hot-spots, making it a useful technique in the search for inhibitors of PPIs (254).

7.1 Identification of a GRK2-interacting peptide

7.1.1 Protein expression and purification of GRK2-domains

For the expression of recombinant GRK2 domains, a bacterial protein expression system was chosen (227). Generally, bacterial expression of recombinant proteins generates high yields of protein for subsequent purification. Disadvantages include protein aggregation and the formation of inclusion bodies, which require harsher conditions for purification. Moreover, the formation of the native conformation can be hindered (255). For the purpose of this study, namely the expression of GRK2 domains for a peptide phage display library screen and protein-protein interactions studies by ELISA technique, neither activity nor the native conformation was required.

In this study, protein expression levels of GRK2KD and GRK2CTD were high, as revealed by SDS-PAGE. Although expression of the C-terminally His-tagged GRK2CTD was lower than that of the N-terminally His-tagged protein. Other groups have reported that the position of the His-tag may affect protein yield (256) and stability (257). The protein expression level of GRK2NTD was rather low, which could reflect instability of the protein. The expressed GRK2-domains could be purified by metal affinity chromatography as evaluated by SDS-PAGE.

7.1.2 A phage display library screen identifies several peptides

The purified C-terminally His-tagged GRK2CTD was used as bait in a peptide phage display library screen, which yielded six 7-mer peptide sequences (Table 7). Two of the peptide sequences (HYIDFRW and HYTDFRW) were identical except for one position. However, as these sequences reappeared in subsequent library screens using different bait-proteins, they unlikely display a consensus sequence, which specifically interacts with a certain protein.

7.1.3 A protein database search was performed for the peptides

A BLAST search for the identified peptide sequences was performed. A BLAST analysis of phage-display derived peptides may yield novel protein interaction partners or inhibitors of protein-protein interactions (222,223).

Peptide IRYVPQT shows sequence homology with cadherin 20

For the sequence IRYVPQT, sequence homology with cadherin 20 was revealed in the BLAST analysis (Table 8).

Cadherin 20 has been identified as a member of the cadherin family of cell-cell adhesion molecules. Cadherins contain extracellular Ca^{2+} -binding domains, transmembrane domains and cytoplasmic domains interacting with intracellular proteins linking them to the cytoskeleton (258). As no further experiments were performed with this peptide, the implications of the finding is not clear.

Peptide IVSLQTP shows sequence homology with NFAT

The BLAST analysis for the peptide sequence IVSLQTP revealed sequence homology with NFAT (Table 8).

The nuclear factor of activated T-cells, cytoplasmic 3 (NFATc3) has recently gained attention as an interaction partner of GRK5.

Gαq, a mediator of cardiac hypertrophic signalling (259,260), stimulates a rise in the intracellular calcium level, thereby promoting calmodulin-mediated nuclear translocation of GRK5 (261). Nuclear accumulation of GRK5 in turn promotes transcription of hypertrophic genes by (i) phosphorylation of histone deacetylase 5 (HDAC5) inducing de-repression of the myocyte enhancer factor 2 (MEF2) (262) and (ii) enhancing DNA binding of NFAT in a kinase-independent manner (261,263).

For GRK2, however, neither nuclear localization (107) nor interaction with NFAT (263) have been reported so far. Thus, the significance of finding a peptide derived from NFAT through a phage display library screen using the GRK2CTD as bait, is unclear.

Moreover, the NFAT-isoform (NFATc2) identified in the BLAST analysis with homology to the peptide sequence IVSLQTP, differs from the one reported to interact with GRK5 (NFATc3).

Peptide ASTLIVF shows sequence homology with WDR76

For the peptide sequence ASTLIVF, the BLAST analysis showed sequence homology with WDR76 (Table 8).

WD repeat-containing proteins are characterized by a series of repetitive approximately 40 amino acids long sequences with a signature C-terminal WD (tryptophan, aspartic acid) dipeptide. WD domains were first identified in the β-subunit of bovine transducin, the main G protein in retinal cells (36,264). Solving of the crystal structure of the

prototypical WD repeat-containing protein Gβγ revealed a seven-bladed β-propeller structure (Figure 30, lower middle panel) (36,265). The propeller blades consisting of four anti-parallel β-strands display a toroidal shape building a funnel (Figure 30, lower left panel). One WD repeat spans strand D of one blade and strands A, B and C of the following blade (Figure 30, lower right panel). Hence, a WD repeat does not correspond to a single blade of the propeller structure. The result of this unique architecture is a highly symmetrical protein stabilized by numerous hydrogen bonds and displaying multiple surfaces for protein-protein interaction (235).

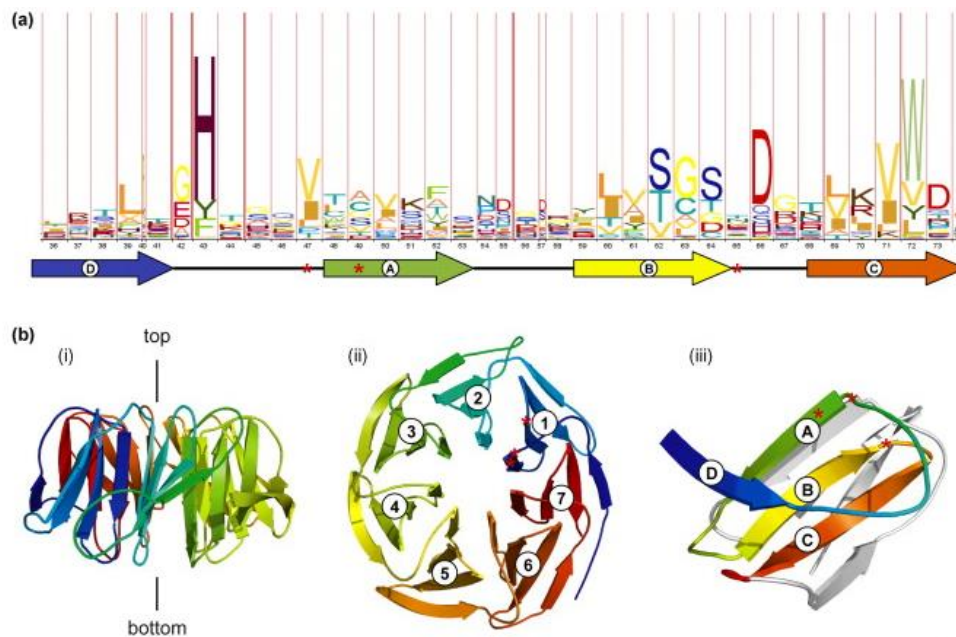


Figure 30: Sequence and structure of WD repeat-containing proteins

WD repeat-containing proteins consist of ~40 amino acid spanning sequences with a characteristic C-terminal WD-dipeptide (upper panel). The highly rigid tertiary protein structure builds a funnel-like shape (lower left panel). A seven-bladed β-propeller structure is found most commonly for WD repeat-containing proteins (lower middle panel). One WD repeat consists of strand D of one blade and strands A-C of the next blade (lower right panel) (235).

Interestingly, whereas secondary and tertiary protein structures are rigidly defined among WD repeat-containing proteins, the primary amino acid sequence is highly variable making the identification of a protein as a WD repeat-containing protein somewhat challenging. Very few amino acid residues are conserved such that e.g. the name-giving WD-dipeptide is not a strict requirement. Still, some key elements are frequently found (Figure 30, upper panel): (i) a GH (glycine, histidine) dipeptide at the C-terminal end of strand D, (ii) three amino acids with small side chains (serine, glycine) at the C-terminal

end of strand B, (iii) and an aspartic acid residue six amino acids before the signature WD dipeptide (235,264,266).

WD repeat-containing proteins are known to interact with PH domains, as e.g. G β γ interacts with GRK2 via its PH domain (267). Moreover, G β γ was also found to interact with other WD repeat-containing proteins, such as RACK1 or WDR26 (268,269). The characteristic β -propeller architecture forms multiple possible protein interactions surfaces on the bottom, at the top and at the sides (268). Thus, a role for WD repeat-containing proteins in scaffolding protein assemblies was proposed (270).

The human WD repeat-containing protein 76 (WDR76) displays the characteristic seven-bladed tertiary protein structure. It was shown to interact *in vivo* with CUL4-DDB1 ubiquitin ligase, for which other WD repeat-containing proteins serve as molecular adaptors mediating substrate targeting (271). The WDR76 orthologue from *Saccharomyces cerevisiae*, Cmr1, in cooperation with other proteins was found to be involved in maintenance of genome integrity. More specifically, it mitigates stress-induced DNA damage during replication (272).

7.1.4 Sequence elongation of the peptide sequence ASTLIVF

The approach of elongating the peptide sequence ASTLIVF according to the homologous sequence of WDR76 was based on the structural relatedness of WDR76 and G β γ . Moreover, targeting of PPIs with small molecules is challenging, because of the necessity to cover a larger protein interface. Thus, it could be that medium-sized compounds (1000-2000 Da) are better suited for inhibition (207).

In addition, the GRK2-inhibitory peptides reported so far are roughly between 14 and 28 amino acids in length (174,187,188,195). For the PepInh, truncation even resulted in the loss of activity (194). This could indicate a requirement for a longer sequence for GRK2-inhibition.

7.1.5 A GRK2-interacting peptide is identified by ELISA

Binding ELISAs and competition ELISAs are versatile methods to study PPIs (273).

In the presented study, ELISA technique was chosen to examine the interaction of GRK2CTD with the elongated peptides WD1 or WD3, respectively. GRK2CTD was shown to interact with WD3 (Figure 21: A), whereas the interaction with WD1 was not significant (Figure 21: B). Interestingly, both peptides, WD1 and WD3, contain the sequence identified in the phage display library screen (ASTLIV). However, WD3 in comparison to WD1 contains more (five vs. four) charged amino acids, which could facilitate electrostatic interactions with GRK2CTD. Similarly, the binding of β ARKct and G β γ has been proposed to rely on electrostatic interactions (188). To rule out unspecific binding of the GRK2CTD to WD3, a WD3-scrambled sequence could be tested for its interaction with GRK2CTD. The differences in charge between the two peptides, WD1 and WD3,

could also affect the coating efficiency. Coating of equal amounts of peptides could be confirmed by detection with a suitable antibody.

Taken together, GRK2CTD binds to WD3, which is an elongated version of a peptide identified in a phage display library screen.

7.2 The GRK2-interacting peptide shows GRK2-inhibitory features *in vitro*

To characterize the GRK2-inhibitory features of the elongated peptides, three different *in vitro* assays were performed. First, the effect of the peptides on the G β -GRK2CTD protein-protein interaction, which is essential for kinase activation and translocation to the plasma membrane, was studied. Second, an *in vitro* phosphorylation assay was chosen to assess, whether the peptides have any influence on the kinase activity. Third, the impact of the peptides on the desensitization of the endogenously expressed bradykinin receptor type 2 was investigated in transiently transfected HEK cells.

7.2.1 The GRK2-inhibitory peptide interferes with the G β -GRK2CTD interaction

In this study, binding of the GRK2CTD to both G β 3 and G β 3-s could be revealed by ELISA technique (Figure 22). This finding is in line with other studies reporting an interaction of GRK2 with G $\beta\gamma$ in general (38,187), and G β 3 and G β 3-s specifically (274).

Interestingly, a G β 3-polymorphism (C825T) linked to the increased occurrence of the shorter splice variant (G β 3s) (275,276), was found to be associated with hypertension. For this shorter splice variant, G β 3-mediated ubiquitination of GRK2 is impaired leading to protein accumulation. Enhanced GRK2 levels, in turn, explain the association with a hypertensive state (274).

One group identified the GRK2-inhibitory compound M119 in a competition ELISA with G $\beta\gamma$ and SIGK, a peptide showing a high affinity for G $\beta\gamma$ (191). This indicates the applicability of a competition ELISA for the identification of compounds interfering with specific protein-protein interactions.

Here, it was shown that WD3 significantly interferes with the G β 3-GRK2CTD interaction in a competition ELISA (Figure 23: A). For the shorter splice variant, G β 3-s, a trend towards disruption of the G β -GRK2CTD interaction could be observed, which was not significant (Figure 23: B). WD1, in contrast did neither influence the binding of GRK2CTD to G β 3 nor G β 3-s (Figure 23: A, B).

The different effects observed for G β 3 and G β 3-s could be attributed to variations in coating efficiency. Equal coating could be confirmed by immunochemical detection. Moreover, the seven-bladed propeller structure found most often in WD repeat-containing proteins is predicted to be most stable (277). G β 3-s, however, lacks around 40 amino acids (275), which could affect the stability of the protein and consequently the outcome of the assay. The high standard deviation as observed for the competition assay with GRK2CTD and G β 3-s (Figure 22) could be an indication for such unstable experimental conditions.

Nevertheless, the results presented here indicate that WD3 interferes with the G β γ -GRK2CTD interaction essential for kinase activation.

7.2.2 The GRK2-inhibitory peptide inhibits GRK2 activity in an *in vitro* phosphorylation assay

Several studies have used *in vitro* phosphorylation assays to investigate the kinase activity of GRK2 in the presence and/or absence of specific compounds (175,178,278). GRK2 phosphorylates a variety of different substrates, most prominently GPCRs (110). In addition, there is an increasing number of studies reporting cytosolic non-receptor substrates of GRK2 (85).

In the presented study, SRSF1, a novel substrate of GRK2 (Quitterer, U., unpublished data) has been used to investigate the impact of the two peptides (WD1 and WD3) on the activity of GRK2. WD3 significantly reduced the phosphorylation of SRSF1 by GRK2, which indicates an inhibition of the kinase function. In contrast, WD1 did not influence the activity of GRK2 towards SRSF1. Remarkably, the potency of WD3 is comparable to paroxetine (Quitterer, U., unpublished data), which has recently been identified as a selective GRK2-inhibitor (178).

However, the inhibitory effect of WD3 in this system was not expected. The GRK2-derived peptide (amino acids 643-670) containing the 'G β γ binding domain' has been shown to inhibit G β γ -mediated GRK2-activity towards a receptor substrate (187). In this study, WD3 has been shown to interfere with the G β -GRK2CTD interaction (Figure 23). To test such a mode of action, a reconstituted system containing a membrane-embedded receptor and G β γ would be required (187). The *in vitro* phosphorylation setup used here lacks both G β γ and a receptor substrate. Nevertheless, the effect observed could be explained by competition of WD3 with the chosen substrate SRSF1 for binding to GRK2. Thus, it would be interesting to perform the phosphorylation assay using different substrates, particularly a receptor substrate. However, receptors are hydrophobic and inherently expressed at low levels, making the experimental procedure more challenging.

Moreover, selectivity of the peptide towards other kinases should be addressed in further experiments. Targeting of GRK2CTD as an allosteric site would be expected to alleviate the problem of unselective kinase-inhibition, which stems from a high sequence conservation of the ATP-binding site (279). Nevertheless, testing of other kinases, e.g. of the AGC kinase family or its subfamily of GRKs, would be desirable, as it could also support the proposed mode of action.

7.2.3 The GRK2-inhibitory peptide inhibits desensitization of the GPCR B2R

The B2R, upon agonist-stimulation with bradykinin, couples to $G\alpha_q$ (280), which leads to increased intracellular calcium levels (281). GRK2 has been reported to phosphorylate B2R in human fibroblasts (282) and to impair agonist-stimulated B2R-signalling as indicated by reduced intracellular calcium levels (283). Moreover, a study using the GRK2-inhibitor RKIP showed enhanced calcium signalling in HEK cells upon stimulation of B2R with its cognate ligand bradykinin (248). B2R is endogenously expressed in HEK cells (281), hence ensuring a stable experimental system to study GRK2-inhibitory effects.

In the presented study, the bradykinin-stimulated rise in the intracellular free calcium concentration in HEK cells was used to investigate the GRK2-inhibitory effect of the transiently expressed peptides WD1, WD2 and WD3. Of the three peptides, only WD3 led to a significantly enhanced maximum calcium signal of agonist-stimulated B2R (Figure 26). These results indicate that WD3 inhibits GRK2-mediated attenuation of bradykinin-stimulated calcium signalling (desensitization).

One study showed that downregulation of endogenous RKIP expression levels using a miRNA diminished the GRK2-inhibitory capacity of RKIP (248). In the presented study, equal amounts of DNA were transfected. However, peptide expression levels were not assessed. Thus, the GRK2-inhibitory effect observed with WD3 in comparison to WD1 and WD2 could also be a result of different peptide expression levels. Immunoblot detection of the peptide expression levels could exclude such an effect.

GRK2 has also been reported to regulate β 2AR (284) and α 2AR (137), which are both known to couple to $G\alpha_s$ and $G\alpha_i$ (45,46). Moreover, GRK2 upregulation has been shown to contribute to the impaired signalling of these receptors in heart failure (130,137). Therefore, elucidation of the effects of the peptides (WD1, WD2 and WD3) on the desensitization of these $G\alpha_{s/i}$ -coupled receptors would be interesting.

7.3 The GRK2-interacting peptide WD3 shows GRK2-inhibitory features *in vivo*

To investigate the *in vivo* effects of the peptide WD3, a transgenic mouse model with cardiac-specific expression of the peptide sequence was established (Figure 28). These mice were then subjected to AAC as an animal model of chronic pressure overload-induced heart failure (143). WD3 retarded the development of cardiac deterioration as compared with a non-transgenic wild-type control mouse.

This result is in agreement with the effects observed in a study using PepInh, a peptide GRK2-inhibitor derived from the first intracellular loop of the hamster β 2AR. Mice with cardiac-specific overexpression of PepInh, showed an improved heart weight to body weight ratio compared to wild-type mice after long-term AAC. Furthermore, their heart function was improved as indicated by measuring the left-ventricular ejection fraction (143).

The transgenic mouse line with cardiac-specific expression of WD3 can be utilized to characterize the *in vivo* effects of WD3 further. Protein expression levels could be assessed by immunoblot detection. Moreover, gene expression profiling could reveal alterations in metabolic or growth-promoting pathways, which have been shown to be affected by GRK2-inhibition in previous studies (143,173).

7.4 Evaluation of the GRK2-inhibitory peptide

7.4.1 Potency and selectivity

The potency of WD3, the GRK2-inhibitory peptide development in this study, was not determined. Nevertheless, the results obtained in the *in vitro* phosphorylation assay indicate an effect comparable to paroxetine (Figure 24 and Quitterer, U., unpublished data). Moreover, the GRK2-inhibitory effect of WD3 is sufficient to exert a cardioprotective effect in an *in vivo* pressure overload model of heart failure.

Another point, which was not addressed in the presented work, is the selectivity of WD3. As mentioned before, targeting of the GRK2CTD is expected to confer selectivity within the GRK-family, because only the members of the β ARK-subfamily (GRK2 and GRK3) are activated by $G\beta\gamma$ (100,101). Whereas GRK2 has been widely studied, less is known about the (patho)physiological role of GRK3. In contrast to GRK2 gene ablation, GRK3-deficient mice develop normally, except for a loss of odorant-receptor desensitization. This is probably a result of the fact that GRK3 is expressed at high levels in the olfactory epithelium (285). The other ubiquitously expressed GRK-isoforms are GRK5 and GRK6 (85). GRK5, the other major GRK-isoform in the heart, is also upregulated in heart failure and thought to contribute to heart failure (286). Thus, selectivity within the GRK-family might not be a requirement, at least not for the treatment of heart failure.

7.4.2 Mechanism of action

The methodical approach outlined in the presented study assumes a mode of action, by which the peptide, WD3, interferes with the G β γ -mediated activation of GRK2. In this study, the competition ELISA with G β 3 and GRK2CTD supports such an inhibitory mechanism (6.4.1.2). Interestingly, the common binding site shared by G β γ effectors identified in one study, suggests that mostly hydrophobic interactions are critical for G β γ -effector interactions (188). WD3 encompasses a hydrophobic region, which backs the effect observed in the competition ELISA. However, electrostatic interactions have been proposed to underlie the binding of β ARKct to G β γ (188). A role for charged amino acids in GRK2-inhibition is also supported by studies with anionic GRK2-inhibitors (96,198). Elongation of the original peptide-sequence identified in the phage display library screen added negatively charged amino acids (6.3.2), which would be in line with the proposed mode of action of these inhibitors (e.g. heparin). To find out, which residues are essential for the GRK2-inhibitory effect of WD3, more studies are needed.

Additionally, the C-terminal domain of GRK2 also contributes to enzyme activation by interacting with anionic phospholipids of the membrane (100,105). Moreover, agonist-occupied GPCRs are potent allosteric activators of GRK activity by inducing a transition toward an active closed conformation. Mutations in the C-terminal tail impaired receptor phosphorylation, suggesting a role for GRK2CTD in receptor-mediated kinase activation (287). Therefore, WD3 as a GRK2CTD-interacting peptide (6.3.3) could also interfere with these mechanisms of activation.

However, the surprising finding, that WD3 inhibits GRK2-mediated phosphorylation of the soluble substrate SRSF1 (Figure 24) is not sufficiently clarified by the above suggested mechanisms of action. WD3 might interfere with the GRK2-SRSF1 interaction, which would explain the results presented in this study. This would be intriguing, because there are little data on the interaction of GRK2 with soluble substrates with regard to the specific sites of interaction. Receptors are known to interact via the GRK2NTD, an interaction blocked by RKIP (91,168). In recent years, there has been an increasing interest in GRK2 non-receptor substrates (85). Thus, substrate-specific inhibition of GRK2-mediated phosphorylation would certainly be of value. However, further studies are needed to decipher the substrate-specificity of WD3-mediated GRK2-inhibition.

7.4.3 Safety of GRK2-inhibition

Systemic and organ-specific side effects of inhibiting the ubiquitously expressed GRK2 need to be addressed.

Even more so considering that GRK2 gene ablation results in embryonic lethality (161). As cardiomyocyte-specific gene ablation produces viable offspring with normal heart structure and function, embryonic lethality in GRK2 gene ablated mice is probably due to

extra cardiac effects (162). Nevertheless, an increased prevalence of cardiac congenital defects has been found to be associated with paroxetine use during the first trimester of pregnancy (288), underscoring the role of GRK2 in cardiac development.

Concerns regarding a long-term enhancement of β -adrenergic signalling stem from animal models of β AR-overexpression (289,290). These mice presented with a phenotype marked by increased cardiac contractility, which later developed into heart failure (289). Furthermore, adrenergic stimulation is inherently toxic to the heart and promotes apoptosis (291).

This problem could be overcome by a time-restricted short-term application after myocardial infarction to halt the development of maladaptive processes. Such an approach was taken by one group studying the effects of adenovirus-mediated β ARKct gene delivery in a large animal model (141). Another possibility would be to limit the use to acute heart failure, as is already the current treatment regimen for inotropic drugs (132). Furthermore, paroxetine has been marketed in 1992 and shows a safety profile comparable to other antidepressants (292). This supports data from GRK2^{+/-} mice, which develop normally and display improved cardiac function (138).

7.5 Outlook

7.5.1 Further development of the prototype

As mentioned before, peptide drugs generally display an unfavourable pharmacokinetic profile (4.5.1). However, there are several options for improving the pharmacokinetic and –dynamic profile of WD3. An alanine-scan could identify amino acid residues, which are essential for the GRK2-inhibitory effect of WD3 (197) and thus, guide approaches towards truncation, introduction of (un)natural amino acids or N-methylation. However, truncation might also result in loss of activity as observed for the GRK2-inhibitory peptide, PepInh (194).

Moreover, cyclisation of the peptide structure could be attempted. Due to their more rigid secondary structure, cyclic peptides tend to display higher affinity for their target proteins. However, cyclisation might also result in loss of activity. Protein-protein interactions are often hydrophobic in nature and do not display highly rigid stereochemical requirements (201). Therefore, they can be accommodated by a number of peptide conformations and sequences. A more rigid peptide conformation might still not fit into the protein-protein interface.

Alternatively, a competition screen, as was performed for the C13 aptamer and identified paroxetine as a GRK2-inhibitor (178), could be performed with WD3 in a similar manner.

7.5.2 Research Applications

The novel approach of targeting the GRK2CTD identified the GRK2-interacting peptide WD3 (Figure 21). In contrast to the compounds interfering with the G β -GRK2 interaction

(β ARKct, M119, gallein), WD3, by directly binding $G\beta\gamma$, might help in elucidating GRK2-specific $G\beta\gamma$ -effector functions. Moreover, WD3 could help in identifying the GRK2-interaction site of known interaction partners or substrates.

8 Conclusion

GRK2 has been implicated as a drug target in a variety of conditions, most importantly for the treatment of heart failure. Efforts towards a clinically approved drug, however, have been unsuccessful to date.

In the presented study, a novel approach is taken by direct targeting of the C-terminal domain of GRK2, thus potentially interfering with G β γ -mediated kinase activation. Screening of a peptide phage display library and subsequent modification of the most promising candidate, led to the development of a peptide inhibitor prototype (WD3), which shows GRK2-inhibitory features in several *in vitro* assays. Moreover, cardiac-specific expression of the WD3 peptide sequence exerts a cardioprotective effect in an animal model of chronic pressure overload.

Thus, the WD3 peptide could serve as lead structure for the development of a more potent and drug-like compound. The WD3-peptide could also prove useful in elucidating GRK2-mediated G β γ effector functions, as it specifically inhibits the G β γ -GRK2 interaction.

However, further research is needed to characterize the interaction of WD3 with GRK2 and the *in vivo* effects in more detail.

9 Acknowledgments

I would like to thank Prof. Dr. Ursula Quitterer for giving me the opportunity to work on this exciting project as part of my PhD and for her support throughout the years. I would also like to thank Prof. Dr. Cornelia Halin for being my co-supervisor.

Special thanks to the group members Dr. Said AbdAlla and Dr. Andreas Langer for their assistance with various laboratory techniques.

Thanks go to my fellow PhD students, Dr. Joshua Abd Alla and Stefan Wolf, for scientific and non-scientific exchange and to our animal caretaker, Marianne Antony, for gentle handling of the mice.

My master students Laura Huber, Selina Obrist, Susanne Driessen, Joëlle Kenel, Natalie Bernath, and Kira Heusler, I would like to thank for the nice working atmosphere.

10 Curriculum vitae

Muriel Grämer

Date of birth March 25th, 1987
Citizen of Gommiswald-Dorf SG

Education

November 2013 – present	PhD Student in the group of Prof. Dr. Ursula Qitterer, ETH Zurich
2013	Federal Diploma for Pharmacists
February-July 2012	Master Thesis in the group of Prof. Dr. Ursula Qitterer, Institute of Pharmaceutical Sciences ETH Zurich, Molecular Pharmacology “Effect of the adaptorprotein 14-3-3 ϵ on the protein levels of GPCRs”
2011-2013	Master’s Degree in Pharmaceutical Sciences, ETH Zurich
2007-2011	Bachelor’s Degree in Pharmaceutical Sciences, ETH Zurich
2000-2006	Kantonsschule Limmattal

11 Publications

Patent application

Abd Alla, J., Graemer, M., Wolf, S., and Quitterer, U. (2016), Invention of a prototype, which is cardioprotective by inhibition of GRK2-mediated phosphorylation of a novel non-receptor GRK2 substrate, the Serine/arginine-rich splicing factor 1 (SRSF1), patent application approved by ETH Transfer (ETH 2016-138)

Journal article

Abd Alla, J., Graemer, M., Fu, X., and Quitterer, U. (2016) Inhibition of G-protein-coupled Receptor Kinase 2 Prevents the Dysfunctional Cardiac Substrate Metabolism in Fatty Acid Synthase Transgenic Mice. *The Journal of biological chemistry* **291**, 2583-2600

Conference contributions

Graemer, M., Kenel, J., and Quitterer, U. (2015) Phage display library screening for a GRK2-inhibitor prototype with less side effects. *DDNZ Symposium 2015* **1**, 40

Abd Alla, J., Graemer, M., and Quitterer, U. (2015) Inhibition of G-protein-coupled receptor kinase 2 (GRK2) retards cardiometabolic remodelling of late stage heart failure. *DDNZ Symposium 2015* **1**, 39

Graemer, M., and Quitterer, U. (2015) Identification of GRK2-interacting peptides. "Deutsche Gesellschaft für Experimentelle und Klinische Pharmakologie und Toxikologie e.V." *Naunyn-Schmiedeberg's archives of pharmacology* **388**, 4

Abd Alla, J., Graemer, M., and Quitterer, U. (2014) Transgenic mice with myocardium-specific over-expression of fatty acid synthase (FASN) develop signs of cardiac hypertrophy and failure. "Deutsche Gesellschaft für Experimentelle und Klinische Pharmakologie und Toxikologie e.V." *Naunyn-Schmiedeberg's archives of pharmacology* **387**, 23

Quitterer, U., Langer, A., Graemer, M., and Abdalla, S. (2014) Transgenic mice show functional heterodimerization between vascular angiotensin II AT1 receptor and bradykinin B2 receptor. "Deutsche Gesellschaft für Experimentelle und Klinische Pharmakologie und Toxikologie e.V." *Naunyn-Schmiedeberg's archives of pharmacology* **387**, 61

12 References

1. Pierce, K. L., Premont, R. T., and Lefkowitz, R. J. (2002) Seven-transmembrane receptors. *Nat Rev Mol Cell Biol* **3**, 639-650
2. Overington, J. P., Al-Lazikani, B., and Hopkins, A. L. (2006) How many drug targets are there? *Nat Rev Drug Discov* **5**, 993-996
3. Strader, C. D., Fong, T. M., Tota, M. R., Underwood, D., and Dixon, R. A. (1994) Structure and function of G protein-coupled receptors. *Annual review of biochemistry* **63**, 101-132
4. Dixon, R. A., Kobilka, B. K., Strader, D. J., Benovic, J. L., Dohlman, H. G., Frielle, T., Bolanowski, M. A., Bennett, C. D., Rands, E., Diehl, R. E., Mumford, R. A., Slater, E. E., Sigal, I. S., Caron, M. G., Lefkowitz, R. J., and Strader, C. D. (1986) Cloning of the gene and cDNA for mammalian beta-adrenergic receptor and homology with rhodopsin. *Nature* **321**, 75-79
5. Palczewski, K., Kumasaka, T., Hori, T., Behnke, C. A., Motoshima, H., Fox, B. A., Le Trong, I., Teller, D. C., Okada, T., Stenkamp, R. E., Yamamoto, M., and Miyano, M. (2000) Crystal structure of rhodopsin: A G protein-coupled receptor. *Science* **289**, 739-745
6. Shonberg, J., Kling, R. C., Gmeiner, P., and Lober, S. (2015) GPCR crystal structures: Medicinal chemistry in the pocket. *Bioorganic & medicinal chemistry* **23**, 3880-3906
7. Fredriksson, R., Lagerstrom, M. C., Lundin, L. G., and Schioth, H. B. (2003) The G-protein-coupled receptors in the human genome form five main families. Phylogenetic analysis, paralogon groups, and fingerprints. *Molecular pharmacology* **63**, 1256-1272
8. Lefkowitz, R. J. (2004) Historical review: a brief history and personal retrospective of seven-transmembrane receptors. *Trends in pharmacological sciences* **25**, 413-422
9. Black, J. B., Premont, R. T., and Daaka, Y. (2016) Feedback Regulation of G Protein-Coupled Receptor Signaling by GRKs and Arrestins. *Seminars in cell & developmental biology*
10. Lagerstrom, M. C., and Schioth, H. B. (2008) Structural diversity of G protein-coupled receptors and significance for drug discovery. *Nat Rev Drug Discov* **7**, 339-357
11. Gilman, A. G. (1987) G proteins: transducers of receptor-generated signals. *Annual review of biochemistry* **56**, 615-649
12. Neer, E. J. (1994) G proteins: critical control points for transmembrane signals. *Protein science : a publication of the Protein Society* **3**, 3-14
13. Neer, E. J. (1995) Heterotrimeric G proteins: organizers of transmembrane signals. *Cell* **80**, 249-257

14. Benovic, J. L., Kuhn, H., Weyand, I., Codina, J., Caron, M. G., and Lefkowitz, R. J. (1987) Functional desensitization of the isolated beta-adrenergic receptor by the beta-adrenergic receptor kinase: potential role of an analog of the retinal protein arrestin (48-kDa protein). *Proceedings of the National Academy of Sciences of the United States of America* **84**, 8879-8882
15. Luttrell, L. M., Ferguson, S. S., Daaka, Y., Miller, W. E., Maudsley, S., Della Rocca, G. J., Lin, F., Kawakatsu, H., Owada, K., Luttrell, D. K., Caron, M. G., and Lefkowitz, R. J. (1999) Beta-arrestin-dependent formation of beta2 adrenergic receptor-Src protein kinase complexes. *Science* **283**, 655-661
16. Luttrell, L. M., Roudabush, F. L., Choy, E. W., Miller, W. E., Field, M. E., Pierce, K. L., and Lefkowitz, R. J. (2001) Activation and targeting of extracellular signal-regulated kinases by beta-arrestin scaffolds. *Proceedings of the National Academy of Sciences of the United States of America* **98**, 2449-2454
17. Lefkowitz, R. J., and Whalen, E. J. (2004) beta-arrestins: traffic cops of cell signaling. *Curr Opin Cell Biol* **16**, 162-168
18. Violin, J. D., and Lefkowitz, R. J. (2007) Beta-arrestin-biased ligands at seven-transmembrane receptors. *Trends in pharmacological sciences* **28**, 416-422
19. Downes, G. B., and Gautam, N. (1999) The G protein subunit gene families. *Genomics* **62**, 544-552
20. Oldham, W. M., and Hamm, H. E. (2008) Heterotrimeric G protein activation by G-protein-coupled receptors. *Nat Rev Mol Cell Biol* **9**, 60-71
21. Willars, G. B. (2006) Mammalian RGS proteins: Multifunctional regulators of cellular signalling. *Seminars in cell & developmental biology* **17**, 363-376
22. Milligan, G., and Kostenis, E. (2006) Heterotrimeric G-proteins: a short history. *Br J Pharmacol* **147 Suppl 1**, S46-55
23. Northup, J. K., Sternweis, P. C., Smigel, M. D., Schleifer, L. S., Ross, E. M., and Gilman, A. G. (1980) Purification of the regulatory component of adenylate cyclase. *Proceedings of the National Academy of Sciences of the United States of America* **77**, 6516-6520
24. Hayes, J. S., and Mayer, S. E. (1981) Regulation of guinea pig heart phosphorylase kinase by cAMP, protein kinase, and calcium. *The American journal of physiology* **240**, E340-349
25. Kamp, T. J., and Hell, J. W. (2000) Regulation of cardiac L-type calcium channels by protein kinase A and protein kinase C. *Circulation research* **87**, 1095-1102
26. Shi, J., Qian, W., Yin, X., Iqbal, K., Grundke-Iqbal, I., Gu, X., Ding, F., Gong, C.-X., and Liu, F. (2011) Cyclic AMP-dependent Protein Kinase Regulates the Alternative Splicing of Tau Exon 10: A MECHANISM INVOLVED IN TAU PATHOLOGY OF ALZHEIMER DISEASE. *Journal of Biological Chemistry* **286**, 14639-14648

27. Codina, J., Hildebrandt, J. D., Sekura, R. D., Birnbaumer, M., Bryan, J., Manclark, C. R., Iyengar, R., and Birnbaumer, L. (1984) Ns and Ni , the stimulatory and inhibitory regulatory components of adenylyl cyclases. Purification of the human erythrocyte proteins without the use of activating regulatory ligands. *The Journal of biological chemistry* **259**, 5871-5886
28. Lyon, A. M., and Tesmer, J. J. (2013) Structural insights into phospholipase C-beta function. *Molecular pharmacology* **84**, 488-500
29. Rhee, S. G. (2001) Regulation of phosphoinositide-specific phospholipase C. *Annual review of biochemistry* **70**, 281-312
30. Carman, C. V., Parent, J.-L., Day, P. W., Pronin, A. N., Sternweis, P. M., Wedegaertner, P. B., Gilman, A. G., Benovic, J. L., and Kozasa, T. (1999) Selective Regulation of G α q/11 by an RGS Domain in the G Protein-coupled Receptor Kinase, GRK2. *Journal of Biological Chemistry* **274**, 34483-34492
31. Day, P. W., Carman, C. V., Sterne-Marr, R., Benovic, J. L., and Wedegaertner, P. B. (2003) Differential interaction of GRK2 with members of the G α q family. *Biochemistry* **42**, 9176-9184
32. Day, P. W., Tesmer, J. J., Sterne-Marr, R., Freeman, L. C., Benovic, J. L., and Wedegaertner, P. B. (2004) Characterization of the GRK2 binding site of Galphaq. *The Journal of biological chemistry* **279**, 53643-53652
33. Hart, M. J., Jiang, X., Kozasa, T., Roscoe, W., Singer, W. D., Gilman, A. G., Sternweis, P. C., and Bollag, G. (1998) Direct stimulation of the guanine nucleotide exchange activity of p115 RhoGEF by Galpha13. *Science* **280**, 2112-2114
34. Worzfeld, T., Wettschureck, N., and Offermanns, S. (2008) G12/G13-mediated signalling in mammalian physiology and disease. *Trends in pharmacological sciences* **29**, 582-589
35. Simonds, W. F., Butrynski, J. E., Gautam, N., Unson, C. G., and Spiegel, A. M. (1991) G-protein beta gamma dimers. Membrane targeting requires subunit coexpression and intact gamma C-A-A-X domain. *The Journal of biological chemistry* **266**, 5363-5366
36. Wall, M. A., Coleman, D. E., Lee, E., Iniguez-Lluhi, J. A., Posner, B. A., Gilman, A. G., and Sprang, S. R. (1995) The structure of the G protein heterotrimer Gi α 1 β 1 γ 2. *Cell* **83**, 1047-1058
37. Clapham, D. E., and Neer, E. J. (1993) New roles for G-protein beta gamma dimers in transmembrane signalling. *Nature* **365**, 403-406
38. Pitcher, J. A., Inglese, J., Higgins, J. B., Arriza, J. L., Casey, P. J., Kim, C., Benovic, J. L., Kwatra, M. M., Caron, M. G., and Lefkowitz, R. J. (1992) Role of beta gamma subunits of G proteins in targeting the beta-adrenergic receptor kinase to membrane-bound receptors. *Science* **257**, 1264-1267

39. Koch, W. J., Hawes, B. E., Allen, L. F., and Lefkowitz, R. J. (1994) Direct evidence that Gi-coupled receptor stimulation of mitogen-activated protein kinase is mediated by G beta gamma activation of p21ras. *Proceedings of the National Academy of Sciences of the United States of America* **91**, 12706-12710
40. Faure, M., Voyno-Yasenetskaya, T. A., and Bourne, H. R. (1994) cAMP and beta gamma subunits of heterotrimeric G proteins stimulate the mitogen-activated protein kinase pathway in COS-7 cells. *The Journal of biological chemistry* **269**, 7851-7854
41. Ikeda, S. R. (1996) Voltage-dependent modulation of N-type calcium channels by G-protein beta gamma subunits. *Nature* **380**, 255-258
42. Herlitze, S., Garcia, D. E., Mackie, K., Hille, B., Scheuer, T., and Catterall, W. A. (1996) Modulation of Ca²⁺ channels by G-protein beta gamma subunits. *Nature* **380**, 258-262
43. Mark, M. D., and Herlitze, S. (2000) G-protein mediated gating of inward-rectifier K⁺ channels. *Eur J Biochem* **267**, 5830-5836
44. Tang, W. J., and Gilman, A. G. (1992) Adenylyl cyclases. *Cell* **70**, 869-872
45. Hermans, E. (2003) Biochemical and pharmacological control of the multiplicity of coupling at G-protein-coupled receptors. *Pharmacology & therapeutics* **99**, 25-44
46. Daaka, Y., Luttrell, L. M., and Lefkowitz, R. J. (1997) Switching of the coupling of the beta2-adrenergic receptor to different G proteins by protein kinase A. *Nature* **390**, 88-91
47. Craft, C. M., Whitmore, D. H., and Wiechmann, A. F. (1994) Cone arrestin identified by targeting expression of a functional family. *The Journal of biological chemistry* **269**, 4613-4619
48. Krupnick, J. G., and Benovic, J. L. (1998) The role of receptor kinases and arrestins in G protein-coupled receptor regulation. *Annual review of pharmacology and toxicology* **38**, 289-319
49. Attramadal, H., Arriza, J. L., Aoki, C., Dawson, T. M., Codina, J., Kwatra, M. M., Snyder, S. H., Caron, M. G., and Lefkowitz, R. J. (1992) Beta-arrestin2, a novel member of the arrestin/beta-arrestin gene family. *The Journal of biological chemistry* **267**, 17882-17890
50. Lohse, M. J., Benovic, J. L., Codina, J., Caron, M. G., and Lefkowitz, R. J. (1990) beta-Arrestin: a protein that regulates beta-adrenergic receptor function. *Science* **248**, 1547-1550
51. Ahn, S., Wei, H., Garrison, T. R., and Lefkowitz, R. J. (2004) Reciprocal regulation of angiotensin receptor-activated extracellular signal-regulated kinases by beta-arrestins 1 and 2. *The Journal of biological chemistry* **279**, 7807-7811
52. Wilden, U., Hall, S. W., and Kuhn, H. (1986) Phosphodiesterase activation by photoexcited rhodopsin is quenched when rhodopsin is phosphorylated and binds

- the intrinsic 48-kDa protein of rod outer segments. *Proceedings of the National Academy of Sciences of the United States of America* **83**, 1174-1178
53. Pierce, K. L., and Lefkowitz, R. J. (2001) Classical and new roles of [beta]-arrestins in the regulation of G-PROTEIN-COUPLED receptors. *Nat Rev Neurosci* **2**, 727-733
 54. Miller, W. E., and Lefkowitz, R. J. (2001) Expanding roles for beta-arrestins as scaffolds and adapters in GPCR signaling and trafficking. *Curr Opin Cell Biol* **13**, 139-145
 55. Noma, T., Lemaire, A., Naga Prasad, S. V., Barki-Harrington, L., Tilley, D. G., Chen, J., Le Corvoisier, P., Violin, J. D., Wei, H., Lefkowitz, R. J., and Rockman, H. A. (2007) Beta-arrestin-mediated beta1-adrenergic receptor transactivation of the EGFR confers cardioprotection. *The Journal of clinical investigation* **117**, 2445-2458
 56. Ahn, S., Shenoy, S. K., Wei, H., and Lefkowitz, R. J. (2004) Differential kinetic and spatial patterns of beta-arrestin and G protein-mediated ERK activation by the angiotensin II receptor. *The Journal of biological chemistry* **279**, 35518-35525
 57. Nuber, S., Zabel, U., Lorenz, K., Nuber, A., Milligan, G., Tobin, A. B., Lohse, M. J., and Hoffmann, C. (2016) β -Arrestin biosensors reveal a rapid, receptor-dependent activation/deactivation cycle. *Nature* **531**, 661-664
 58. Calebiro, D., Nikolaev, V. O., Gagliani, M. C., de Filippis, T., Dees, C., Tacchetti, C., Persani, L., and Lohse, M. J. (2009) Persistent cAMP-signals triggered by internalized G-protein-coupled receptors. *PLoS Biol* **7**, e1000172
 59. Ferrandon, S., Feinstein, T. N., Castro, M., Wang, B., Bouley, R., Potts, J. T., Gardella, T. J., and Vilardaga, J. P. (2009) Sustained cyclic AMP production by parathyroid hormone receptor endocytosis. *Nature chemical biology* **5**, 734-742
 60. Irannejad, R., Tomshine, J. C., Tomshine, J. R., Chevalier, M., Mahoney, J. P., Steyaert, J., Rasmussen, S. G., Sunahara, R. K., El-Samad, H., Huang, B., and von Zastrow, M. (2013) Conformational biosensors reveal GPCR signalling from endosomes. *Nature* **495**, 534-538
 61. Tsvetanova, N. G., Irannejad, R., and von Zastrow, M. (2015) GPCR signaling via heterotrimeric G proteins from endosomes. *The Journal of biological chemistry*
 62. Thomsen, Alex R. B., Plouffe, B., Cahill, Thomas J., III, Shukla, Arun K., Tarrasch, Jeffrey T., Dosey, Annie M., Kahsai, Alem W., Strachan, Ryan T., Pani, B., Mahoney, Jacob P., Huang, L., Breton, B., Heydenreich, Franziska M., Sunahara, Roger K., Skiniotis, G., Bouvier, M., and Lefkowitz, Robert J. (2016) GPCR-G Protein- β -Arrestin Super-Complex Mediates Sustained G Protein Signaling. *Cell* **166**, 907-919
 63. Shukla, A. K., Westfield, G. H., Xiao, K., Reis, R. I., Huang, L. Y., Tripathi-Shukla, P., Qian, J., Li, S., Blanc, A., Oleskie, A. N., Dosey, A. M., Su, M., Liang, C. R., Gu, L. L., Shan, J. M., Chen, X., Hanna, R., Choi, M., Yao, X. J., Klink, B. U.,

- Kahsai, A. W., Sidhu, S. S., Koide, S., Penczek, P. A., Kossiakoff, A. A., Woods, V. L., Jr., Kobilka, B. K., Skiniotis, G., and Lefkowitz, R. J. (2014) Visualization of arrestin recruitment by a G-protein-coupled receptor. *Nature* **512**, 218-222
64. Oakley, R. H., Laporte, S. A., Holt, J. A., Caron, M. G., and Barak, L. S. (2000) Differential affinities of visual arrestin, beta arrestin1, and beta arrestin2 for G protein-coupled receptors delineate two major classes of receptors. *The Journal of biological chemistry* **275**, 17201-17210
65. Oakley, R. H., Laporte, S. A., Holt, J. A., Barak, L. S., and Caron, M. G. (2001) Molecular determinants underlying the formation of stable intracellular G protein-coupled receptor-beta-arrestin complexes after receptor endocytosis*. *The Journal of biological chemistry* **276**, 19452-19460
66. Lee, M.-H., Appleton, K. M., Strungs, E. G., Kwon, J. Y., Morinelli, T. A., Peterson, Y. K., Laporte, S. A., and Luttrell, L. M. (2016) The conformational signature of β -arrestin2 predicts its trafficking and signalling functions. *Nature* **531**, 665-668
67. Goodman, O. B., Jr., Krupnick, J. G., Santini, F., Gurevich, V. V., Penn, R. B., Gagnon, A. W., Keen, J. H., and Benovic, J. L. (1996) Beta-arrestin acts as a clathrin adaptor in endocytosis of the beta2-adrenergic receptor. *Nature* **383**, 447-450
68. Sibley, D. R., Benovic, J. L., Caron, M. G., and Lefkowitz, R. J. (1987) Molecular mechanisms of beta-adrenergic receptor desensitization. *Advances in experimental medicine and biology* **221**, 253-273
69. Lohse, M. J., Andexinger, S., Pitcher, J., Trukawinski, S., Codina, J., Faure, J. P., Caron, M. G., and Lefkowitz, R. J. (1992) Receptor-specific desensitization with purified proteins. Kinase dependence and receptor specificity of beta-arrestin and arrestin in the beta 2-adrenergic receptor and rhodopsin systems. *The Journal of biological chemistry* **267**, 8558-8564
70. Laporte, S. A., Oakley, R. H., Zhang, J., Holt, J. A., Ferguson, S. S., Caron, M. G., and Barak, L. S. (1999) The beta2-adrenergic receptor/betaarrestin complex recruits the clathrin adaptor AP-2 during endocytosis. *Proceedings of the National Academy of Sciences of the United States of America* **96**, 3712-3717
71. Zhang, J., Ferguson, S. S., Barak, L. S., Menard, L., and Caron, M. G. (1996) Dynamin and beta-arrestin reveal distinct mechanisms for G protein-coupled receptor internalization. *The Journal of biological chemistry* **271**, 18302-18305
72. Trejo, J., and Coughlin, S. R. (1999) The cytoplasmic tails of protease-activated receptor-1 and substance P receptor specify sorting to lysosomes versus recycling. *The Journal of biological chemistry* **274**, 2216-2224
73. Staehelin, M., and Simons, P. (1982) Rapid and reversible disappearance of beta-adrenergic cell surface receptors. *The EMBO journal* **1**, 187-190
74. Morrison, K. J., Moore, R. H., Carsrud, N. D., Trial, J., Millman, E. E., Tuvim, M., Clark, R. B., Barber, R., Dickey, B. F., and Knoll, B. J. (1996) Repetitive

- endocytosis and recycling of the beta 2-adrenergic receptor during agonist-induced steady state redistribution. *Molecular pharmacology* **50**, 692-699
75. Oakley, R. H., Laporte, S. A., Holt, J. A., Barak, L. S., and Caron, M. G. (1999) Association of beta-arrestin with G protein-coupled receptors during clathrin-mediated endocytosis dictates the profile of receptor resensitization. *The Journal of biological chemistry* **274**, 32248-32257
76. Irannejad, R., and von Zastrow, M. (2014) GPCR signaling along the endocytic pathway. *Curr Opin Cell Biol* **27**, 109-116
77. Huang, Z. M., Gao, E., Chuprun, J. K., and Koch, W. J. (2014) GRK2 in the Heart: A GPCR Kinase and Beyond. *Antioxidants & redox signaling*
78. Wisler, J. W., DeWire, S. M., Whalen, E. J., Violin, J. D., Drake, M. T., Ahn, S., Shenoy, S. K., and Lefkowitz, R. J. (2007) A unique mechanism of beta-blocker action: carvedilol stimulates beta-arrestin signaling. *Proceedings of the National Academy of Sciences of the United States of America* **104**, 16657-16662
79. Rajagopal, K., Whalen, E. J., Violin, J. D., Stiber, J. A., Rosenberg, P. B., Premont, R. T., Coffman, T. M., Rockman, H. A., and Lefkowitz, R. J. (2006) Beta-arrestin2-mediated inotropic effects of the angiotensin II type 1A receptor in isolated cardiac myocytes. *Proceedings of the National Academy of Sciences of the United States of America* **103**, 16284-16289
80. Violin, J. D., DeWire, S. M., Yamashita, D., Rominger, D. H., Nguyen, L., Schiller, K., Whalen, E. J., Gowen, M., and Lark, M. W. (2010) Selectively engaging beta-arrestins at the angiotensin II type 1 receptor reduces blood pressure and increases cardiac performance. *The Journal of pharmacology and experimental therapeutics* **335**, 572-579
81. Tobin, A. B., Butcher, A. J., and Kong, K. C. (2008) Location, location, location...site-specific GPCR phosphorylation offers a mechanism for cell-type-specific signalling. *Trends in pharmacological sciences* **29**, 413-420
82. Benovic, J. L., DeBlasi, A., Stone, W. C., Caron, M. G., and Lefkowitz, R. J. (1989) Beta-adrenergic receptor kinase: primary structure delineates a multigene family. *Science* **246**, 235-240
83. Krupnick, J. G., Gurevich, V. V., and Benovic, J. L. (1997) Mechanism of quenching of phototransduction. Binding competition between arrestin and transducin for phosphorhodopsin. *The Journal of biological chemistry* **272**, 18125-18131
84. Premont, R. T., Macrae, A. D., Aparicio, S. A., Kendall, H. E., Welch, J. E., and Lefkowitz, R. J. (1999) The GRK4 subfamily of G protein-coupled receptor kinases. Alternative splicing, gene organization, and sequence conservation. *The Journal of biological chemistry* **274**, 29381-29389

85. Gurevich, E. V., Tesmer, J. J. G., Mushegian, A., and Gurevich, V. V. (2012) G protein-coupled receptor kinases: More than just kinases and not only for GPCRs. *Pharmacology and Therapeutics* **133**, 40-69
86. Lodowski, D. T., Tesmer, V. M., Benovic, J. L., and Tesmer, J. J. (2006) The structure of G protein-coupled receptor kinase (GRK)-6 defines a second lineage of GRKs. *The Journal of biological chemistry* **281**, 16785-16793
87. Tesmer, J. J., Tesmer, V. M., Lodowski, D. T., Steinhagen, H., and Huber, J. (2010) Structure of human G protein-coupled receptor kinase 2 in complex with the kinase inhibitor balanol. *J Med Chem* **53**, 1867-1870
88. Homan, K. T., Larimore, K. M., Elkins, J. M., Szklarz, M., Knapp, S., and Tesmer, J. J. (2015) Identification and structure-function analysis of subfamily selective G protein-coupled receptor kinase inhibitors. *ACS chemical biology* **10**, 310-319
89. Allen, S. J., Parthasarathy, G., Darke, P. L., Diehl, R. E., Ford, R. E., Hall, D. L., Johnson, S. A., Reid, J. C., Rickert, K. W., Shipman, J. M., Soisson, S. M., Zuck, P., Munshi, S. K., and Lumb, K. J. (2015) Structure and Function of the Hypertension Variant A486V of G Protein-coupled Receptor Kinase 4. *Journal of Biological Chemistry* **290**, 20360-20373
90. Homan, K. T., Waldschmidt, H. V., Glukhova, A., Cannavo, A., Song, J., Cheung, J. Y., Koch, W. J., Larsen, S. D., and Tesmer, J. J. (2015) Crystal Structure of G Protein-Coupled Receptor Kinase 5 in Complex with a Rationally Designed Inhibitor. *The Journal of biological chemistry*
91. Palczewski, K., Buczylko, J., Lebioda, L., Crabb, J. W., and Polans, A. S. (1993) Identification of the N-terminal region in rhodopsin kinase involved in its interaction with rhodopsin. *The Journal of biological chemistry* **268**, 6004-6013
92. Beautrait, A., Michalski, K. R., Lopez, T. S., Mannix, K. M., McDonald, D. J., Cutter, A. R., Medina, C. B., Hebert, A. M., Francis, C. J., Bouvier, M., Tesmer, J. J., and Sterne-Marr, R. (2014) Mapping the putative G protein-coupled receptor (GPCR) docking site on GPCR kinase 2: insights from intact cell phosphorylation and recruitment assays. *The Journal of biological chemistry* **289**, 25262-25275
93. Homan, K. T., Wu, E., Wilson, M. W., Singh, P., Larsen, S. D., and Tesmer, J. J. (2014) Structural and functional analysis of g protein-coupled receptor kinase inhibition by paroxetine and a rationally designed analog. *Molecular pharmacology* **85**, 237-248
94. Pitcher, J. A., Freedman, N. J., and Lefkowitz, R. J. (1998) G protein-coupled receptor kinases. *Annual review of biochemistry* **67**, 653-692
95. Ribas, C., Penela, P., Murga, C., Salcedo, A., Garcia-Hoz, C., Jurado-Pueyo, M., Aymerich, I., and Mayor, F., Jr. (2007) The G protein-coupled receptor kinase (GRK) interactome: role of GRKs in GPCR regulation and signaling. *Biochimica et biophysica acta* **1768**, 913-922

96. Homan, K. T., and Tesmer, J. J. (2014) Structural insights into G protein-coupled receptor kinase function. *Curr Opin Cell Biol* **27C**, 25-31
97. Sato, P. Y., Chuprun, J. K., Schwartz, M., and Koch, W. J. (2015) The evolving impact of g protein-coupled receptor kinases in cardiac health and disease. *Physiological reviews* **95**, 377-404
98. Inglese, J., Koch, W. J., Caron, M. G., and Lefkowitz, R. J. (1992) Isoprenylation in regulation of signal transduction by G-protein-coupled receptor kinases. *Nature* **359**, 147-150
99. Hisatomi, O., Matsuda, S., Satoh, T., Kotaka, S., Imanishi, Y., and Tokunaga, F. (1998) A novel subtype of G-protein-coupled receptor kinase, GRK7, in teleost cone photoreceptors. *FEBS letters* **424**, 159-164
100. Pitcher, J. A., Touhara, K., Payne, E. S., and Lefkowitz, R. J. (1995) Pleckstrin homology domain-mediated membrane association and activation of the beta-adrenergic receptor kinase requires coordinate interaction with G beta gamma subunits and lipid. *The Journal of biological chemistry* **270**, 11707-11710
101. Pitcher, J. A., Fredericks, Z. L., Stone, W. C., Premont, R. T., Stoffel, R. H., Koch, W. J., and Lefkowitz, R. J. (1996) Phosphatidylinositol 4,5-bisphosphate (PIP₂)-enhanced G protein-coupled receptor kinase (GRK) activity. Location, structure, and regulation of the PIP₂ binding site distinguishes the GRK subfamilies. *The Journal of biological chemistry* **271**, 24907-24913
102. Daaka, Y., Pitcher, J. A., Richardson, M., Stoffel, R. H., Robishaw, J. D., and Lefkowitz, R. J. (1997) Receptor and G betagamma isoform-specific interactions with G protein-coupled receptor kinases. *Proceedings of the National Academy of Sciences of the United States of America* **94**, 2180-2185
103. Inglese, J., Freedman, N. J., Koch, W. J., and Lefkowitz, R. J. (1993) Structure and mechanism of the G protein-coupled receptor kinases. *The Journal of biological chemistry* **268**, 23735-23738
104. Eichmann, T., Lorenz, K., Hoffmann, M., Brockmann, J., Krasel, C., Lohse, M. J., and Quitterer, U. (2003) The amino-terminal domain of G-protein-coupled receptor kinase 2 is a regulatory Gbeta gamma binding site. *The Journal of biological chemistry* **278**, 8052-8057
105. DebBurman, S. K., Ptasienski, J., Boetticher, E., Lomasney, J. W., Benovic, J. L., and Hosey, M. M. (1995) Lipid-mediated regulation of G protein-coupled receptor kinases 2 and 3. *The Journal of biological chemistry* **270**, 5742-5747
106. Thiyagarajan, M. M., Stracquatano, R. P., Pronin, A. N., Evanko, D. S., Benovic, J. L., and Wedegaertner, P. B. (2004) A predicted amphipathic helix mediates plasma membrane localization of GRK5. *The Journal of biological chemistry* **279**, 17989-17995

107. Johnson, L. R., Robinson, J. D., Lester, K. N., and Pitcher, J. A. (2013) Distinct Structural Features of G Protein-Coupled Receptor Kinase 5 (GRK5) Regulate Its Nuclear Localization and DNA-Binding Ability. *PLoS one* **8**, e62508
108. Stoffel, R. H., Randall, R. R., Premont, R. T., Lefkowitz, R. J., and Inglese, J. (1994) Palmitoylation of G protein-coupled receptor kinase, GRK6. Lipid modification diversity in the GRK family. *The Journal of biological chemistry* **269**, 27791-27794
109. Premont, R. T., Macrae, A. D., Stoffel, R. H., Chung, N., Pitcher, J. A., Ambrose, C., Inglese, J., MacDonald, M. E., and Lefkowitz, R. J. (1996) Characterization of the G protein-coupled receptor kinase GRK4. Identification of four splice variants. *The Journal of biological chemistry* **271**, 6403-6410
110. Benovic, J. L., Strasser, R. H., Caron, M. G., and Lefkowitz, R. J. (1986) Beta-adrenergic receptor kinase: identification of a novel protein kinase that phosphorylates the agonist-occupied form of the receptor. *Proceedings of the National Academy of Sciences of the United States of America* **83**, 2797-2801
111. Nobles, K. N., Xiao, K., Ahn, S., Shukla, A. K., Lam, C. M., Rajagopal, S., Strachan, R. T., Huang, T.-Y., Bressler, E. A., Hara, M. R., Shenoy, S. K., Gygi, S. P., and Lefkowitz, R. J. (2011) Distinct Phosphorylation Sites on the β 2-Adrenergic Receptor Establish a Barcode That Encodes Differential Functions of β -Arrestin. *Sci. Signal.* **4**, ra51-
112. Bouvier, M., Hausdorff, W. P., De Blasi, A., O'Dowd, B. F., Kobilka, B. K., Caron, M. G., and Lefkowitz, R. J. (1988) Removal of phosphorylation sites from the beta 2-adrenergic receptor delays onset of agonist-promoted desensitization. *Nature* **333**, 370-373
113. Benovic, J. L., Pike, L. J., Cerione, R. A., Staniszewski, C., Yoshimasa, T., Codina, J., Caron, M. G., and Lefkowitz, R. J. (1985) Phosphorylation of the mammalian beta-adrenergic receptor by cyclic AMP-dependent protein kinase. Regulation of the rate of receptor phosphorylation and dephosphorylation by agonist occupancy and effects on coupling of the receptor to the stimulatory guanine nucleotide regulatory protein. *The Journal of biological chemistry* **260**, 7094-7101
114. Bouvier, M., Leeb-Lundberg, L. M., Benovic, J. L., Caron, M. G., and Lefkowitz, R. J. (1987) Regulation of adrenergic receptor function by phosphorylation. II. Effects of agonist occupancy on phosphorylation of alpha 1- and beta 2-adrenergic receptors by protein kinase C and the cyclic AMP-dependent protein kinase. *The Journal of biological chemistry* **262**, 3106-3113
115. Kim, J., Ahn, S., Ren, X. R., Whalen, E. J., Reiter, E., Wei, H., and Lefkowitz, R. J. (2005) Functional antagonism of different G protein-coupled receptor kinases for beta-arrestin-mediated angiotensin II receptor signaling. *Proceedings of the National Academy of Sciences of the United States of America* **102**, 1442-1447

116. Ren, X.-R., Reiter, E., Ahn, S., Kim, J., Chen, W., and Lefkowitz, R. J. (2005) Different G protein-coupled receptor kinases govern G protein and β -arrestin-mediated signaling of V2 vasopressin receptor. *Proceedings of the National Academy of Sciences of the United States of America* **102**, 1448-1453
117. Carman, C. V., Som, T., Kim, C. M., and Benovic, J. L. (1998) Binding and phosphorylation of tubulin by G protein-coupled receptor kinases. *The Journal of biological chemistry* **273**, 20308-20316
118. Kahsai, A. W., Zhu, S., and Fenteany, G. (2010) G protein-coupled receptor kinase 2 activates radixin, regulating membrane protrusion and motility in epithelial cells. *Biochimica et biophysica acta* **1803**, 300-310
119. Cant, S. H., and Pitcher, J. A. (2005) G protein-coupled receptor kinase 2-mediated phosphorylation of ezrin is required for G protein-coupled receptor-dependent reorganization of the actin cytoskeleton. *Molecular biology of the cell* **16**, 3088-3099
120. Ruiz-Gomez, A., Humrich, J., Murga, C., Quitterer, U., Lohse, M. J., and Mayor, F., Jr. (2000) Phosphorylation of phosducin and phosducin-like protein by G protein-coupled receptor kinase 2. *The Journal of biological chemistry* **275**, 29724-29730
121. Muller, S., Straub, A., Schroder, S., Bauer, P. H., and Lohse, M. J. (1996) Interactions of phosducin with defined G protein beta gamma-subunits. *The Journal of biological chemistry* **271**, 11781-11786
122. Pronin, A. N., Morris, A. J., Surguchov, A., and Benovic, J. L. (2000) Synucleins are a novel class of substrates for G protein-coupled receptor kinases. *The Journal of biological chemistry* **275**, 26515-26522
123. Patial, S., Luo, J., Porter, K. J., Benovic, J. L., and Parameswaran, N. (2010) G-protein-coupled-receptor kinases mediate TNF α -induced NF κ B signalling via direct interaction with and phosphorylation of I κ B α . *The Biochemical journal* **425**, 169-178
124. Freedman, N. J., Kim, L. K., Murray, J. P., Exum, S. T., Brian, L., Wu, J. H., and Peppel, K. (2002) Phosphorylation of the platelet-derived growth factor receptor-beta and epidermal growth factor receptor by G protein-coupled receptor kinase-2. Mechanisms for selectivity of desensitization. *The Journal of biological chemistry* **277**, 48261-48269
125. Sterne-Marr, R., Tesmer, J. J., Day, P. W., Stracquatano, R. P., Cilente, J. A., O'Connor, K. E., Pronin, A. N., Benovic, J. L., and Wedegaertner, P. B. (2003) G protein-coupled receptor Kinase 2/G α q/11 interaction. A novel surface on a regulator of G protein signaling homology domain for binding G α subunits. *The Journal of biological chemistry* **278**, 6050-6058
126. Sallese, M., Mariggio, S., D'Urbano, E., Iacovelli, L., and De Blasi, A. (2000) Selective regulation of Gq signaling by G protein-coupled receptor kinase 2: direct

- interaction of kinase N terminus with activated galphaq. *Molecular pharmacology* **57**, 826-831
127. Naga Prasad, S. V., Barak, L. S., Rapacciuolo, A., Caron, M. G., and Rockman, H. A. (2001) Agonist-dependent recruitment of phosphoinositide 3-kinase to the membrane by beta-adrenergic receptor kinase 1. A role in receptor sequestration. *The Journal of biological chemistry* **276**, 18953-18959
 128. Premont, R. T., Claing, A., Vitale, N., Freeman, J. L., Pitcher, J. A., Patton, W. A., Moss, J., Vaughan, M., and Lefkowitz, R. J. (1998) beta2-Adrenergic receptor regulation by GIT1, a G protein-coupled receptor kinase-associated ADP ribosylation factor GTPase-activating protein. *Proceedings of the National Academy of Sciences of the United States of America* **95**, 14082-14087
 129. Shiina, T., Arai, K., Tanabe, S., Yoshida, N., Haga, T., Nagao, T., and Kurose, H. (2001) Clathrin box in G protein-coupled receptor kinase 2. *The Journal of biological chemistry* **276**, 33019-33026
 130. Ungerer, M., Bohm, M., Elce, J. S., Erdmann, E., and Lohse, M. J. (1993) Altered expression of beta-adrenergic receptor kinase and beta 1-adrenergic receptors in the failing human heart. *Circulation* **87**, 454-463
 131. Penela, P., Murga, C., Ribas, C., Lafarga, V., and Mayor Jr, F. (2010) The complex G protein-coupled receptor kinase 2 (GRK2) interactome unveils new physiopathological targets. *British Journal of Pharmacology* **160**, 821-832
 132. (2016) 2016 ESC Guidelines for the diagnosis and treatment of acute and chronic heart failure: The Task Force for the diagnosis and treatment of acute and chronic heart failure of the European Society of Cardiology (ESC). Developed with the special contribution of the Heart Failure Association (HFA) of the ESC. *European journal of heart failure*
 133. Bristow, M. R., Ginsburg, R., Minobe, W., Cubicciotti, R. S., Sageman, W. S., Lurie, K., Billingham, M. E., Harrison, D. C., and Stinson, E. B. (1982) Decreased catecholamine sensitivity and beta-adrenergic-receptor density in failing human hearts. *The New England journal of medicine* **307**, 205-211
 134. Bristow, M. R., Ginsburg, R., Umans, V., Fowler, M., Minobe, W., Rasmussen, R., Zera, P., Menlove, R., Shah, P., Jamieson, S., and et al. (1986) Beta 1- and beta 2-adrenergic-receptor subpopulations in nonfailing and failing human ventricular myocardium: coupling of both receptor subtypes to muscle contraction and selective beta 1-receptor down-regulation in heart failure. *Circulation research* **59**, 297-309
 135. Communal, C., Singh, K., Sawyer, D. B., and Colucci, W. S. (1999) Opposing effects of beta(1)- and beta(2)-adrenergic receptors on cardiac myocyte apoptosis : role of a pertussis toxin-sensitive G protein. *Circulation* **100**, 2210-2212
 136. Chen, M., Sato, P. Y., Chuprun, J. K., Peroutka, R. J., Otis, N. J., Ibeti, J., Pan, S., Sheu, S. S., Gao, E., and Koch, W. J. (2013) Prodeath signaling of G protein-

- coupled receptor kinase 2 in cardiac myocytes after ischemic stress occurs via extracellular signal-regulated kinase-dependent heat shock protein 90-mediated mitochondrial targeting. *Circulation research* **112**, 1121-1134
137. Lymeropoulos, A., Rengo, G., Funakoshi, H., Eckhart, A. D., and Koch, W. J. (2007) Adrenal GRK2 upregulation mediates sympathetic overdrive in heart failure. *Nature medicine* **13**, 315-323
 138. Rockman, H. A., Choi, D. J., Akhter, S. A., Jaber, M., Giros, B., Lefkowitz, R. J., Caron, M. G., and Koch, W. J. (1998) Control of myocardial contractile function by the level of beta-adrenergic receptor kinase 1 in gene-targeted mice. *The Journal of biological chemistry* **273**, 18180-18184
 139. Koch, W. J., Rockman, H. A., Samama, P., Hamilton, R. A., Bond, R. A., Milano, C. A., and Lefkowitz, R. J. (1995) Cardiac function in mice overexpressing the beta-adrenergic receptor kinase or a beta ARK inhibitor. *Science* **268**, 1350-1353
 140. Rockman, H. A., Chien, K. R., Choi, D. J., Iaccarino, G., Hunter, J. J., Ross, J., Jr., Lefkowitz, R. J., and Koch, W. J. (1998) Expression of a beta-adrenergic receptor kinase 1 inhibitor prevents the development of myocardial failure in gene-targeted mice. *Proceedings of the National Academy of Sciences of the United States of America* **95**, 7000-7005
 141. Raake, P. W., Schlegel, P., Ksienzyk, J., Reinkober, J., Barthelmes, J., Schinkel, S., Pleger, S., Mier, W., Haberkorn, U., Koch, W. J., Katus, H. A., Most, P., and Muller, O. J. (2013) AAV6.betaARKct cardiac gene therapy ameliorates cardiac function and normalizes the catecholaminergic axis in a clinically relevant large animal heart failure model. *European heart journal* **34**, 1437-1447
 142. Iaccarino, G., Tomhave, E. D., Lefkowitz, R. J., and Koch, W. J. (1998) Reciprocal in vivo regulation of myocardial G protein-coupled receptor kinase expression by beta-adrenergic receptor stimulation and blockade. *Circulation* **98**, 1783-1789
 143. Abd Alla, J., Graemer, M., Fu, X., and Quitterer, U. (2016) Inhibition of G-protein-coupled Receptor Kinase 2 Prevents the Dysfunctional Cardiac Substrate Metabolism in Fatty Acid Synthase Transgenic Mice. *The Journal of biological chemistry* **291**, 2583-2600
 144. Raake, P. W., Vinge, L. E., Gao, E., Boucher, M., Rengo, G., Chen, X., DeGeorge, B. R., Jr., Matkovich, S., Houser, S. R., Most, P., Eckhart, A. D., Dorn, G. W., 2nd, and Koch, W. J. (2008) G protein-coupled receptor kinase 2 ablation in cardiac myocytes before or after myocardial infarction prevents heart failure. *Circulation research* **103**, 413-422
 145. Gros, R., Benovic, J. L., Tan, C. M., and Feldman, R. D. (1997) G-protein-coupled receptor kinase activity is increased in hypertension. *The Journal of clinical investigation* **99**, 2087-2093

146. Liu, S., Premont, R. T., Kontos, C. D., Zhu, S., and Rockey, D. C. (2005) A crucial role for GRK2 in regulation of endothelial cell nitric oxide synthase function in portal hypertension. *Nature medicine* **11**, 952-958
147. Avendano, M. S., Lucas, E., Jurado-Pueyo, M., Martinez-Revelles, S., Vila-Bedmar, R., Mayor, F., Jr., Salaices, M., Briones, A. M., and Murga, C. (2014) Increased nitric oxide bioavailability in adult GRK2 hemizygous mice protects against angiotensin II-induced hypertension. *Hypertension* **63**, 369-375
148. Tutunea-Fatan, E., Caetano, F. A., Gros, R., and Ferguson, S. S. (2015) GRK2 Targeted Knock-down Results in Spontaneous Hypertension, and Altered Vascular GPCR Signaling. *The Journal of biological chemistry*
149. Eckhart, A. D., Ozaki, T., Tevæarai, H., Rockman, H. A., and Koch, W. J. (2002) Vascular-targeted overexpression of G protein-coupled receptor kinase-2 in transgenic mice attenuates beta-adrenergic receptor signaling and increases resting blood pressure. *Molecular pharmacology* **61**, 749-758
150. Garcia-Guerra, L., Nieto-Vazquez, I., Vila-Bedmar, R., Jurado-Pueyo, M., Zalba, G., Diez, J., Murga, C., Fernandez-Veledo, S., Mayor, F., Jr., and Lorenzo, M. (2010) G protein-coupled receptor kinase 2 plays a relevant role in insulin resistance and obesity. *Diabetes* **59**, 2407-2417
151. Vila-Bedmar, R., Cruces-Sande, M., Lucas, E., Willemen, H. L., Heijnen, C. J., Kavelaars, A., Mayor, F., Jr., and Murga, C. (2015) Reversal of diet-induced obesity and insulin resistance by inducible genetic ablation of GRK2. *Science signaling* **8**, ra73
152. Anis, Y., Leshem, O., Reuveni, H., Wexler, I., Ben Sasson, R., Yahalom, B., Laster, M., Raz, I., Ben Sasson, S., Shafir, E., and Ziv, E. (2004) Antidiabetic effect of novel modulating peptides of G-protein-coupled kinase in experimental models of diabetes. *Diabetologia* **47**, 1232-1244
153. Cipolletta, E., Campanile, A., Santulli, G., Sanzari, E., Leosco, D., Campiglia, P., Trimarco, B., and Iaccarino, G. (2009) The G protein coupled receptor kinase 2 plays an essential role in beta-adrenergic receptor-induced insulin resistance. *Cardiovascular research* **84**, 407-415
154. Usui, I., Imamura, T., Satoh, H., Huang, J., Babendure, J. L., Hupfeld, C. J., and Olefsky, J. M. (2004) GRK2 is an endogenous protein inhibitor of the insulin signaling pathway for glucose transport stimulation. *The EMBO journal* **23**, 2821-2829
155. Usui, I., Imamura, T., Babendure, J. L., Satoh, H., Lu, J. C., Hupfeld, C. J., and Olefsky, J. M. (2005) G protein-coupled receptor kinase 2 mediates endothelin-1-induced insulin resistance via the inhibition of both Galphaq/11 and insulin receptor substrate-1 pathways in 3T3-L1 adipocytes. *Molecular endocrinology* **19**, 2760-2768

156. Nemeth, E. F. (2002) The search for calcium receptor antagonists (calcilytics). *J Mol Endocrinol* **29**, 15-21
157. Marie, P. J. (2010) The calcium-sensing receptor in bone cells: a potential therapeutic target in osteoporosis. *Bone* **46**, 571-576
158. Uzawa, T., Hori, M., Ejiri, S., and Ozawa, H. (1995) Comparison of the effects of intermittent and continuous administration of human parathyroid hormone(1-34) on rat bone. *Bone* **16**, 477-484
159. Ward, D. T., and Riccardi, D. (2012) New concepts in calcium-sensing receptor pharmacology and signalling. *Br J Pharmacol* **165**, 35-48
160. Lorenz, S., Frenzel, R., Paschke, R., Breitwieser, G. E., and Miedlich, S. U. (2007) Functional desensitization of the extracellular calcium-sensing receptor is regulated via distinct mechanisms: role of G protein-coupled receptor kinases, protein kinase C and beta-arrestins. *Endocrinology* **148**, 2398-2404
161. Jaber, M., Koch, W. J., Rockman, H., Smith, B., Bond, R. A., Sulik, K. K., Ross, J., Jr., Lefkowitz, R. J., Caron, M. G., and Giros, B. (1996) Essential role of beta-adrenergic receptor kinase 1 in cardiac development and function. *Proceedings of the National Academy of Sciences of the United States of America* **93**, 12974-12979
162. Matkovich, S. J., Diwan, A., Klanke, J. L., Hammer, D. J., Marreez, Y., Odley, A. M., Brunskill, E. W., Koch, W. J., Schwartz, R. J., and Dorn, G. W., 2nd. (2006) Cardiac-specific ablation of G-protein receptor kinase 2 redefines its roles in heart development and beta-adrenergic signaling. *Circulation research* **99**, 996-1003
163. Metaye, T., Levillain, P., Kraimps, J. L., and Perdrisot, R. (2008) Immunohistochemical detection, regulation and antiproliferative function of G-protein-coupled receptor kinase 2 in thyroid carcinomas. *The Journal of endocrinology* **198**, 101-110
164. Wei, Z., Hurtt, R., Ciccarelli, M., Koch, W. J., and Doria, C. (2012) Growth inhibition of human hepatocellular carcinoma cells by overexpression of G-protein-coupled receptor kinase 2. *Journal of cellular physiology* **227**, 2371-2377
165. Penela, P., Rivas, V., Salcedo, A., and Mayor, F., Jr. (2010) G protein-coupled receptor kinase 2 (GRK2) modulation and cell cycle progression. *Proceedings of the National Academy of Sciences of the United States of America* **107**, 1118-1123
166. Nogues, L., Reglero, C., Rivas, V., Salcedo, A., Lafarga, V., Neves, M., Ramos, P., Mendiola, M., Berjon, A., Stamatakis, K., Zhou, X. Z., Lu, K. P., Hardisson, D., Mayor, F., Jr., and Penela, P. (2016) G Protein-coupled Receptor Kinase 2 (GRK2) Promotes Breast Tumorigenesis Through a HDAC6-Pin1 Axis. *EBioMedicine*
167. Pollesello, P. (2014) Drug discovery and development for acute heart failure drugs: Are expectations too high? *International journal of cardiology*
168. Lorenz, K., Lohse, M. J., and Quitterer, U. (2003) Protein kinase C switches the Raf kinase inhibitor from Raf-1 to GRK-2. *Nature* **426**, 574-579

169. Yeung, K., Seitz, T., Li, S., Janosch, P., McFerran, B., Kaiser, C., Fee, F., Katsanakis, K. D., Rose, D. W., Mischak, H., Sedivy, J. M., and Kolch, W. (1999) Suppression of Raf-1 kinase activity and MAP kinase signalling by RKIP. *Nature* **401**, 173-177
170. Deiss, K., Kisker, C., Lohse, M. J., and Lorenz, K. (2012) Raf kinase inhibitor protein (RKIP) dimer formation controls its target switch from Raf1 to G protein-coupled receptor kinase (GRK) 2. *Journal of Biological Chemistry* **287**, 23407-23417
171. Hengst, U., Albrecht, H., Hess, D., and Monard, D. (2001) The phosphatidylethanolamine-binding protein is the prototype of a novel family of serine protease inhibitors. *The Journal of biological chemistry* **276**, 535-540
172. Schmid, E., Neef, S., Berlin, C., Tomasovic, A., Kahlert, K., Nordbeck, P., Deiss, K., Denzinger, S., Herrmann, S., Wettwer, E., Weidendorfer, M., Becker, D., Schafer, F., Wagner, N., Ergun, S., Schmitt, J. P., Katus, H. A., Weidemann, F., Ravens, U., Maack, C., Hein, L., Ertl, G., Muller, O. J., Maier, L. S., Lohse, M. J., and Lorenz, K. (2015) Cardiac RKIP induces a beneficial beta-adrenoceptor-dependent positive inotropy. *Nature medicine* **21**, 1298-1306
173. Fu, X., Koller, S., Alla, J. A., and Qwitterer, U. (2013) Inhibition of G-protein-coupled Receptor Kinase 2 (GRK2) Triggers the Growth-promoting Mitogen-activated Protein Kinase (MAPK) Pathway. *Journal of Biological Chemistry* **288**, 7738-7755
174. Pao, C. S., Barker, B. L., and Benovic, J. L. (2009) Role of the amino terminus of G protein-coupled receptor kinase 2 in receptor phosphorylation. *Biochemistry* **48**, 7325-7333
175. Mayer, G., Wulffen, B., Huber, C., Brockmann, J., Flicke, B., Neumann, L., Hafenbradl, D., Klebl, B. M., Lohse, M. J., Krasel, C., and Blind, M. (2008) An RNA molecule that specifically inhibits G-protein-coupled receptor kinase 2 in vitro. *RNA (New York, N.Y.)* **14**, 524-534
176. Tesmer, V. M., Lennarz, S., Mayer, G., and Tesmer, J. J. (2012) Molecular mechanism for inhibition of g protein-coupled receptor kinase 2 by a selective RNA aptamer. *Structure* **20**, 1300-1309
177. Hafner, M., Vianini, E., Albertoni, B., Marchetti, L., Grune, I., Gloeckner, C., and Famulok, M. (2008) Displacement of protein-bound aptamers with small molecules screened by fluorescence polarization. *Nature protocols* **3**, 579-587
178. Thal, D. M., Homan, K. T., Chen, J., Wu, E. K., Hinkle, P. M., Huang, Z. M., Chuprun, J. K., Song, J., Gao, E., Cheung, J. Y., Sklar, L. A., Koch, W. J., and Tesmer, J. J. (2012) Paroxetine is a direct inhibitor of g protein-coupled receptor kinase 2 and increases myocardial contractility. *ACS chemical biology* **7**, 1830-1839

179. Schumacher, S. M., Gao, E., Zhu, W., Chen, X., Chuprun, J. K., Feldman, A. M., JJ, G. T., and Koch, W. J. (2015) Paroxetine-mediated GRK2 inhibition reverses cardiac dysfunction and remodeling after myocardial infarction. *Science translational medicine* **7**, 277ra231
180. Setyawan, J., Koide, K., Diller, T. C., Bunnage, M. E., Taylor, S. S., Nicolaou, K. C., and Brunton, L. L. (1999) Inhibition of protein kinases by balanol: specificity within the serine/threonine protein kinase subfamily. *Molecular pharmacology* **56**, 370-376
181. Homan, K. T., and Tesmer, J. J. (2015) Molecular basis for small molecule inhibition of G protein-coupled receptor kinases. *ACS chemical biology* **10**, 246-256
182. Thal, D. M., Yeow, R. Y., Schoenau, C., Huber, J., and Tesmer, J. J. (2011) Molecular mechanism of selectivity among G protein-coupled receptor kinase 2 inhibitors. *Molecular pharmacology* **80**, 294-303
183. Harding, V. B., Jones, L. R., Lefkowitz, R. J., Koch, W. J., and Rockman, H. A. (2001) Cardiac beta ARK1 inhibition prolongs survival and augments beta blocker therapy in a mouse model of severe heart failure. *Proceedings of the National Academy of Sciences of the United States of America* **98**, 5809-5814
184. Akhter, S. A., Eckhart, A. D., Rockman, H. A., Shotwell, K., Lefkowitz, R. J., and Koch, W. J. (1999) In vivo inhibition of elevated myocardial beta-adrenergic receptor kinase activity in hybrid transgenic mice restores normal beta-adrenergic signaling and function. *Circulation* **100**, 648-653
185. Williams, M. L., Hata, J. A., Schroder, J., Rampersaud, E., Petrofski, J., Jakoi, A., Milano, C. A., and Koch, W. J. (2004) Targeted beta-adrenergic receptor kinase (betaARK1) inhibition by gene transfer in failing human hearts. *Circulation* **109**, 1590-1593
186. Volkers, M., Weidenhammer, C., Herzog, N., Qiu, G., Spaich, K., von Wegner, F., Peppel, K., Muller, O. J., Schinkel, S., Rabinowitz, J. E., Hippe, H. J., Brinks, H., Katus, H. A., Koch, W. J., Eckhart, A. D., Friedrich, O., and Most, P. (2011) The inotropic peptide betaARKct improves betaAR responsiveness in normal and failing cardiomyocytes through G(betaagamma)-mediated L-type calcium current disinhibition. *Circulation research* **108**, 27-39
187. Koch, W. J., Inglese, J., Stone, W. C., and Lefkowitz, R. J. (1993) The binding site for the beta gamma subunits of heterotrimeric G proteins on the beta-adrenergic receptor kinase. *The Journal of biological chemistry* **268**, 8256-8260
188. Scott, J. K., Huang, S. F., Gangadhar, B. P., Samoriski, G. M., Clapp, P., Gross, R. A., Taussig, R., and Smrcka, A. V. (2001) Evidence that a protein-protein interaction 'hot spot' on heterotrimeric G protein betagamma subunits is used for recognition of a subclass of effectors. *The EMBO journal* **20**, 767-776

189. Ghosh, M., Peterson, Y. K., Lanier, S. M., and Smrcka, A. V. (2003) Receptor- and nucleotide exchange-independent mechanisms for promoting G protein subunit dissociation. *The Journal of biological chemistry* **278**, 34747-34750
190. Davis, T. L., Bonacci, T. M., Sprang, S. R., and Smrcka, A. V. (2005) Structural and molecular characterization of a preferred protein interaction surface on G protein beta gamma subunits. *Biochemistry* **44**, 10593-10604
191. Bonacci, T. M., Mathews, J. L., Yuan, C., Lehmann, D. M., Malik, S., Wu, D., Font, J. L., Bidlack, J. M., and Smrcka, A. V. (2006) Differential targeting of Gbetagamma-subunit signaling with small molecules. *Science* **312**, 443-446
192. Casey, L. M., Pistner, A. R., Belmonte, S. L., Migdalovich, D., Stolpnik, O., Nwakanma, F. E., Vorobiof, G., Dunaevsky, O., Matavel, A., Lopes, C. M., Smrcka, A. V., and Blaxall, B. C. (2010) Small molecule disruption of G beta gamma signaling inhibits the progression of heart failure. *Circulation research* **107**, 532-539
193. Bluml, K., Schnepf, W., Schroder, S., Beyermann, M., Macias, M., Oschkinat, H., and Lohse, M. J. (1997) A small region in phosducin inhibits G-protein betagamma-subunit function. *The EMBO journal* **16**, 4908-4915
194. Benovic, J. L., Onorato, J., Lohse, M. J., Dohlman, H. G., Staniszewski, C., Caron, M. G., and Lefkowitz, R. J. (1990) Synthetic peptides of the hamster beta 2-adrenoceptor as substrates and inhibitors of the beta-adrenoceptor kinase. *Br J Clin Pharmacol* **30 Suppl 1**, 3S-12S
195. Winstel, R., Ihlenfeldt, H.-G., Jung, G., Krasel, C., and Lohse, M. J. (2005) Peptide inhibitors of G protein-coupled receptor kinases. *Biochemical Pharmacology* **70**, 1001-1008
196. Carotenuto, A., Cipolletta, E., Gomez-Monterrey, I., Sala, M., Vernieri, E., Limatola, A., Bertamino, A., Musella, S., Sorriento, D., Grieco, P., Trimarco, B., Novellino, E., Iaccarino, G., and Campiglia, P. (2013) Design, synthesis and efficacy of novel G protein-coupled receptor kinase 2 inhibitors. *European journal of medicinal chemistry* **69**, 384-392
197. Gomez-Monterrey, I., Carotenuto, A., Cipolletta, E., Sala, M., Vernieri, E., Limatola, A., Bertamino, A., Musella, S., Grieco, P., Trimarco, B., Novellino, E., Iaccarino, G., and Campiglia, P. (2014) SAR study and conformational analysis of a series of novel peptide G protein-coupled receptor kinase 2 inhibitors. *Biopolymers* **101**, 121-128
198. Benovic, J. L., Stone, W. C., Caron, M. G., and Lefkowitz, R. J. (1989) Inhibition of the beta-adrenergic receptor kinase by polyanions. *The Journal of biological chemistry* **264**, 6707-6710
199. Lohse, M. J., Benovic, J. L., Caron, M. G., and Lefkowitz, R. J. (1990) Multiple pathways of rapid beta 2-adrenergic receptor desensitization. Delineation with specific inhibitors. *The Journal of biological chemistry* **265**, 3202-3211

200. Schulte-Michels, J., Wolf, A., Aatz, S., Engelhard, K., Sieben, A., Martinez-Osuna, M., Haberlein, F., and Haberlein, H. (2016) alpha-Hederin inhibits G protein-coupled receptor kinase 2-mediated phosphorylation of beta2-adrenergic receptors. *Phytomedicine : international journal of phytotherapy and phytopharmacology* **23**, 52-57
201. Tsomaia, N. (2015) Peptide therapeutics: targeting the undruggable space. *European journal of medicinal chemistry* **94**, 459-470
202. Lipinski, C. A., Lombardo, F., Dominy, B. W., and Feeney, P. J. (2001) Experimental and computational approaches to estimate solubility and permeability in drug discovery and development settings. *Advanced drug delivery reviews* **46**, 3-26
203. Ladner, R. C., Sato, A. K., Gorzelany, J., and de Souza, M. (2004) Phage display-derived peptides as therapeutic alternatives to antibodies. *Drug discovery today* **9**, 525-529
204. Kovalainen, M., Monkare, J., Riikonen, J., Pesonen, U., Vlasova, M., Salonen, J., Lehto, V. P., Jarvinen, K., and Herzig, K. H. (2015) Novel delivery systems for improving the clinical use of peptides. *Pharmacol Rev* **67**, 541-561
205. Moroz, E., Matorri, S., and Leroux, J. C. (2016) Oral delivery of macromolecular drugs: Where we are after almost 100years of attempts. *Advanced drug delivery reviews* **101**, 108-121
206. Fosgerau, K., and Hoffmann, T. (2015) Peptide therapeutics: current status and future directions. *Drug discovery today* **20**, 122-128
207. Wojcik, P., and Berlicki, L. (2016) Peptide-based inhibitors of protein-protein interactions. *Bioorganic & medicinal chemistry letters* **26**, 707-713
208. Licht, T., Tsurulnikov, L., Reuveni, H., Yarnitzky, T., and Ben-Sasson, S. A. (2003) Induction of pro-angiogenic signaling by a synthetic peptide derived from the second intracellular loop of S1P3 (EDG3). *Blood* **102**, 2099-2107
209. Karatas, H., Townsend, E. C., Cao, F., Chen, Y., Bernard, D., Liu, L., Lei, M., Dou, Y., and Wang, S. (2013) High-affinity, small-molecule peptidomimetic inhibitors of MLL1/WDR5 protein-protein interaction. *Journal of the American Chemical Society* **135**, 669-682
210. Rengo, G., Lymperopoulos, A., Leosco, D., and Koch, W. J. (2011) GRK2 as a novel gene therapy target in heart failure. *Journal of molecular and cellular cardiology* **50**, 785-792
211. Greenberg, B. (2015) Gene therapy for heart failure. *Journal of cardiology* **66**, 195-200
212. Greenberg, B., Butler, J., Felker, G. M., Ponikowski, P., Voors, A. A., Desai, A. S., Barnard, D., Bouchard, A., Jaski, B., Lyon, A. R., Pogoda, J. M., Rudy, J. J., and Zsebo, K. M. (2016) Calcium upregulation by percutaneous administration of gene therapy in patients with cardiac disease (CUPID 2): a randomised,

- multinational, double-blind, placebo-controlled, phase 2b trial. *Lancet (London, England)* **387**, 1178-1186
213. Akhter, S. A., Skaer, C. A., Kypson, A. P., McDonald, P. H., Peppel, K. C., Glower, D. D., Lefkowitz, R. J., and Koch, W. J. (1997) Restoration of beta-adrenergic signaling in failing cardiac ventricular myocytes via adenoviral-mediated gene transfer. *Proceedings of the National Academy of Sciences of the United States of America* **94**, 12100-12105
 214. Smith, G. P. (1985) Filamentous fusion phage: novel expression vectors that display cloned antigens on the virion surface. *Science* **228**, 1315-1317
 215. Molek, P., Strukelj, B., and Bratkovic, T. (2011) Peptide phage display as a tool for drug discovery: targeting membrane receptors. *Molecules* **16**, 857-887
 216. Rahbarnia, L., Farajnia, S., Babaei, H., Majidi, J., Veisi, K., Ahmadzadeh, V., and Akbari, B. (2016) Evolution of phage display technology: from discovery to application. *Journal of drug targeting*, 1-9
 217. Hamzeh-Mivehroud, M., Alizadeh, A. A., Morris, M. B., Church, W. B., and Dastmalchi, S. (2013) Phage display as a technology delivering on the promise of peptide drug discovery. *Drug discovery today* **18**, 1144-1157
 218. Pande, J., Szewczyk, M. M., and Grover, A. K. (2010) Phage display: concept, innovations, applications and future. *Biotechnology advances* **28**, 849-858
 219. Zou, Q., and Yang, K. L. (2016) Identification of peptide inhibitors of penicillinase using a phage display library. *Analytical biochemistry* **494**, 4-9
 220. Burritt, J. B., Quinn, M. T., Jutila, M. A., Bond, C. W., and Jesaitis, A. J. (1995) Topological mapping of neutrophil cytochrome b epitopes with phage-display libraries. *The Journal of biological chemistry* **270**, 16974-16980
 221. Smith, G. P., and Petrenko, V. A. (1997) Phage Display. *Chemical reviews* **97**, 391-410
 222. Wu, J., Wu, M. C., Zhang, L. F., Lei, J. Y., Feng, L., and Jin, J. (2009) Identification of binding peptides of the ADAM15 disintegrin domain using phage display. *Journal of biosciences* **34**, 213-220
 223. Gnanasekar, M., Suleman, F. G., Ramaswamy, K., and Caldwell, J. D. (2009) Identification of sex hormone binding globulin-interacting proteins in the brain using phage display screening. *International journal of molecular medicine* **24**, 421-426
 224. Shiuan, D., Chen, Y. H., Lin, H. K., Huang, K. J., Tai, D. F., and Chang, D. K. (2016) Discovering Peptide Inhibitors of Human Squalene Synthase Through Screening the Phage-Displayed Cyclic Peptide c7c Library. *Applied biochemistry and biotechnology* **179**, 597-609
 225. Smrcka, A. V., and Scott, J. K. (2002) Discovery of ligands for beta gamma subunits from phage-displayed peptide libraries. *Methods in enzymology* **344**, 557-576

226. Gallagher, S. R., and Desjardins, P. (2008) Quantitation of Nucleic Acids and Proteins. in *Current Protocols Essential Laboratory Techniques*, John Wiley & Sons, Inc. pp
227. Studier, F. W., and Moffatt, B. A. (1986) Use of bacteriophage T7 RNA polymerase to direct selective high-level expression of cloned genes. *Journal of molecular biology* **189**, 113-130
228. Bradford, M. M. (1976) A rapid and sensitive method for the quantitation of microgram quantities of protein utilizing the principle of protein-dye binding. *Analytical biochemistry* **72**, 248-254
229. Altschul, S. F., Madden, T. L., Schaffer, A. A., Zhang, J., Zhang, Z., Miller, W., and Lipman, D. J. (1997) Gapped BLAST and PSI-BLAST: a new generation of protein database search programs. *Nucleic acids research* **25**, 3389-3402
230. Grynkiewicz, G., Poenie, M., and Tsien, R. Y. (1985) A new generation of Ca²⁺ indicators with greatly improved fluorescence properties. *The Journal of biological chemistry* **260**, 3440-3450
231. Wu, J. H., Hagaman, J., Kim, S., Reddick, R. L., and Maeda, N. (2002) Aortic constriction exacerbates atherosclerosis and induces cardiac dysfunction in mice lacking apolipoprotein E. *Arteriosclerosis, thrombosis, and vascular biology* **22**, 469-475
232. Devlin, J. J., Panganiban, L. C., and Devlin, P. E. (1990) Random peptide libraries: a source of specific protein binding molecules. *Science* **249**, 404-406
233. Pero, S. C., Oligino, L., Daly, R. J., Soden, A. L., Liu, C., Roller, P. P., Li, P., and Krag, D. N. (2002) Identification of novel non-phosphorylated ligands, which bind selectively to the SH2 domain of Grb7. *The Journal of biological chemistry* **277**, 11918-11926
234. Mohrluder, J., Hoffmann, Y., Stangler, T., Hanel, K., and Willbold, D. (2007) Identification of clathrin heavy chain as a direct interaction partner for the gamma-aminobutyric acid type A receptor associated protein. *Biochemistry* **46**, 14537-14543
235. Stirnimann, C. U., Petsalaki, E., Russell, R. B., and Muller, C. W. (2010) WD40 proteins propel cellular networks. *Trends in biochemical sciences* **35**, 565-574
236. Lodowski, D. T., Pitcher, J. A., Capel, W. D., Lefkowitz, R. J., and Tesmer, J. J. (2003) Keeping G proteins at bay: a complex between G protein-coupled receptor kinase 2 and Gbetagamma. *Science* **300**, 1256-1262
237. Jitsukawa, T., Nakajima, S., Sugawara, I., and Watanabe, H. (1989) Increased coating efficiency of antigens and preservation of original antigenic structure after coating in ELISA. *Journal of immunological methods* **116**, 251-257
238. Inglese, J., Luttrell, L. M., Iniguez-Lluhi, J. A., Touhara, K., Koch, W. J., and Lefkowitz, R. J. (1994) Functionally active targeting domain of the beta-adrenergic receptor kinase: an inhibitor of G beta gamma-mediated stimulation of type II

- adenylyl cyclase. *Proceedings of the National Academy of Sciences of the United States of America* **91**, 3637-3641
239. Touhara, K., Inglese, J., Pitcher, J. A., Shaw, G., and Lefkowitz, R. J. (1994) Binding of G protein beta gamma-subunits to pleckstrin homology domains. *The Journal of biological chemistry* **269**, 10217-10220
240. Mumby, S. M., Casey, P. J., Gilman, A. G., Gutowski, S., and Sternweis, P. C. (1990) G protein gamma subunits contain a 20-carbon isoprenoid. *Proceedings of the National Academy of Sciences of the United States of America* **87**, 5873-5877
241. Xu, X., Yang, D., Ding, J. H., Wang, W., Chu, P. H., Dalton, N. D., Wang, H. Y., Bermingham, J. R., Jr., Ye, Z., Liu, F., Rosenfeld, M. G., Manley, J. L., Ross, J., Jr., Chen, J., Xiao, R. P., Cheng, H., and Fu, X. D. (2005) ASF/SF2-regulated CaMKII δ alternative splicing temporally reprograms excitation-contraction coupling in cardiac muscle. *Cell* **120**, 59-72
242. Braun, A. P., and Schulman, H. (1995) The multifunctional calcium/calmodulin-dependent protein kinase: from form to function. *Annual review of physiology* **57**, 417-445
243. Maier, L. S., Zhang, T., Chen, L., DeSantiago, J., Brown, J. H., and Bers, D. M. (2003) Transgenic CaMKII δ C overexpression uniquely alters cardiac myocyte Ca²⁺ handling: reduced SR Ca²⁺ load and activated SR Ca²⁺ release. *Circulation research* **92**, 904-911
244. Leeb-Lundberg, L. M. F., Marceau, F., Müller-Esterl, W., Pettibone, D. J., and Zuraw, B. L. (2005) International Union of Pharmacology. XLV. Classification of the Kinin Receptor Family: from Molecular Mechanisms to Pathophysiological Consequences. *Pharmacological Reviews* **57**, 27-77
245. Palmer, R. M., Ferrige, A. G., and Moncada, S. (1987) Nitric oxide release accounts for the biological activity of endothelium-derived relaxing factor. *Nature* **327**, 524-526
246. Blaukat, A., Pizard, A., Breit, A., Wernstedt, C., Alhenc-Gelas, F., Muller-Esterl, W., and Dikic, I. (2001) Determination of bradykinin B2 receptor in vivo phosphorylation sites and their role in receptor function. *The Journal of biological chemistry* **276**, 40431-40440
247. Simpson, A. W. (2013) Fluorescent measurement of [Ca(2)(+)]_c: basic practical considerations. *Methods in molecular biology* **937**, 3-36
248. Fu, X. (2013) *MOLECULAR MECHANISMS UNDERLYING GRK2 INHIBITION BY RKIP in vitro AND in vivo*, Diss., Eidgenössische Technische Hochschule ETH Zürich, Nr. 21513, 2013
249. Gulick, J., Subramaniam, A., Neumann, J., and Robbins, J. (1991) Isolation and characterization of the mouse cardiac myosin heavy chain genes. *The Journal of biological chemistry* **266**, 9180-9185

250. Choi, D. J., Koch, W. J., Hunter, J. J., and Rockman, H. A. (1997) Mechanism of beta-adrenergic receptor desensitization in cardiac hypertrophy is increased beta-adrenergic receptor kinase. *The Journal of biological chemistry* **272**, 17223-17229
251. Evron, T., Daigle, T. L., and Caron, M. G. (2012) GRK2: multiple roles beyond G protein-coupled receptor desensitization. *Trends in pharmacological sciences* **33**, 154-164
252. Ivanov, A. A., Khuri, F. R., and Fu, H. (2013) Targeting protein-protein interactions as an anticancer strategy. *Trends in pharmacological sciences* **34**, 393-400
253. Nevola, L., and Giralt, E. (2015) Modulating protein-protein interactions: the potential of peptides. *Chemical communications (Cambridge, England)* **51**, 3302-3315
254. Arkin, M. R., and Wells, J. A. (2004) Small-molecule inhibitors of protein-protein interactions: progressing towards the dream. *Nat Rev Drug Discov* **3**, 301-317
255. Bowden, G. A., and Georgiou, G. (1990) Folding and aggregation of beta-lactamase in the periplasmic space of Escherichia coli. *The Journal of biological chemistry* **265**, 16760-16766
256. Woestenenk, E. A., Hammarstrom, M., van den Berg, S., Hard, T., and Berglund, H. (2004) His tag effect on solubility of human proteins produced in Escherichia coli: a comparison between four expression vectors. *Journal of structural and functional genomics* **5**, 217-229
257. Li, D. F., Feng, L., Hou, Y. J., and Liu, W. (2013) The expression, purification and crystallization of a ubiquitin-conjugating enzyme E2 from *Agrocybe aegerita* underscore the impact of His-tag location on recombinant protein properties. *Acta crystallographica. Section F, Structural biology and crystallization communications* **69**, 153-157
258. Kools, P., Van Imschoot, G., and van Roy, F. (2000) Characterization of three novel human cadherin genes (CDH7, CDH19, and CDH20) clustered on chromosome 18q22-q23 and with high homology to chicken cadherin-7. *Genomics* **68**, 283-295
259. Mende, U., Kagen, A., Cohen, A., Aramburu, J., Schoen, F. J., and Neer, E. J. (1998) Transient cardiac expression of constitutively active Galphaq leads to hypertrophy and dilated cardiomyopathy by calcineurin-dependent and independent pathways. *Proceedings of the National Academy of Sciences of the United States of America* **95**, 13893-13898
260. D'Angelo, D. D., Sakata, Y., Lorenz, J. N., Boivin, G. P., Walsh, R. A., Liggett, S. B., and Dorn, G. W., 2nd. (1997) Transgenic Galphaq overexpression induces cardiac contractile failure in mice. *Proceedings of the National Academy of Sciences of the United States of America* **94**, 8121-8126

261. Gold, J. I., Martini, J. S., Hullmann, J., Gao, E., Chuprun, J. K., Lee, L., Tilley, D. G., Rabinowitz, J. E., Bossuyt, J., Bers, D. M., and Koch, W. J. (2013) Nuclear translocation of cardiac G protein-Coupled Receptor kinase 5 downstream of select Gq-activating hypertrophic ligands is a calmodulin-dependent process. *PloS one* **8**, e57324
262. Martini, J. S., Raake, P., Vinge, L. E., DeGeorge, B. R., Jr., Chuprun, J. K., Harris, D. M., Gao, E., Eckhart, A. D., Pitcher, J. A., and Koch, W. J. (2008) Uncovering G protein-coupled receptor kinase-5 as a histone deacetylase kinase in the nucleus of cardiomyocytes. *Proceedings of the National Academy of Sciences of the United States of America* **105**, 12457-12462
263. Hullmann, J. E., Grisanti, L. A., Makarewich, C. A., Gao, E., Gold, J. I., Chuprun, J. K., Tilley, D. G., Houser, S. R., and Koch, W. J. (2014) GRK5-mediated exacerbation of pathological cardiac hypertrophy involves facilitation of nuclear NFAT activity. *Circulation research* **115**, 976-985
264. Fong, H. K., Hurley, J. B., Hopkins, R. S., Miake-Lye, R., Johnson, M. S., Doolittle, R. F., and Simon, M. I. (1986) Repetitive segmental structure of the transducin beta subunit: homology with the CDC4 gene and identification of related mRNAs. *Proceedings of the National Academy of Sciences of the United States of America* **83**, 2162-2166
265. Sondek, J., Bohm, A., Lambright, D. G., Hamm, H. E., and Sigler, P. B. (1996) Crystal structure of a G-protein beta gamma dimer at 2.1A resolution. *Nature* **379**, 369-374
266. Smith, T. F. (2008) Diversity of WD-repeat proteins. *Sub-cellular biochemistry* **48**, 20-30
267. Wang, D. S., Shaw, R., Winkelmann, J. C., and Shaw, G. (1994) Binding of PH domains of beta-adrenergic receptor kinase and beta-spectrin to WD40/beta-transducin repeat containing regions of the beta-subunit of trimeric G-proteins. *Biochemical and biophysical research communications* **203**, 29-35
268. Chen, S., Spiegelberg, B. D., Lin, F., Dell, E. J., and Hamm, H. E. (2004) Interaction of Gbetagamma with RACK1 and other WD40 repeat proteins. *Journal of molecular and cellular cardiology* **37**, 399-406
269. Sun, Z., Tang, X., Lin, F., and Chen, S. (2011) The WD40 repeat protein WDR26 binds Gbetagamma and promotes Gbetagamma-dependent signal transduction and leukocyte migration. *The Journal of biological chemistry* **286**, 43902-43912
270. Cartier, A., Parent, A., Labrecque, P., Laroche, G., and Parent, J. L. (2011) WDR36 acts as a scaffold protein tethering a G-protein-coupled receptor, Galphaq and phospholipase Cbeta in a signalling complex. *Journal of cell science* **124**, 3292-3304

271. Higa, L. A., Wu, M., Ye, T., Kobayashi, R., Sun, H., and Zhang, H. (2006) CUL4-DDB1 ubiquitin ligase interacts with multiple WD40-repeat proteins and regulates histone methylation. *Nature cell biology* **8**, 1277-1283
272. Gallina, I., Colding, C., Henriksen, P., Beli, P., Nakamura, K., Offman, J., Mathiasen, D. P., Silva, S., Hoffmann, E., Groth, A., Choudhary, C., and Lisby, M. (2015) Cmr1/WDR76 defines a nuclear genotoxic stress body linking genome integrity and protein quality control. *Nat Commun* **6**, 6533
273. Arkin, M. R., Glicksman, M. A., Fu, H., Havel, J. J., and Du, Y. (2004) Inhibition of Protein-Protein Interactions: Non-Cellular Assay Formats. in *Assay Guidance Manual* (Sittampalam, G. S., Coussens, N. P., Nelson, H., Arkin, M., Auld, D., Austin, C., Bejcek, B., Glicksman, M., Inglese, J., Iversen, P. W., Li, Z., McGee, J., McManus, O., Minor, L., Napper, A., Peltier, J. M., Riss, T., Trask, O. J., Jr., and Weidner, J. eds.), Bethesda (MD). pp
274. Zha, Z., Han, X. R., Smith, M. D., Lei, Q. Y., Guan, K. L., and Xiong, Y. (2016) Hypertension-associated C825T polymorphism impairs the function of Gbeta3 to target GRK2 ubiquitination. *Cell discovery* **2**, 16005
275. Siffert, W., Roszkopf, D., Siffert, G., Busch, S., Moritz, A., Erbel, R., Sharma, A. M., Ritz, E., Wichmann, H. E., Jakobs, K. H., and Horsthemke, B. (1998) Association of a human G-protein beta3 subunit variant with hypertension. *Nature genetics* **18**, 45-48
276. Klenke, S., Kussmann, M., and Siffert, W. (2011) The GNB3 C825T polymorphism as a pharmacogenetic marker in the treatment of hypertension, obesity, and depression. *Pharmacogenetics and genomics* **21**, 594-606
277. Murzin, A. G. (1992) Structural principles for the propeller assembly of beta-sheets: the preference for seven-fold symmetry. *Proteins* **14**, 191-201
278. Murga, C., Ruiz-Gomez, A., Garcia-Higuera, I., Kim, C. M., Benovic, J. L., and Mayor, F., Jr. (1996) High affinity binding of beta-adrenergic receptor kinase to microsomal membranes. Modulation of the activity of bound kinase by heterotrimeric G protein activation. *The Journal of biological chemistry* **271**, 985-994
279. Johnson, L. N. (2009) Protein kinase inhibitors: contributions from structure to clinical compounds. *Quarterly reviews of biophysics* **42**, 1-40
280. Liao, J. K., and Homcy, C. J. (1993) The G proteins of the G alpha i and G alpha q family couple the bradykinin receptor to the release of endothelium-derived relaxing factor. *The Journal of clinical investigation* **92**, 2168-2172
281. Kramarenko, II, Bunni, M. A., Morinelli, T. A., Raymond, J. R., and Garnovskaya, M. N. (2009) Identification of functional bradykinin B(2) receptors endogenously expressed in HEK293 cells. *Biochem Pharmacol* **77**, 269-276

282. Blaukat, A., Alla, S. A., Lohse, M. J., and Muller-Esterl, W. (1996) Ligand-induced phosphorylation/dephosphorylation of the endogenous bradykinin B2 receptor from human fibroblasts. *The Journal of biological chemistry* **271**, 32366-32374
283. Koller, S. D. (2012) *Kinase-dependent and kinase-independent functions of G-protein-coupled receptor kinase 2 (GRK2)*, Diss., Eidgenössische Technische Hochschule ETH Zürich, Nr. 20333, 2012
284. Lohse, M. J., Lefkowitz, R. J., Caron, M. G., and Benovic, J. L. (1989) Inhibition of beta-adrenergic receptor kinase prevents rapid homologous desensitization of beta 2-adrenergic receptors. *Proceedings of the National Academy of Sciences of the United States of America* **86**, 3011-3015
285. Peppel, K., Boekhoff, I., McDonald, P., Breer, H., Caron, M. G., and Lefkowitz, R. J. (1997) G Protein-coupled Receptor Kinase 3 (GRK3) Gene Disruption Leads to Loss of Odorant Receptor Desensitization. *Journal of Biological Chemistry* **272**, 25425-25428
286. Traynham, C. J., Hullmann, J., and Koch, W. J. (2016) "Canonical and non-canonical actions of GRK5 in the heart". *Journal of molecular and cellular cardiology* **92**, 196-202
287. Sterne-Marr, R., Leahey, P. A., Bresee, J. E., Dickson, H. M., Ho, W., Ragusa, M. J., Donnelly, R. M., Amie, S. M., Krywy, J. A., Brookins-Danz, E. D., Orakwue, S. C., Carr, M. J., Yoshino-Koh, K., Li, Q., and Tesmer, J. J. (2009) GRK2 activation by receptors: role of the kinase large lobe and carboxyl-terminal tail. *Biochemistry* **48**, 4285-4293
288. Wurst, K. E., Poole, C., Ephross, S. A., and Olshan, A. F. (2010) First trimester paroxetine use and the prevalence of congenital, specifically cardiac, defects: a meta-analysis of epidemiological studies. *Birth defects research. Part A, Clinical and molecular teratology* **88**, 159-170
289. Engelhardt, S., Hein, L., Wiesmann, F., and Lohse, M. J. (1999) Progressive hypertrophy and heart failure in beta1-adrenergic receptor transgenic mice. *Proceedings of the National Academy of Sciences of the United States of America* **96**, 7059-7064
290. Liggett, S. B., Tepe, N. M., Lorenz, J. N., Canning, A. M., Jantz, T. D., Mitarai, S., Yatani, A., and Dorn, G. W., 2nd. (2000) Early and delayed consequences of beta(2)-adrenergic receptor overexpression in mouse hearts: critical role for expression level. *Circulation* **101**, 1707-1714
291. Mann, D. L., Kent, R. L., Parsons, B., and Cooper, G. t. (1992) Adrenergic effects on the biology of the adult mammalian cardiocyte. *Circulation* **85**, 790-804
292. Purgato, M., Papola, D., Gastaldon, C., Trespidi, C., Magni, L. R., Rizzo, C., Furukawa, T. A., Watanabe, N., Cipriani, A., and Barbui, C. (2014) Paroxetine versus other anti-depressive agents for depression. *The Cochrane database of systematic reviews*, Cd006531

13 Appendix

13.1 Sequencing of GRK2NTD6xCHis

Sequencing of pET3dGRK2NTD6xCHis (amino acids 1-190 of GRK2), clone 6

```
NATTTTGTACTTTAAGAAGGAGATATA CCATGG CCGCGGACCTGGAGGCGGTGCTGGCCGACGTGAGCTACCTGATGGC
GATGGAGAAGAGCAAGGCCACGCCGGCGCGCGCCAGCAAGAAGATACTGCTGCCCGAGCCCAGCATCCGCAGTGTGCAT
GCAGAAGTACCTGGAGGACCGGGGCGAGGTGACCTTTGAGAAGATCTTTTCCCAGAAGCTGGGGTACCTGCTCTTCCGAGA
CTTCTGCCTGAACCACCTGGAGGAGGCCAGGCCCTTGGTGGAAATTCATGAGGAGATCAAGAAGTACGAGAAGCTGGAGAC
GGAGGAGGAGCGTGTGGCCCGCAGCCGGGAGATCTTCGACTCATAACATCATGAAGGAGCTGCTGGCCTGCTCGCATCCCTT
CTCGAAGAGTGCCACTGAGCATGTCCAAGGCCACCTGGGGAAGAAGCAGGTGCCTCCGGATCTCTTCCAGCCATACATCGA
AGAGATTTGTCAAAACCTCCGAGGGGACGTGTTCCAGAAATTCATTGAGAGCGATAAGTTCACACGGTTTTGCCAGTGGAA
GAATGTGGAGCTCAACATCCACCTGACCATGAATGAC CACCATCACCATCACCAT TAAGGATCCGGCTGCTAACAAAGCCC
GAAAGGAAGCTGAGTTGGCTGCTGCCACCGCTGACCAATAACTAGCATAAACCCTTGGGGCCTTAAACCGGGTCTTGAGGG
GTTTTTTGCTGAAAGGAGGAACTATATCCGGATATCCACAGGACGGGTGTTGGTCCCATGATCGCGTAGTCGATAGTGGCT
CCAAGTAGCGAAGCGAGCAGGACTGGGGCGGGCCAAAGCGGTCCGACAGTGCTCCGAGAACGGGTGCGCATAGAAATTC
ATCAACGCATATAGCGCTAGCAGCACGCCATAGTGACTGGCGATGCTGTCCGAATGGACGATATCCCAGCAAGAGGCCCGC
AGTACCGGCATAACCAAGCCTATGCCTACAGCATCCAGGG
```

CCATGG: NcoI restriction site

ATG: Start codon

XXX: hexahistidine tag

TAA: Stop codon

GGATCC: BamHI restriction site

```
Query 4 GCGGACCTGGAGGCGGTGCTGGCCGACGTGAGCTACCTGATGGCGATGGAGAAGAGCAAG 63
|
Sbjct 270 GCGGACCTGGAGGCGGTGCTGGCCGACGTGAGCTACCTGATGGCCATGGAGAAGAGCAAG 329

Query 64 GCCACGCCGGCCGCGCGCGCCAGCAAGAAGATACTGCTGCCCGAGCCCAGCATCCGCAGT 123
|
Sbjct 330 GCCACGCCGGCCGCGCGCGCCAGCAAGAAGATCCTGCTGCCCGAGCCCAGCATCCGCAGT 389

Query 124 GTCATGCAGAAGTACCTGGAGGACCGGGGCGAGGTGACCTTTGAGAAGATCTTTTCCAG 183
|
Sbjct 390 GTCATGCAGAAGTACCTGGAGGACCGGGGCGAGGTGACCTTTGAGAAGATCTTTTCCAG 449

Query 184 AAGCTGGGGTACCTGCTCTTCCGAGACTTCTGCCTGAACCACCTGGAGGAGGCCAGGCC 243
|
Sbjct 450 AAGCTGGGGTACCTGCTCTTCCGAGACTTCTGCCTGAACCACCTGGAGGAGGCCAGGCC 509

Query 244 TTGGTGGAAATTCATGAGGAGATCAAGAAGTACGAGAAGCTGGAGACGGAGGAGGAGCGT 303
|
Sbjct 510 TTGGTGGAAATTCATGAGGAGATCAAGAAGTACGAGAAGCTGGAGACGGAGGAGGAGCGT 569

Query 304 GTGGCCCGCAGCCGGGAGATCTTCGACTCATAACATCATGAAGGAGCTGCTGGCCTGCTCG 363
|
Sbjct 570 GTGGCCCGCAGCCGGGAGATCTTCGACTCATAACATCATGAAGGAGCTGCTGGCCTGCTCG 629

Query 364 CATCCCTTCTCGAAGAGTGCCACTGAGCATGTCCAAGGCCACCTGGGGAAGAAGCAGGTG 423
|
Sbjct 630 CATCCCTTCTCGAAGAGTGCCACTGAGCATGTCCAAGGCCACCTGGGGAAGAAGCAGGTG 689

Query 424 CCTCCGGATCTCTTCCAGCCATACATCGAAGAGATTTGTCAAAACCTCCGAGGGGACGTG 483
|
Sbjct 690 CCTCCGGATCTCTTCCAGCCATACATCGAAGAGATTTGTCAAAACCTCCGAGGGGACGTG 749

Query 484 TTCCAGAAATTCATTGAGAGCGATAAGTTCACACGGTTTTGCCAGTGGAAAGATGTGGAG 543
|
Sbjct 750 TTCCAGAAATTCATTGAGAGCGATAAGTTCACACGGTTTTGCCAGTGGAAAGATGTGGAG 809

Query 544 CTCAACATCCACCTGACCATGAATGAC 570
|
Sbjct 810 CTCAACATCCACCTGACCATGAATGAC 836
```



```

Query 727 CCGTGGAGCTGCCCGACTCCTTCTCCCTGAACTACGCTCCCTGCTGGAGGGGTGCTGC 786
          |||
Sbjct 1495 CCGTGGAGCTGCCCGACTCCTTCTCCCTGAACTACGCTCCCTGCTGGAGGGGTGCTGC 1554

Query 787 AGAGGGATGTCAACCGGAGATTGGGCTGCCTGGGCCGAGGGGCTCAGGAGGTGAAAGAGA 846
          |||
Sbjct 1555 AGAGGGATGTCAACCGGAGATTGGGCTGCCTGGGCCGAGGGGCTCAGGAGGTGAAAGAGA 1614

Query 847 GCCCCTTTTTC 857
          |||
Sbjct 1615 GCCCCTTTTTC 1625

```

13.3 Sequencing of GRK2KD6xCHis

Sequencing of pET3dGRK2KD6xCHis (amino acids 191-453 of GRK2), clone 1

```

TATTTTGTTTTACTTTAAGAAGGAGATATA CCATGG CCTTCAGCGTGCATCGCATCATTGGGCGCGGGGGCTTTGGCGAGG
TCTATGGGTGCCGGAAGGCTGACACAGGCAAGATGTACGCCATGAAGTGCCTGGACAAAAAGCGCATCAAGATGAAGCAGG
GGGAGACCCTGGCCCTGAACGAGCGCATCATGCTCTCGCTCGTCAGCACTGGGGACTGCCATTTCATTGTCTGCATGTCAT
ACGCGTTCCACACGCCAGACAAGCTCAGCTTCATCCTGGACCTCATGAACGGTGGGGACCTGCACTACCACCTCTCCCAGC
ACGGGGTCTTCTCAGAGGCTGACATGCGCTTCTATGCGGCCGAGATCATCCTGGGCCTGGAGCACATGCACAACCGCTTCG
TGGTCTACCGGGACCTGAAGCCAGCCAACATCCTTCTGGACGAGCATGGCCACGTGCGGATCTCGGACCTGGGCCTGGCCT
GTGACTTCTCCAAGAAGAAGCCCCATGCCAGCGTGGGCACCCACGGGTACATGGCTCCGGAGGTCTGCAGAAGGGCGTGG
CCTACGACAGCAGTGCCGACTGGTTCTCTCTGGGGTGCATGCTCTTCAAGTTGCTGCGGGGGCACAGCCCCTTCCGGCAGC
ACAAGACCAAAGACAAGCATGAGATCGACCCGCATGACGCTGACGATGGCCGTGGAGCTGCCGACTCCTTCTCCCCTGAAC
TACGCTCCCTGCTGGAGGGGTGCTGCAGAGGGATGTCAACCGGAGATTGGGCTGCCTGGGCCGAGGGGCTCAGGAGGTGA
AAGAGAGCCCCTTTTTT CACCATCACCATCACCAT TAA GGATCC GGCTGCTAACAAAGCCCGAAAGGAAAGCTGAGTTGGCT
GCTGCCACCGCTGAGCAATAACTAGCATAAACCCTTGGGGCCTCTAAACGGGTCTTGAGGGGTTTTTTGCTGAAAGGAGGA
ACTATATCCGGATATCCACAGGACGGGTGTGGTCGCCATG

```

CCATGG: NcoI restriction site

ATG: Start codon

XXX: hexahistidine tag

TAA: Stop codon

GGATCC: BamHI restriction site

```

Query 46 CTTCAGCGTGCATCGCATCATTGGGCGCGGGGGCTTTGGCGAGGTCTATGGGTGCCGGAA 105
          |||
Sbjct 836 CTTCAGCGTGCATCGCATCATTGGGCGCGGGGGCTTTGGCGAGGTCTATGGGTGCCGGAA 895

Query 106 GGCTGACACAGGCAAGATGTACGCCATGAAGTGCCTGGACAAAAAGCGCATCAAGATGAA 165
          |||
Sbjct 896 GGCTGACACAGGCAAGATGTACGCCATGAAGTGCCTGGACAAAAAGCGCATCAAGATGAA 955

Query 166 GCAGGGGAGACCCTGGCCCTGAACGAGCGCATCATGCTCTCGCTCGTCAGCACTGGGGA 225
          |||
Sbjct 956 GCAGGGGAGACCCTGGCCCTGAACGAGCGCATCATGCTCTCGCTCGTCAGCACTGGGGA 1015

Query 226 CTGCCATTTCATTGTCTGCATGTCATACGCGTTCCACACGCCAGACAAGCTCAGCTTCAT 285
          |||
Sbjct 1016 CTGCCATTTCATTGTCTGCATGTCATACGCGTTCCACACGCCAGACAAGCTCAGCTTCAT 1075

Query 286 CCTGGACCTCATGAACGGTGGGGACCTGCACTACCACCTCTCCCAGCACGGGGTCTTCTC 345
          |||
Sbjct 1076 CCTGGACCTCATGAACGGTGGGGACCTGCACTACCACCTCTCCCAGCACGGGGTCTTCTC 1135

Query 346 AGAGGCTGACATGCGCTTCTATGCGCCGAGATCATCCTGGGCCTGGAGCACATGCACAA 405
          |||
Sbjct 1136 AGAGGCTGACATGCGCTTCTATGCGCCGAGATCATCCTGGGCCTGGAGCACATGCACAA 1195

```

```

Query 406 CCGCTTCGTGGTCTACCGGGACCTGAAGCCAGCCAACATCCTTCTGGACGAGCATGGCCA 465
          |||
Sbjct 1196 CCGCTTCGTGGTCTACCGGGACCTGAAGCCAGCCAACATCCTTCTGGACGAGCATGGCCA 1255

Query 466 CGTGGCGATCTCGGACCTGGGCCTGGCCTGTGACTTCTCCAAGAAGAAGCCCCATGCCAG 525
          |||
Sbjct 1256 CGTGGCGATCTCGGACCTGGGCCTGGCCTGTGACTTCTCCAAGAAGAAGCCCCATGCCAG 1315

Query 526 CGTGGGCACCCACGGGTACATGGCTCCGGAGGTCCTGCAGAAGGGCGTGGCCTACGACAG 585
          |||
Sbjct 1316 CGTGGGCACCCACGGGTACATGGCTCCGGAGGTCCTGCAGAAGGGCGTGGCCTACGACAG 1375

Query 586 CAGTGCCGACTGGTTCTCTCTGGGGTGCATGCTCTTCAAGTTGCTGCGGGGGCAGAGCCC 645
          |||
Sbjct 1376 CAGTGCCGACTGGTTCTCTCTGGGGTGCATGCTCTTCAAGTTGCTGCGGGGGCAGAGCCC 1435

Query 646 CTTCCGGCAGCACAAAGACCAAGACAAGCATGAGATCGACCGCATGACGCTGACGATGGC 705
          |||
Sbjct 1436 CTTCCGGCAGCACAAAGACCAAGACAAGCATGAGATCGACCGCATGACGCTGACGATGGC 1495

Query 706 CGTGGAGCTGCCCGACTCCTTCTCCCCTGAACTACGCTCCCTGCTGGAGGGGTTGCTGCA 765
          |||
Sbjct 1496 CGTGGAGCTGCCCGACTCCTTCTCCCCTGAACTACGCTCCCTGCTGGAGGGGTTGCTGCA 1555

Query 766 GAGGGATGTCAACCGGAGATTGGGCTGCCTGGGCCGAGGGGCTCAGGAGGTGAAAGAGAG 825
          |||
Sbjct 1556 GAGGGATGTCAACCGGAGATTGGGCTGCCTGGGCCGAGGGGCTCAGGAGGTGAAAGAGAG 1615

Query 826 CCCCTTTTTCC 836
          |||
Sbjct 1616 CCCCTTTTTCC 1626

```

13.4 Sequencing of 6xNHISGRK2CTD

Sequencing of pET3d6xNHISGRK2CTD (amino acids 454-689 of GRK2), clone 4

```

TGNTATTTTTGTTTACTTTAAGAAGGAGATATAC CATGACC CATCACCATCACCATCACCGCTCCCTGGACTGGCAGATGG
TCTTCTTGCAGAAGTACCCTCCCCGCTGATCCCCCAGAGGGGAGGTGAACGCGGCCGACGCCTTCGACATTGGCTCCT
TCGATGAGGAGGACACAAAAGGAATCAAGTTACTGGACAGTGATCAGGAGCTCTACCGCAACTCCCCCTCACCATCTCGG
AGCGGTGGCAGCAGGAGGTGGCAGAGACTGTCTTCGACACCATCAACGCTGAGACAGACCGGCTGGAGGCTCGCAAGAAAG
CCAAGAACAAGCAGCTGGGCCATGAGGAAGACTACGCCCTGGGCAAGGACTGCATCATGCATGGCTACATGTCCAAGATGG
GCAACCCCTTCTTGACCCAGTGGCAGCGGGGCTACTTCTACCTGTTCCTCAACCGCCTCGAGTGGCGGGGCGAGGGCGAGG
CCCCGAGAGCCTGCTGACCATGGAGGAGATCCAGTCCGGTGGAGGAGACGCAGATCAAGGAGCGCAAGTGCCTGCTCCTCA
AGATCCGCGGTGGGAAACAGTTCAATTTTGCAGTGCATAGCGACCCTGAGCTGGTGCAGTGGAAAGAAGGAGCTGCGCGACG
CCTACCGCGAGGCCAGCAGCTGGTGCAGCGGGTGCCCAAGATGAAGAACAAAGCCGCGCTCGCCCGTGGTGGAGCTGAGCA
AGGTGCCGCTGGTCCAGCGGGCAGTGCCAACGGCCTCTGA GGATCCGGCTGCTAACAAAGCCCCGAAAGGAAGCTGAGTTG
GCTGCTGCCACCGCTGAGCAATAACTAGCATAAACCCTTGGGGCCTCTAAACCGGGTCTTGAGGGGTTTTTTGCTGAAAGGA
GGAATATATCCGGATATCCACAGGACGGGTGTGGTGCCTATGATCGCGTAGTCGATAGTGGCTCCAAGTAGCGAAGCGAG
CAGGACTGGGCGGGCGCCAAAGCGGTTCGGACAGTGCTCCG

```

ATG: Start codon

CATGA: BspHI restriction site, not reconstituted

XXX: hexahistidine tag

TGA: Stop codon

GGATCC: BamHI restriction site

```

Query 59 CCGCTCCCTGGACTGGCAGATGGTCTTCTTGCAGAAGTACCCTCCCCCGCTGATCCCCC 118
          |||
Sbjct 1625 CCGCTCCCTGGACTGGCAGATGGTCTTCTTGCAGAAGTACCCTCCCCCGCTGATCCCCC 1684

Query 119 ACGAGGGGAGGTGAACGCGGCCGACGCCTTCGACATTGGCTCCTTCGATGAGGAGGACAC 178
          |||
Sbjct 1685 ACGAGGGGAGGTGAACGCGGCCGACGCCTTCGACATTGGCTCCTTCGATGAGGAGGACAC 1744

Query 179 AAAAGGAATCAAGTTACTGGACAGTGATCAGGAGCTCTACCGCAACTTCCCCCTCACCAT 238
          |||
Sbjct 1745 AAAAGGAATCAAGTTACTGGACAGTGATCAGGAGCTCTACCGCAACTTCCCCCTCACCAT 1804

```

```

Query 239   CTCGGAGCGGTGGCAGCAGGAGGTGGCAGAGACTGTCTTCGACACCATCAACGCTGAGAC 298
          |||
Sbjct 1805   CTCGGAGCGGTGGCAGCAGGAGGTGGCAGAGACTGTCTTCGACACCATCAACGCTGAGAC 1864

Query 299   AGACCGGCTGGAGGCTCGCAAGAAAGCCAAGAACAAGCAGCTGGGCCATGAGGAAGACTA 358
          |||
Sbjct 1865   AGACCGGCTGGAGGCTCGCAAGAAAGCCAAGAACAAGCAGCTGGGCCATGAGGAAGACTA 1924

Query 359   CGCCCTGGGCAAGGACTGCATCATGCATGGCTACATGTCCAAGATGGGCAACCCCTTCCT 418
          |||
Sbjct 1925   CGCCCTGGGCAAGGACTGCATCATGCATGGCTACATGTCCAAGATGGGCAACCCCTTCCT 1984

Query 419   GACCCAGTGGCAGCGGCGGTACTTCTACCTGTTCCCAACCGCCTCGAGTGGCGGGGCGA 478
          |||
Sbjct 1985   GACCCAGTGGCAGCGGCGGTACTTCTACCTGTTCCCAACCGCCTCGAGTGGCGGGGCGA 2044

Query 479   GGGCGAGCCCCGCAGAGCCTGCTGACCATGGAGGAGATCCAGTCGGTGGAGGAGACGCA 538
          |||
Sbjct 2045   GGGCGAGCCCCGCAGAGCCTGCTGACCATGGAGGAGATCCAGTCGGTGGAGGAGACGCA 2104

Query 539   GATCAAGGAGCGCAAGTGCCTGCTCCTCAAGATCCGCGGTGGGAAACAGTTCATTTTGA 598
          |||
Sbjct 2105   GATCAAGGAGCGCAAGTGCCTGCTCCTCAAGATCCGCGGTGGGAAACAGTTCATTTTGA 2164

Query 599   GTGCGATAGCGACCCTGAGCTGGTGCAGTGAAGAAGGAGCTGCGCGACGCCCTACCGCGA 658
          |||
Sbjct 2165   GTGCGATAGCGACCCTGAGCTGGTGCAGTGAAGAAGGAGCTGCGCGACGCCCTACCGCGA 2224

Query 659   GGCCAGCAGCTGGTGCAGCGGGTGCCEAAGATGAAGAACAAGCCGCGCTCGCCCGTGGT 718
          |||
Sbjct 2225   GGCCAGCAGCTGGTGCAGCGGGTGCCEAAGATGAAGAACAAGCCGCGCTCGCCCGTGGT 2284

Query 719   GGAGCTGAGCAAGGTGCCGCTGGTCCAGCGCGGCAGTGCCAACGGCCTCTGA 770
          |||
Sbjct 2285   GGAGCTGAGCAAGGTGCCGCTGGTCCAGCGCGGCAGTGCCAACGGCCTCTGA 2336

```

13.5 Sequencing of GRK2CTD6xCHis

Sequencing of pET3dGRK2CTD6CHis (amino acids 454-689 of GRK2) clone 4

```

TTCTCTGATATTTTTGTTTACTTTAAGAAGGAGATATAC CATGA CCCGCTCCCTGGACTGGCAGATGGTCTTCTTGCAGAA
GTACCCTCCCCCGCTGATCCCCCACGAGGGGAGGTGAACGCGGGCCGACGCCTTCGACATTGGCTCCTTCGATGAGGAGGA
CACAAAAGGAATCAAGTTACTGGACAGTGATCAGGAGCTCTACCGCAACTTCCCCTCACCATCTCGGAGCGGTGGCAGCA
GGAGGTGGCAGAGACTGTCTTCGACACCATCAACGCTGAGACAGACCGGCTGGAGGCTCGCAAGAAAGCCAAGAACAAGCA
GCTGGGCCATGAGGAAGACTACGCCCTGGGCAAGGACTGCATCATGCATGGCTACATGTCCAAGATGGGCAACCCCTTCCT
GACCCAGTGGCAGCGGCGGTACTTCTACCTGTTCCCAACCGCCTCGAGTGGCGGGGCGAGGGCGAGGCCCCGCAGAGCCT
GCTGACCATGGAGGAGATCCAGTTCGGTGGAGGAGACGCAGATCAAGGAGCGCAAGTGCCTGCTCCTCAAGATCCGCGGTGG
GAAACAGTTTCATTTTGCAGTGGGATAGCGACCCTGAGCTGGTGCAGTGAAGAAGGAGCTGCGCGACGCCCTACCGGAGGC
CCAGCAGCTGGTGCAGCGGGTGCCEAAGATGAAGAACAAGCCGCGCTCGCCCGTGGTGGAGCTGAGCAAGGTGCCGCTGGT
CCAGCGCGGCAGTGCCAACGGCCTC GACCATCACCATCACCATTGAGGATCC GGCTGCTAACAAGCCCGAAAGGAAGCTG
AGTTGGCTGCTGCCACCGCTGAGCAATAACTAGCATAACCCCTTGGGGCCTCTAAACGGGTCTTGAGGGGTTTTTTGCTGA
AAGGAGGAAGTATATCCGGATATCCACAGGACGGGTGTGGTCCGATGATCGCGTAGTCGATAGTGGCTCCAAGTAGCGAA
CGAGCAGGACTGGGCGGGCCAAAGCGGTCCGACAGT

```

ATG: Start codon

CATGA: BspHI restriction site, not reconstituted

XXXX: hexahistidine tag

TGA: Stop codon

GGATCC: BamHI restriction site

```

Query 1     CGCTCCCTGGACTGGCAGATGGTCTTCTTGCAGAAGTACCCTCCCCCGCTGATCCCCCA 60
          |||
Sbjct 1626   CGCTCCCTGGACTGGCAGATGGTCTTCTTGCAGAAGTACCCTCCCCCGCTGATCCCCCA 1685

```


Query	61	CGAGGGGAGGTGAACGCGGCCGACGCCTTCGACATTGGCTCCTTCGATGAGGAGGACACA	120
Sbjct	1686	CGAGGGGAGGTGAACGCGGCCGACGCCTTCGACATTGGCTCCTTCGATGAGGAGGACACA	1745
Query	121	AAAGGAATCAAGTTACTGGACAGTGATCAGGAGCTTACCGCAACTTCCCCCTCACCATC	180
Sbjct	1746	AAAGGAATCAAGTTACTGGACAGTGATCAGGAGCTTACCGCAACTTCCCCCTCACCATC	1805
Query	181	TCCGAGCGGTGGCAGCAGGAGGTGGCAGAGACTGTCTTCGACACCATCAACGCTGAGACA	240
Sbjct	1806	TCCGAGCGGTGGCAGCAGGAGGTGGCAGAGACTGTCTTCGACACCATCAACGCTGAGACA	1865
Query	241	GACCGGCTGGAGGCTCGCAAGAAAGCCAAGAACAAGCAGCTGGGCCATGAGGAAGACTAC	300
Sbjct	1866	GACCGGCTGGAGGCTCGCAAGAAAGCCAAGAACAAGCAGCTGGGCCATGAGGAAGACTAC	1925
Query	301	GCCCTGGGCAAGGACTGCATCATGCATGGCTACATGTCCAAGATGGGCAACCCCTTCTTG	360
Sbjct	1926	GCCCTGGGCAAGGACTGCATCATGCATGGCTACATGTCCAAGATGGGCAACCCCTTCTTG	1985
Query	361	ACCCAGTGGCAGCGGCGGTACTTCTACCTGTTCCCAACCGCCTCGAGTGGCGGGGCGAG	420
Sbjct	1986	ACCCAGTGGCAGCGGCGGTACTTCTACCTGTTCCCAACCGCCTCGAGTGGCGGGGCGAG	2045
Query	421	GGCGAGGCCCGCAGAGCCTGCTGACCATGGAGGAGATCCAGTCGGTGGAGGAGACGCAG	480
Sbjct	2046	GGCGAGGCCCGCAGAGCCTGCTGACCATGGAGGAGATCCAGTCGGTGGAGGAGACGCAG	2105
Query	481	ATCAAGGAGCGCAAGTGCCTGCTCCTCAAGATCCGCGGTGGGAAACAGTTCATTTTGCAG	540
Sbjct	2106	ATCAAGGAGCGCAAGTGCCTGCTCCTCAAGATCCGCGGTGGGAAACAGTTCATTTTGCAG	2165
Query	541	TGCGATAGCGACCCTGAGCTGGTGCAGTGAAGAAGGAGCTGCGCGACGCCTACCGCGAG	600
Sbjct	2166	TGCGATAGCGACCCTGAGCTGGTGCAGTGAAGAAGGAGCTGCGCGACGCCTACCGCGAG	2225
Query	601	GCCCAGCAGCTGGTGCAGCGGGTGCCCAAGATGAAGAACAAGCCGCGCTCGCCCGTGGTG	660
Sbjct	2226	GCCCAGCAGCTGGTGCAGCGGGTGCCCAAGATGAAGAACAAGCCGCGCTCGCCCGTGGTG	2285
Query	661	GAGCTGAGCAAGGTGCCGCTGGTCCAGCGCGGCAGTGCCAACGGCCTC	708
Sbjct	2286	GAGCTGAGCAAGGTGCCGCTGGTCCAGCGCGGCAGTGCCAACGGCCTC	2333

13.6 Sequencing of pcDNA3WD1

Sequencing of pcDNA3WD1 (MASTLIVGHWDGNMSLVDRRT)

CTAGAGAACCCACTGCTTACTGGCTTATCGAAATTAATACGACTCACTATAGGGAGACCCAAGCTTGGTACCGAGCTC **BGA**
TCCATGGCCAGCACCTGATCGTGGGCCACTGGGACGGCAACATGAGCCTGGTGGACAGGAGGACC **TGA**CTCGAGCATGCA
TCTAGAGGGCCCTATTCTATAGTGTACCTAAATGCTAGAGCTCGCTGATCAGCCTCGACTGTGCCTTCTAGTTGCCAGCC
ATCTGTTGTTTGCCCTCCCCGCTGCCTTCCTTGACCCTGGAAGGTGCCACTCCCCTGTCCTTCTCAATAAAAATGAGGA
AATTGCATCGCATTGTCTGAGTAGGTGTCAATCTATTCTGGGGGTGGGGTGGGGCAGGACAGCAAGGGGGAGGATTGGGA
AGACAATAGCAGGCATGCTGGGGATGCGGTGGGCTCTATGGCTTCTGAGGCGGAAAGAACCAGCTGGGGCTCTAGGGGGTA
TCCCCACGCGCCCTGTAGCGGCGCATTAAGCGCGGCGGGTGTGGTGGTTACGCGCAGCGTGACCGCTACACTTGCCAGCGC
CCTAGCGCCCGCTCCTTTCGCTTCTTCCCTTCCCTTCTCGCCACGTTTCGCCGGCTTTCCCCGTCAAGCTCTAAATCGGGG
GCTCCCTTTAGGGTTCGGATTTAGTGCTTTACGGCACCTCGACCCAAAAAATTGATTAGGGTGATGGTTCACGTAGTGG
GCCATCGCCCTGATAGACGGTTTTTTCGCCCTTTGACGTTGGAGTCCACGTTCTTTAATAGTGGACTCTTGTTCCAAACTGG
AACAACTCAACCCTATCTCGGTCTATTCTTTTGAATTTATAAGGGATTTTGCCGATTTCCGGCCTATTGGTTAAAAAATGA
GCTGATTTAACAAAAATTAACGGAATTAATCTGTGGAATGTGTGTGTCAGTTAGGGTGTGGAAAGTCCCAGGCTCCCCA
GCAGGCAGAAGTATGCAAAGCATGCATCTCAATTAGTCAGCAACCAGGTGTGGAAAGTCCCAGGCTCCCAGCAGGCAGA
AGTATGCAAAGCATGCATCTCAATTAGTCAGCAACCATAGTCCCGCCCTAACTCCGCCCATCCCGCCCTAACTCCGCC
AGTTCGCCCATTY

ATG: Start codon

GGATCC: BamHI restriction site

TGA: Stop codon

CTCGAG: XhoI restriction site

13.7 Sequencing of pcDNA3WD2

Sequencing of pcDNA3WD2 (MFLAEDASTLIVGHWDGNMSL)

```
CAGAGCTCTCTGGCTAACTAGAGAACCCACTGCTTACTGGCTTATCGAAATTAATACGACTCACTATAGGGAGACCCAAGC
TTGGTACCGAGCTCGGATCCATGTTCCCTGGCCGAGGACGCCAGCACCCCTGATCGTGGGCCACTGGGACGGCAACATGAGCC
TGTGACTCGAGCATGCATCTAGAGGGCCCTATTCTATAGTGTACCTAAATGCTAGAGCTCGCTGATCAGCCTCGACTGTG
CCTTCTAGTTGCCAGCCATCTGTTGTTTGGCCCTCCCCCGTGCCTTCCTTGACCCTGGAAGGTGCCACTCCCCTGTCCTT
TCCTAATAAAAATGAGGAAATTCATCGCATTGTCTGAGTAGGTGTCACTTCTATTCTGGGGGGTGGGGTGGGGCAGGACAGC
AAGGGGGAGGATTGGGAAGACAATAGCAGGCATGCTGGGGATGCGGTGGGCTCTATGGCTTCTGAGGCGGAAAGAACCAGC
TGGGGCTCTAGGGGGTATCCCCACGCGCCCTGTAGCGGCGCATTAAAGCGGGCGGGTGTGGTGGTTACGCGCAGCGTGACC
GCTACACTTGCCAGCGCCCTAGCGCCCGCTCCTTTTCGCTTTCTTCCCTTCCTTTCTCGCCACGTTTCGCCGGCTTTCCCGT
CAAGCTCTAAATCGGGGGCTCCCTTTAGGGTTCGGATTTAGTGTCTTACGGCACCTCGACCCCAAAAACTTGATTAGGGT
GATGGTTCACGTAGTGGCCATCGCCCTGATAGACGGTTTTTTCGCCCTTTGACGTTGGAGTCCACGTTCTTTAATAGTGGA
CTCTTGTTCAAACTGGAACAACACTCAACCCTATCTCGGTCTATTCTTTGATTTATAAGGGATTTTGCCGATTTTCGGCC
TATTGGTTAAAAAATGAGCTGATTTAACAAAAATTTAACGCGAATTAATTTCTGTGGAATGTGTGTGTCAGTTAGGGTGTGGAA
AGTCCCCAGGCTCCCCAGCAGGCAGAAGTATGCAAAGCATGCATCTCAATTAGTCAGCAACCAGGTGTGGGAAAGTCCCCA
GGCTCCCCAGCAGGCAGAAGTATGCAAAGCATGCATCTCATTAGTCAGCAACCATAGTCCCGCCCC
```

ATG: Start codon

GGATCC: BamHI restriction site

TGA: Stop codon

CTCGAG: XhoI restriction site

13.8 Sequencing of pcDNA3WD3

Sequencing of pcDNA3WD3 (MERSSFSSFDLAEDASTLIVF)

```
ACTAGAGAACCCACTGCTTACTGGCTTATCGAAATTAATACGACTCACTATAGGGAGACCCAAGCTTGGTACCGAGCTCGG
ATCCATGGAGAGGAGCAGCTTCAGCAGCTTCGACTTCCTGGCYGAGGACGCCAGCACCCCTGATCGTGTTCTGACTCGAGCA
TGCATCTAGAGGGCCCTATTCTATAGTGTACCTAAATGCTAGAGCTCGCTGATCAGCCTCGACTGTGCCTTCTAGTTGCC
AGCCATCTGTTGTTTGGCCCTCCCCCGTGCCTTCCTTGACCCTGGAAGGTGCCACTCCCCTGTCCTTTCTAATAAAAATG
AGGAAATTGCATCGCATTGTCTGAGTAGGTGTCACTTCTATTCTGGGGGGTGGGGTGGGGCAGGACAGCAAGGGGGAGGATT
GGGAAGACAATAGCAGGCATGCTGGGGATGCGGTGGGCTCTATGGCTTCTGAGGCGGAAAGAACCAGCTGGGGCTCTAGGG
GGTATCCCCACGCGCCCTGTAGCGGCGCATTAAAGCGGGCGGGTGTGGTGGTTACGCGCAGCGTGACCGCTACACTTGCCA
GCGCCCTAGCGCCCGCTCCTTTTCGCTTTCTTCCCTTCCTTTCTCGCCACGTTTCGCCGGCTTTCCCGTCAAGCTCTAAATC
GGGGGCTCCCTTTAGGGTTCGGATTTAGTGTCTTACGGCACCTCGACCCCAAAAACTTGATTAGGGTGTGGTTACAGTA
GTGGGCCATCGCCCTGATAGACGGTTTTTTCGCCCTTTGACGTTGGAGTCCACGTTCTTTAATAGTGGACTCTTGTTCAAA
CTGGAACAACACTCAACCCTATCTCGGTCTATTCTTTGATTTATAAGGGATTTTGCCGATTTTCGGCCTATTGGTTAAAAA
ATGAGCTGATTTAACAAAAATTTAACGCGAATTAATTTCTGTGGAATGTGTGTGTCAGTTAGGGTGTGGAAAGTCCCCAGGCTC
CCCAGCAGGCAGAAGTATGCAAAGCATGCATCTCAATTAGTCAGCAACCAGGTGTGGAAAGTCCCCAGGCTCCCCAGCAGG
```

CAGAAGTATGCAAAGCATGCATCTCAATTAGTCAGCAACCATAGTCCCGCCCTAACTCCGCCATCCCGCCCTAAATCCG
GCCAGTTCC

ATG: Start codon

GGATCC: BamHI restriction site

TGA: Stop codon

CTCGAG: XhoI restriction site

13.9 Sequencing of pMHCWD3

Sequencing of pMHCWD3 (MERSSFSSFDLAEDASTLIVF) clone 2

CTCCCCATAAGAGTTTGA**CTCGAC****ATG**GAGAGGAGCAGCTTCAGCAGCTTCGACTTCTGGCCGAGGACGCCAGCACCT
GATCGTGTTC**TGA****AAGCTT**GATGGGTGGCATCCCTGTGACCCCTCCCCAGTGCCTCTCCTGGCCCTGGAAGTTGCCACTCC
AGTGCCCAACCAGCCTTGTCCATAATAAAATTAAGTTGCATCATTTTTGTCTGACTAGGTGTCTTCTATAAATATTATGGGGTG
GAGGGGGGTGGTATGGAGCAAGGGGCAAGTTGGGAAGACAACCTGTAGGGCTGCGGGTCTATTGGGAACCAAGCTGGAG
TGCAGTGGCACAATCTTGGCTCACTGCAATCTCCGCCTCCTGGGTTCAAGCGATTCTCCTGCCTCAGCCTCCCAGTTGTT
GGGATTCCAGGCATGCATGACCAGGCTCAGCTAATTTTTGTTTTTTGGTAGAGACGGGGTTTACCATATTGGCCAGGCT
GGTCTCCAACCTCCTAATCTCAGGTGATCTACCCACCTTGGCCTCCCAAATTGCTGGGATTACAGGCGTGAACCACTGCTCC
CTTCCCTGTCTTCTGATTTTAAAATAACTATAACCAGCAGGAGGACGTCAGACACAGCATAGGCTACCTGGCCATGCCCA
ACCGTGGGACATTTGAGTTGCTTGGCTTGGCACTGTCTCTCATGCGTTGGGTCCACTCAGTAGATGCCTGTTGAATTCCT
GCAGCCCGGGGATCCACTAGTTCTAGAGCGGCCGTTTTAACTAGTATACACGTGGCGCCCGGGCGGCCACCAGCGGTG
GAGCTCCAGCTTTTGTTCCTTTAGTGAGGGTTAATTTTCGAGCTTGGCGTAATCATGGTCATAGCTGTTTCTGTGTGAAA
TTGTTATCCGCTCACAAATCCACACAACATACGAGCCGGAAGCATAAAGTGTAAGCCTGGGGTGCCTAATGAGTGAGCTA
ACTCACATTAATTGCGTTGCGCTCACTGCCCCGCTTCCAGTCGGGAAACCTGTCGTGCCAGCTGCATTAATGAATCGGCCA
ACGCSCGGGGAARAGGCGGTTTGGCGTATTGGGCGCTCTTCCGCTTCTCGGTCA

ATG: Start codon

CTCGAC: SalI restriction site

TGA: Stop codon

AAGCTT: HindIII restriction site